UNIVERSITA' DEGLI STUDI DI PARMA

Dottorato di ricerca in Biochimica e Biologia Molecolare

Ciclo XXIII: 2008-2010

Biochemical characterization of human kynurenine aminotransferase II (hKAT II): a drug target for cognitive diseases

Coordinatore:
Chiar.mo Prof. Gian Luigi Rossi

Tutor:
Chiar.mo Prof. Andrea Mozzarelli

Co-Tutor:
Prof.ssa Barbara Campanini

Dottoranda:
Dott.ssa Elisabetta Passera

GENERAL INTRODUCTION

Kynurenine aminotransferase (KAT) is a pyridoxal 5'-phosphate dependent enzyme, which catalyzes the irreversible transamination of L-kynurenine (KYN) to produce kynurenic acid (KYNA). KYN is the central metabolite in the Kynurenine pathway (KP), the main tryptophan degradation pathway in most living organisms. The scientific interest in KP is unceasing because some of its enzymes and metabolites (kynurenines) mediate relevant physiological functions and associated pathological states of the immune and nervous systems. In particular, KYNA is a neuroinhibitory metabolite of the KP, acting as a broad-spectrum endogenous antagonist of ionotropic excitatory amino acid receptors and α7 nicotinic acetylcholine receptors, which are involved in cognitive functions like learning and memory. Since these antagonistic effects are seen at KYNA concentrations found in the mammalian brain, elevations in the brain KYNA has been hypothesized as an important factor contributing to the pathogenesis and progression of neurological or psychiatric diseases that are associated to cognitive impairment, including schizophrenia and Alzheimer's disease. In human and rodent brains four proteins named KAT I, II, III and IV, have been reported to be involved in KYNA synthesis. In view of its biochemical properties, KAT II is the prevalent isoform responsible for KYN degradation in mammalian brain to give KYNA. Therefore, human KAT II is a potential drug target in the treatment of neurophatological conditions characterized by a glutamatergic and cholinergic hypofunction related to an excess of KYNA, like Schizophrenia and Alzheimer's disease. Despite hKAT II is considered a potential regulatory target for maintaining physiological concentrations of KYNA, a thorough biochemical characterization of this enzyme is still missing. The principal aim of this study was a detailed assessment of hKAT II in regards its biochemical and functional characteristics. In particular, the activity of hKAT II towards the natural substrates kynurenine and α-aminoadipate, and the inhibitors (R)-2-amino-4-(4-(ethylsulfonyl)-4-oxobutanoic acid and sulfinic acid was investigated. Moreover, we determined for the first time the intrinsic β-lytic activity towards the substrate analog β-chloroalanine of hKAT II and a variant carrying the Y142F mutation, expected, on the basis of structural evaluations, to exhibit a decreased propensity for β-elimination, a side reaction common to transaminases. The biochemical investigation has allowed us to develop two efficient and rapid assays to screen hKAT II inhibitors: i) a continuous assay based on the absorbance of the natural substrate L-KYN, that allows fast measurement of enzyme activity and determination of inhibition mechanisms; and ii) a 96-well plate suited, end-point assay based on the coupling of hKAT II activity to two reporter reactions. These assays are of interest in the high-throughput screening for specific hKAT II inhibitors. The availability of these assays and a detailed spectroscopic analysis allowed to demonstrate that (R)-2-amino-4-(4-(ethylsulfonyl)-4-oxobutanoic acid and sulfinic acid, reported to be selective and potent rat KAT II inhibitors, are actually substrate for the human ortholog, rather than pure competitive inhibitors. As a part of the activities carried out during the thesis, we carried out attemps to increase the expression yield of soluble hKAT II. Recombinant expression of hKAT II was investigated by a novel culture method, called EnBase^{TM}, or enzyme-based-substrate-delivery (BioSilta). EnBase^{TM} (BioSilta) is an enhanced novel microbial culture system in which enzyme-based supply of glucose allows a glucose-limited growth, providing high cell densities and high recombinant protein yields. The avaibility of higher amounts of hKAT II, together with the tools developed for the high-throughput screening of hKAT II specific inhibitors will be useful in the development of novel drugs for cognitive dysfunction.

CONTENTS

CHAPTER 1

INTRODUCTION

The kynurenine pathway

In mammalian tissues, the most important route of non proteinogenic tryptophan metabolism is the "Kynurenine Pathway" (*1*) (KP; Scheme 1), a cascade of enzymatic steps which convert tryptophan to nicotinamide adenine dinucleotide (NAD) (*2*). The term "Kynurenine Pathway" is derived from the central metabolite L-kynurenine (L-KYN) and is different from the use of tryptophan for the formation of the neurotransmitter serotonin and the related neurohormone melatonin (*3*). In humans the KP occurs both peripherally and centrally and involves many enzymes, including two heme-dependent enzymes, indoleamine-2,3-dioxygenase(*4*) (IDO; EC: 1.13.11.52) and tryptophan-2,3-dioxygenase(*5*) (TDO; EC 1.13.11.11), which catalyze the oxidative ring opening of tryptophan. They differ in their tissue localization and regulation(*6*). TDO is predominantly expressed in the liver, constitutes the major source of KYN in non-inflammatory conditions, and is activated by glucocortinoids (*7*). IDO is present both in brain (neurons, glial cells) and in peripheral tissues (*8*) and is stimulated by proinflammatory cytokines (*9*). The product of this reaction is formyl-kynurenine, which is further degraded to KYN by kynurenine formylase (*10*). KYN can be further metabolized by three different enzymes: kynurenine 3-monooxygenase (KMO), yielding 3-hydroxykynurenine (3-HKYN), kynureninase which forms anthranilic acid (HANA) and kynurenine aminotransferase (KAT) which catalyzes the transamination of KYN to a side chain keto acid intermediate which spontaneously undergoes to an intramolecular cyclization yielding kynurenic acid (KYNA) (*11*). The transamination reaction which forms KYNA is irreversible and constitutes a dead-end arm of the KP, since there is no enzyme that further metabolises KYNA. 3-HK is metabolized by the same KATs to yield xanthurenic acid, another metabolic inert side product of the pathway, or by kynureninase to give rise to 3-hydroxyanthranilic acid. 3-hydroxyanthranilic acid 3,4 dioxygenase then converts 3-hydroxyanthranilic acid to α-amino-ω-carboxymuconic acid semialdehyde, which either rearranges non enzimatically to form quinolinic acid (QUIN), or serves as a substrate for 2-amino-3-carboxymuconic acid semialdehyde decarboxylase yielding picolinic acid and its downstream metabolites. Finally, QUIN is metabolized by quinolinic acid phosphoribosyltransferase, yielding nicotinic acid mononucleotide and subsequent degradation products including the end product NAD^+.

All the enzymes required for this catabolic cascade are present in the brain (*12*), but their cerebral activity is much lower than in the peripheral organs such as the liver and kidney (*13, 14*). Indeed, the KP mainly occurs in systemic tissues, especially in the liver, while most of the tryptophan in the CNS is converted to indolamines or utilized in protein synthesis (*15*). The activities of both TDO and IDO in the brain are normally very low under regular physiological conditions, thus the cerebral

KP pathway is driven mainly by blood-derived KYN, which can readily cross the blood-brain barrier (BBB) by using the same tryptophan neutral amino acid transporter (*12, 16*). However, unlike tryptophan, which serves as a substrate for serotonine biosynthesis in neurons, brain KYN is preferentially metabolized in astrocytes and microglial cells. Indeed, in mammalian brain all enzymes of the KP are primarily expressed in astrocytes and/or in microglial cells, rather than in neurons. As brain KYN derives to a significant extent (about 60%) (*17*) from the peripheral circulation, fluctuations in peripheral KYN formation have significant influence on brain kynurenines formation.

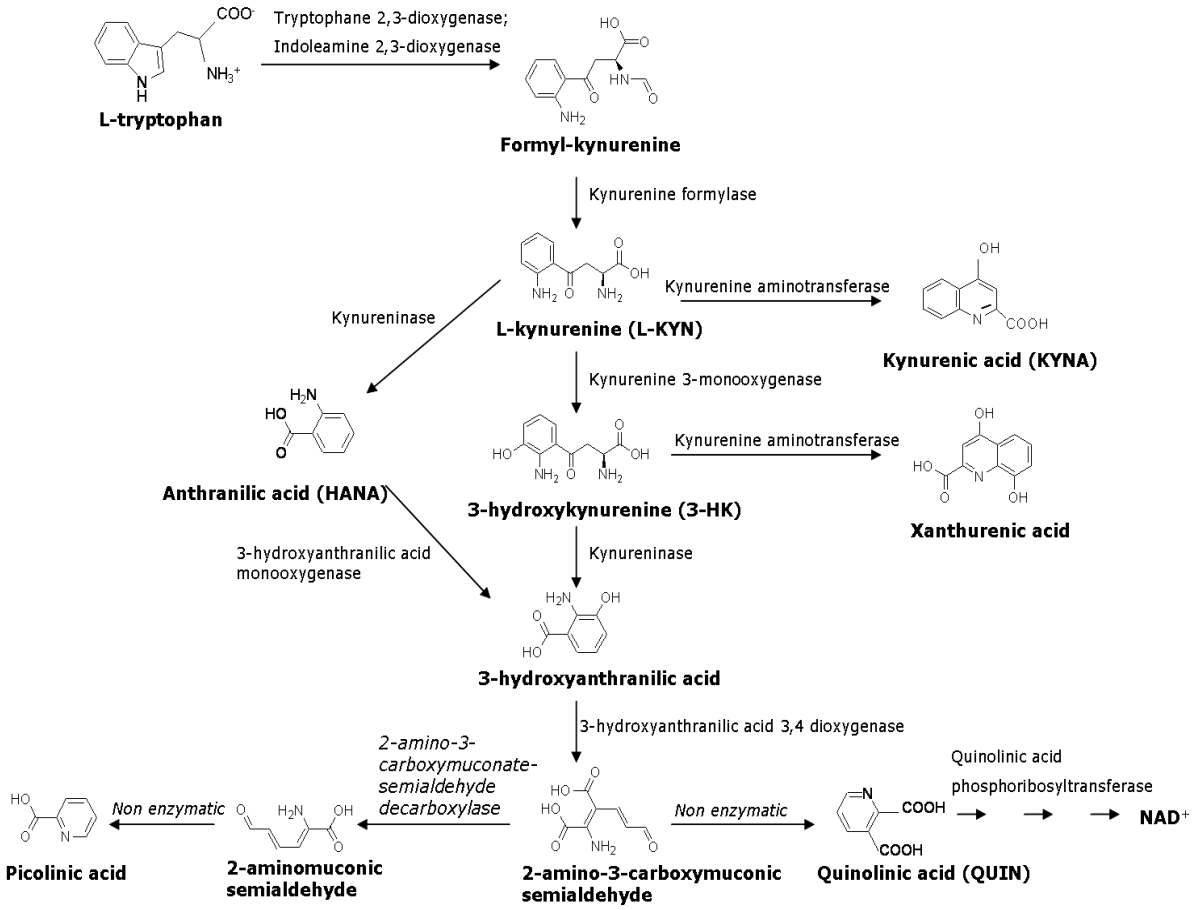

Scheme 1. Kynurenine pathway in mammalian cells.

Blood-borne KYN, after entering the brain from the periphery, is sequestrated into either astrocytes or microglia for further degradation. In the brain, the subsequent intracellular degradation of KYN is primarily dictated by the differential distribution of individual KP's enzymes in astrocytes and microglial cells (*12, 18-20*). Astrocytes do not appear to contain kynurenine 3-monooxygenase and therefore favour KYNA synthesis, whereas microglial cells possess very little KAT activity and preferentially form intermediates of the QUIN branch of the pathway (*20*). In the brain the formation

of KYNA and QUIN is therefore spatially separated: in astrocytes KYN is irreversibly transaminated to KYNA (the "KYNA branch" of the KP), which cannot be metabolized further intracellularly, but is promptly released from the cell. In contrast, 3-HK and its downstream product QUIN are preferentially synthesized in microglial cells and then further degraded enzymatically (the "QUIN branch" of the KP). This cellular compartimentalization probably accounts for the fact that no functional interaction between the two KP arms are observed when either KAT or KMO are specifically inhibited. The independence of the two branches of the KP is maintained under both physiological and pathological conditions (*21*).

The levels of brain kynurenines are often abnormal as a result of pathogenic events (*22*). Cerebral KP metabolism is always stimulated in response to physical injury, resulting in the rapid up-regulation of QUIN, 3-HK and KYNA formation (*12*). Inflammatory conditions, such as viral invasion, presence of bacterial lipopolysaccarides or interferon stimulation are accompanied by an increased activity of indoleamine 2,3-dioxygenase and kynurenine hydroxylase, causing substantial increases in the production of kynurenine (*18, 23*). Substantial (often 100- to 1000-fold) elevations in 3-HK and QUIN are seen when microglial cells are activated or when macrophages infiltrate the brain during immunological impairment, such as viral or other infections, neuroinflammation or ischemic and traumatic conditions (*24*). Because of the very low KAT activity in microglia and other cells of monocyte origin, the synthesis of KYNA is less affected (*13*).

Kynurenine 3-monooxygenase (KMO), which converts L-KYN to 3-hydroxykynurenine along the "QUIN branch" of the KP, is increasingly viewed as a major gatekeeper of the kynurenine pathway (*25*). This enzyme shows much higher activity in peripheral tissues than in the brain. Because of its low K_m for KYN (approximately 20 μM), this microglial enzyme is more rapidly saturated by brain KYN concentrations than astrocytic KATs (K_m values: ~4 mM) (*26*). It follows that cerebral KMO exerts preferential control over the fate of KYN within the brain.

Qualitatively, the characteristics of enzymes along the "QUIN branch" of the pathway does not appear to differ between the brain and the periphery. Moreover, kynurenine 3-monooxygenase, kynureninase, 3-hydroxyanthranilic acid oxygenase and quinolinc acid phosphoribosyltransferase present in the brain have been confirmed to be identical with those expressed in the periphery, using specific antibodies and molecular cloning (*13*). On the contrary, comparison of peripheral and central nervous system (CNS) KATs reveals a more complex picture since peripheral organs contains several aminotransferases capable of forming KYNA from L-KYN (*27*), whereas L-KYN transamination to produce KYNA in the CNS of mammals is carried out by four distinct enzymes, KAT I, II, III and IV, constituting the KATs family (*28-32*). Although all the four isoforms are present in the mammalian brain to a different extent, only KAT I and KAT II have been thoroughly characterized with regard to their role in cerebral KYNA synthesis (*33, 34*). This two isoforms differ, in particular, by substrate specificity, with KAT I showing a lower substrate specificity than KAT II for L-KYN (*33*). Moreover, the intrinsic catalytic promiscuity of KAT I is enhanced by its β-lyase

activity (*35, 36*). Therefore, KAT II has been considered the principal isoform responsible for the synthesis of KYNA in the rodent and human brain (*33, 34, 37*).

Physiological relevance of kynurenines

In the periphery, the role of the KP appears to be primarily directed toward the maintenance of NAD homeostasis, with other KP metabolites excreted unchanged in high concentrations in the urine (*13*), hence the collective term "kynurenines" for KP metabolites. Although all kynurenines are found in high concentration in urine, none of them has so far been assigned a relevant physiological function in peripheral organs (*13*). Instead, in mammalian CNS the KP is of particular biological interest because it leads to four neuroactive metabolites: KYNA and QUIN, which exert respectively neuroinhibitory and neuroexcitatory activity through interaction with glutamate and nicotinic receptors, and 3-HKYN and HANA, which promote neuronal damage by generating neurotoxic free radicals. The synthesis of these neuroactive kynurenines within the CNS has been implicated not only in mediating several physiological functions of the nervous systems, but also in the pathogenesis of different neurological disorders (*11, 14*). The first indication that kynurenines might play a role in the brain was provided by Lapin (*38*) (1978), who noted convulsion after an intracerebral injection of QUIN in mice. Soon thereafter, ionophoretically applied QUIN was found to excite rat cortical neurons (*39*), and intracerebrally injected QUIN was shown to cause excitotoxic lesions in rat brain (*40, 41*). In the last decades the physiophatological effects of neuroactive kynurenines have been intensively investigated. Neuroactive metabolites of tryptophan along the KP have been implicated in the pathophysiology of a variety of neurological and psychiatric diseases (*13, 42*) either chronic like Alzheimer's (*43*), Parkinson's (*44*) and Huntington's disease (*45, 46*), Schizophrenia and cognitive impairment (*47-50*), Multiple sclerosis (*51*), Amyotropic lateral sclerosis (*52*), or caused by acute insult like ischemia, stroke and head trauma (*13*).

Among the neuroactive kynurenines, KYNA has recently received most of the attention. Indeed, it has been demonstrated by *in vivo* studies that KYNA participates in normal brain function as endogenous modulator of excitatory neurotransmission (*53, 54*). Most physiological effects associates with KYNA, including neuroprotective properties, have been attributed to its antagonistic activity on ionotropic glutamate and α7 nicotinic acetylcholine receptors, both of which are involved in regulating neuronal plasticity and cognitive functions like learning and memory (*55*). Several recent studies emphasized the effects of KYNA on the physiological functions related to these receptors.

Glutamate and nicotinic acetylcholine receptors

Glutamate and nicotinic acetylcholine receptors are ligand–gated channels selective for cations. Both these receptors are transmembrane ion channels that are opened or closed in response to

the binding, on an allosteric binding site, of a chemical messenger, a neurotransmitter. The ion channel is regulated by a ligand and is usually very selective to one or more ions like Na^+, K^+ or Ca^{2+}. Such receptors are located at synapses and convert the chemical signal of presynaptically released neurotransmitter directly and very quickly into a postsynaptic electrical signal.

Ionotropic glutamate receptors, which mediate most of the fast excitatory synaptic transmissions in the CNS, consists of 3 subtypes: kainate receptors, alpha-amino-3-hydroxy-5-methyl-4-isoxazole propionic acid (AMPA) receptors and N-methyl-D-aspartate (NMDA) receptors. Activation of glutamate receptors is responsible for basal excitatory synaptic transmission and for mechanisms which underlie learning and memory such as long-term potentiation and long-term depression (*56, 57*). However, any event or process leading to a sudden or chronic increase in the activity of glutamate receptors often induces the death of neurons (*58*). Indeed, over-activation of glutamate receptors leads to a rise of intracellular Ca^{2+} that promotes neuronal cells damage by both activating destructive enzymes and increasing the formation of reactive oxygen species(*59*). The neuronal damage that characterizes chronic neurodegenerative disorders such as Parkinson's disease and follows cerebral insults as stroke, ischemia, trauma, hypoxia, hypoglicemia and hepatic encephalopathy, is believed to result, in part, from increased activity of glutamate receptors (*60*). N-Methyl-D-aspartate receptor (NMDAR) is a specific type of glutamate-gated ion channel ubiquitously distributed throughout the brain, fundamental to excitatory neurotransmission and critical for normal CNS function. Its role relates to memory functions, learning processes and mental performance. The activation of NMDA receptor requires co-binding by two ligands: glutamate and glycine (Figure 1). The co-agonist glycine binds to a "strychnine-insensitive" glycine modulatory site on the NMDA receptor, which must be occupied in order for glutamate to open the channel (*61*). Therefore, the availability of glycine at the co-agonist site plays a critical role in the optimal NMDA receptor functioning. Activation of NMDA receptor result in the opening of an ion channel that allows flow of Na^+ and Ca^{2+} ions into the cells and K^+ out of the cells. Calcium flux through NMDARs is thought to play a role in synaptic plasticy, a cellular mechanism which is believed to underlie memory and learning. Abnormal over-activation of MNDARs has been suggested to lead to neuronal cell death observed in many acute and chronic disorders such as ischemia, stroke, and Huntington's disease (*62*).

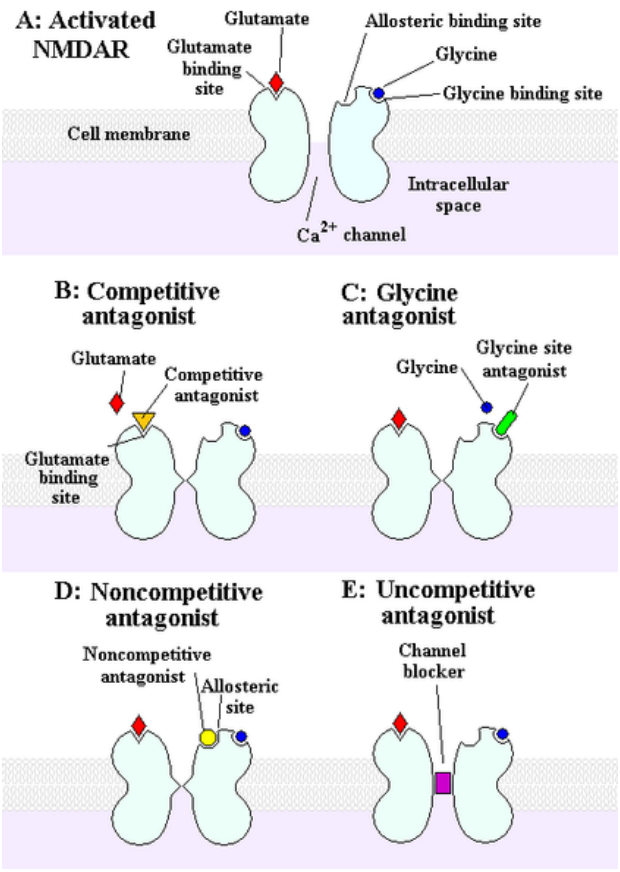

Figure 1. Simplified model of NMDAR activation and various types of NMDAR blockers.

Nicotinic acetylcholine receptors (nAChRs) are grouped into muscle, neuronal and α-bungarotoxin– sensitive, based on pharmacology and tissue–specific expression. Neuronal nAChRs are trans-membrane allosteric proteins formed by five subunits (*63*). They can be holigomers as well as heteroligomers made up from the combination of different α subunits or α and β subunits (*64*). Numerous type of functional neuronal nAChRs have been so far identified. As with all ligand-gated ion channels, opening of the nAChR channel pore requires the binding of a chemical messenger. Like the other type of acetylcholine receptors, muscarinic acetylcholine receptors (mAChRs), the nAChR is triggered by the binding of the neurotransmitter acetylcholine (ACh). However, whereas muscarinic receptors are activated by muscarine, nicotinic receptors are also opened by nicotine. Hence, the name "nicotinic". Agonist, such as endogenous acetylcholine or exogenous nicotine, stabilize the open conformation of the nAChR channel for several milliseconds. While open, the nAChRs channel transiently permeates cations before closing back; in particular, Na^+ enters the cell and K^+ exits. The net flow of positively-charged ions is inward. With a sufficient number of channels opening at once, the intracellular Na^+ concentration rises to the point at which the positive charge within the cell is enough to depolarize the membrane and produce an intracellular ionic signal. Although sodium and potassium carry most of nAChR current, calcium can also make a significant contribution (*55, 65, 66*). Figure 2 illustrates sites on a nAChR

that can alter function. Competitive antagonists and partial agonists can occupy the agonist binding sites. Open channel blockers, such as phenylcyclidine, can bind within the pore. Moreover, there are multiple sites for other noncompetitive inhibitors and modulators.

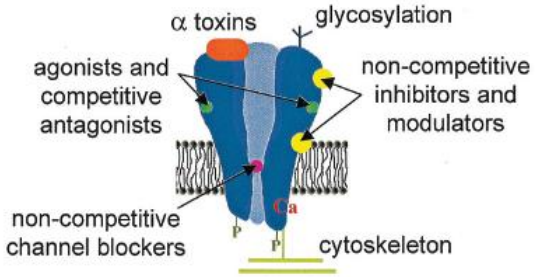

Figure 2. A representation of the allosteric sites on a nAChR, showing three of the five subunits that form the pentameric receptor-channel complex (*67*).

The structural diversity of nicotinic receptors provides the flexibility necessary for them to play multiple and varied roles in synaptic transmission throughout the CNS. In particular, receptor channels made up entirely of the α_7 subunit (α_7 nAChRs), are widely distributed in the mammalian CNS and are characterized by high calcium permeability and rapid activation and desensitization kinetics (*68*). Cholinergic mechanisms mediated by α_7 nAChRs influence a number of cognitive functions and modulates a wide variety of behaviours (*63*). Behavioural and pharmacologic studies carried out in rats have suggested that α_7nAChRs are essential for memory (*69*). Nicotinic AChRs also have roles during development and neuronal plasticity (*70*). Biological changes that inappropriately alter nicotinic mechanisms could immediately influence the release of many neurotransmitters and alter excitatory neurotransmission. Nicotinic cholinergic dysfunctions in the brain are intimately involved in the pathogenesis of a number of neurological disorders, including Alzheimer's disease, Parkinson's disease, Down Syndrome, schizophrenia and some form of epilepsy (*63*). As example, during the progression of Alzheimer's disease, cholinergic inputs decreased as well as the number of nAChRs in some brain area (*71, 72*). Loss of nicotinic-based mechanism is likely to contribute to the overall cognitive deficits associated with Alzheimer's disease (*67*).

KYNA as an endogenous antagonist of ionotropic glutamate and nicotinic acetylcholine receptors

KYNA, which is produced and released by astrocytes in the brain, is unique in three aspects. First, the transamination reaction, where the side chain of KYN cyclizes to form KYNA, is irreversible. Second, there is no catabolic enzymes that further metabolizes KYNA. Third, KYNA is not taken up by glia cells or neurons. Thus, following its irreversible transamination from KYN in astrocytes, newly formed KYNA is rapidly released into the extracellular milieu (*73, 74*), where it has access to

neuronal membrane receptors. The only known mechanism that clears KYNA from the extracellular space in the CNS is a non specific acid transporter that eliminates KYNA from the brain (*13, 75*). Furthermore, rapid renal excretion seems to be the single most important mechanism of brain KYNA disposition in the rat (*76*). Under normal physiologic conditions, tissue concentration of KYNA in human brain range between 0.2 and 1.5 μM (*75, 77*). The KYNA content of the rat brain is substantially lower (≈ 20 nM) (*78*).

The neuroactive properties of KYNA have long been attributed to its action as a competitive antagonist at the glycine site on NMDA receptors. At low micromolar concentrations ($IC_{50} \cong$ 10-15 μM) (*79, 80*) , it specifically blocks the NMDARs activity via a competitive antagonism of glycine at the "strychnine-insensitive" glycine modulatory site on the NMDA receptor (*81*), see Figure 1. At higher concentrations ($IC_{50} \cong$ 200-500 μM), KYNA acts as a competitive antagonist at the agonist recognition site of the NMDA receptor (*79, 82, 83*). Furthermore, in even higher dose, (IC_{50} 0.1 – 1 mM), this tryptophan metabolite is able to antagonize also AMPA and kainate receptors (*11, 14, 84*). Therefore, KYNA is considered a broad-spectrum endogenous antagonist of ionotropic excitatory amino acid receptors (*74, 85*). More recently, it has been discovered that at physiologically relevant concentrations (IC 50 ≅ 7 μM))(*80*), KYNA non-competitively antagonizes α7 nicotinic acetylcholine receptor (α7nAChRs) more effectively than NMDA receptors(*80*). This action, which may play a part in the ability of KYNA to generate a deficit in the sensory system (*86, 87*), has been suggested to be mediated by its binding to sites located on the N-terminal domain of the α7-nACh receptor subunit (*63*). In the light of present data, α7nAChRs could be considered a preferential target for endogenous KYNA *in vivo* (*88*) and it is likely that fluctuations in endogenous brain KYNA levels preferentially affect α7nAChRs function (*80*), activation of which at the presynaptic site is involved in regulating neuronal plasticity in the brain (*68, 70, 89-91*).

Considering that KYNA levels in mammalian brains, including humans, range from low nanomolar to low micromolar (*75*), it has long been a matter of controversy whether endogenous KYNA levels are sufficiently high to block NMDA receptor activity with physiological or pathological relevance. Some lines of evidence indicate that the glycine coagonist site on NMDA receptors may not be fully saturated (*92-94*), so that even quite low KYNA concentrations under physiological conditions could be sufficient to maintain a partial antagonism at the glycine receptor (*14*). Moreover, a recent study (*95*) suggests that as KYNA is synthesized and released from brain astrocytes (*96*), especially from those in close opposition to glutamatergic synapses (*97*), the concentration of KYNA in glutamatergic boutons might be high enough not only to block both the glycine-site of the NMDA receptor and the α7 nicotinic receptor, but also the agonist recognition site of the NMDA receptor, thus producing significant actions on brain glutamatergic and cholinergic neurotransmission.

KYNA as a ligand of GPR35

G protein-coupled receptors (GPCRs) are seven-transmembrane domain receptors that constitute the largest and most diverse protein family in mammalian genomes. Their primary function is to transduce extracellular stimuli into intracellular signals through interaction of their intracellular domains with heterotrimeric G proteins. Depending on the type of G protein to which the receptor is coupled, a variety of downstream signalling pathways can be activated (*98*). GPCRs are involved in a wide variety of physiological processes, such as the visual sense, the sense of smell, behavioral and mood regulation, regulation of immune system activity and inflammation. In human, in addition to about 160 characterized receptors, an equal number of genes encode proteins belonging to this family of receptors, but their ligands and functions remain to be determined and they are so called “orphan” G protein-coupled receptors (*99, 100*).

In a recent study, KYNA has been identified as an endogenous ligand of an orphan G protein-coupled receptor, GPR35, that is predominantly expressed in immune cells and gastrointestinal tissue (*98*). In particular, KYNA elicited a specific rise in Ca^{2+} in cells expressing human GPR35, with a medium effective concentration (EC_{50}) of 39 μM. The reported EC_{50} value of KYNA on human GPR35 activation is comparable with the concentration required for NMDA receptor antagonism. The discovery of KYNA as an endogenous ligand for GPR35 further highlighted the importance of this kynurenine metabolite in regulating biological functions. Kynurenine metabolic pathway is indeed activated during inflammatory conditions, such as viral invasion, bacterial lipopolysaccharides (LPS), or interferon-γ-stimulation (*101, 102*). The activation of tryptophan metabolism causes a reduced plasma tryptophan level and an elevated KYNA concentration (*42*). The predominant expression of GPR35 in immune cells and the elevation of KYNA levels during inflammation, suggest that this receptor-ligand pair may play important roles in immunological regulation.

In addition to above described physiological functions, KYNA is also involved in maintaining physiological arterial blood pressure. In rats, the region of the rostral and caudal medulla in the CNS play an important role in regulating cardiovascular function (*103-105*). Spontaneously hypertensive rats that have higher arterial blood pressure were found to have significantly lower KAT activity and KYNA content in their rostral and caudal medulla than the control rats (*106*). Injection of KYNA into the rostral ventrolateral medulla of these rats significantly decreased their arterial pressure (*107*), which suggest that KYNA is involved in maintaining physiological arterial blood pressure.

Other neuroactive kynurenines

In addition to KYNA, the KP generates others three neuroactive compounds, the excitotoxic NMDARs agonist quinolinic acid (QUIN), and the free radical generators 3-hydroxykynurenine (3-HK) and 3-hydroxyanthranilic acid (HANA).

QUIN is the only known endogenous compound with the ability to selectively activate the NMDA subtype of glutamate receptors, causing increased neuronal firing (*108*). QUIN has been shown to enhance synaptosomal glutamate release and to inhibit the glutamate uptake into astrocytes, resulting in an increased glutamate concentration into the synaptic cleft and at the presynaptic level (*109*). It is documented that CNS infection and immune activation are associated with accumulation of QUIN in the brain and cerebral spinal fluid, as a consequence of IDO and TDO over-activation (*18, 23*). Substantial (often 100-to 1000 fold) elevations in QUIN are seen when microglia cells are activated or when macrophages infiltrate the brain during immunological compromise, such as viral or other infections, neuroinflammation or ischemic and traumatic conditions (*24*). Elevated QUIN concentrations are responsible for over-activation of NMDA receptors and have been shown to concur to neuronal damage occurring in CNS inflammations. The mechanism for QUIN neuroexcitocytotoxicity in human astrocytes and neurons has recently been clarified (*110*). QUIN-induced cytotoxic effects on neurons and astrocytes are likely to be mediated by an over activation of NMDA receptors with subsequent induction of nitric oxide synthase and excessive nitric oxide-mediated free radical damage. The concentration of QUIN in cerebral tissue, between 40 and 400 nM (*13, 111-113*), and its low receptor affinity ($IC_{50} > 100$ μM) are difficult to reconcile with its high cytotoxicity. It appears that the high in vivo potency of QUIN, particularly as an excitotoxin, is caused by a combination of factors, including the absence of effective removal mechanisms for extracellular QUIN (*85*) and its ability to readily generate damage-promoting free radicals. In fact, it also induces lipid peroxidation (*114*) and the production of reactive oxygen species (*115*).

3-HK, a biological precursor of QUIN, is present in the human brain at a concentration range between 15 and 400 nM. Also 3-HK has neurotoxic properties, but in contrast to QUIN and KYNA, the neurotoxicity of 3-HK is not mediated by the direct interaction with specific recognition sites, but by generating toxic free radicals (*116*), which initiate a cascade of intracellular events resulting in cellular oxidative damage. Applications of 3-HK at micromolar levels (1-100 μM) to striatal neuronal cultures causes time and dose-dependent death, which is significantly reduced by co-treatment with catalase, suggesting that neurotoxic effects of 3-HK are due to hydrogen peroxide production (*108*). In addition, the immediate 3-HK degradation product, 3-hydroxyanthranilic acid, has also been shown to be neurotoxic (*117*), as it readily undergoes auto-oxidation with the production of superoxide and hydrogen peroxide thus promoting oxidative protein damage (*118*).

KYNA as an astrocyte-derived neuromodulator

KYNA has unique neuroinhibitory properties, which have been intensively investigated in the last years. A large body of studies has demonstrated that this compound is significantly involved in basal neurophysiological processes in the brain, particularly in the modulation of behaviour and cognition (*119*). Early *in vivo* studies on KYNA neurophysiological effects concerned the hypothesis of this KP metabolite as an endogenous neuroprotective agent endowed with antiexcitotoxic and anticonvulsant properties. As over-activation of glutamate receptors promotes neuronal cells damage, a mechanism capable of preventing glutamate receptors from being over-stimulated seems essential for maintaining the normal physiological condition in the CNS. The antagonist activity of KYNA on NMDA receptors, whose excessive activation results in excitotoxic nerve cell loss, prompted the hypothesis that KYNA may exert neuroprotective properties, likely acting as an endogenous anti-excitotoxic agent limiting neurotoxicity arising from NMDA receptors over-stimulation (*13*). This hypothesis was first investigated in rats brain, showing that KYNA prevented the neurotoxic effects induced by the local application of the related brain metabolite QUIN (*85*). Furthermore, pharmacologically administration of KYNA, or its pro-drugs analogues able to cross the blood brain barrier readily than the parent compound, have anticonvulsive effects and provide neuronal protection against brain damage resulting from ischemia, hypoxia or traumatic brain injury (*85, 120-122*). Nevertheless, it is possible to dissociate KYNA's antiexcitotoxic and anticonvulsant properties, which can be realized at nanomolar concentrations (*15, 122, 123*), from its potentially harmful effects on cognition at much higher levels (*87*).

The neurophysiological aspect of endogenous KYNA that has recently gained most attention is its modulatory function on glutamatergic and cholinergic neurotransmission. The antagonist activity of KYNA on NMDA and α7-nAChR receptors, which are intimately involved in synaptic plasticity and cognitive functions, prompted the hypothesis that KYNA may function as a unique glial modulator of cholinergic and glutamatergic activity, capable of influencing cognitive functions mediated by these neurotransmitters systems (*13, 79, 81*). A large number of *in vivo* experiments in rodents have demonstrated that nanomolar (i.e. endogenous) concentrations of KYNA in the prefrontal cortex cause a decrease in the extracellular levels of three neurotransmitters known to be associated with cognitive functions, i.e., glutamate, acetylcholine and dopamine. Interestingly, these modulatory effects are bidirectional, i.e., a selective reduction in KYNA formation substantially enhances the extracellular presence of these neurotransmitters (*54, 124, 125*). These results validated the role of KYNA as an endogenous modulator of cognitive processes closely linked to glutamatergic, dopaminergic and cholinergic neurotransmission. Moreover, KYNA' s bidirectional control over these neurotransmitters is of special interest in view of the fact that KYNA' s levels are abnormally high in the brain and cerebrospinal fluid of individuals with schizophrenia (*47-49*) and in those with Alzheimer's disease (*43*), suggesting that increased levels of KYNA may contribute to glutamatergic and cholinergic–mediated cognitive dysfunction involved

in these two neuropathological conditions. The complexity of the neurophysiological actions of KYNA in the CNS implies its pathophysiological significance in situation of clinically relevant receptor impairments (*126*).

KYNA's imbalance in neurodegenerative disorders

In recent years mounting attention has been paid to the possible physiopathological role of dysregulations in normal brain KYNA concentration. As fluctuations in the endogenous brain levels of KYNA influence glutamatergic, dopaminergic and cholinergic neurotransmission (*53, 54*), dysfunction of cerebral KYNA synthesis has been hypothesized as an important factor contributing to the pathogenesis and progression of neurological or psychiatric diseases that are associated with impaired cholinergic and/or glutamatergic neurotransmission. The hypothesis of a causative role of KYNA in neurophatological processes gained momentum because of reports of changes in its brain content in several neurological and psychiatric diseases (Table 1). Cerebral KYNA levels are increased in patients with Alzheimer's disease (*43*), Down's syndrome (*127*) and schizophrenia (*47-50*), and levels are decreased in patients with end-stage Parkinson's disease (*44*) and Huntington's disease (*45, 46*).

INCREASED KYNA		**DECREASED KYNA**	
Disease state	*Reference*	*Disease state*	*Reference*
Schizophrenia	(*47, 49, 50*)	Parkinson's disease	(*44*)
Alzheimer's disease	(*43*)	Huntington's disease	(*45, 46*)
Down's syndrome	(*127*)	Infantile spasms	(*128*)
Amyotrophic lateral sclerosis	(*52*)	Multiple sclerosis	(*51*)
Cerebral malaria	(*129*)		
HIV infection	(*130, 131*)		

Table 1. Altered brain and cerebrospinal fluid KYNA levels in selected diseases states.

Neurochemistry studies demonstrated that KYNA acts as a negative regulator of glutamatergic neurotransmission, that in turns modulates extracellular dopamine levels (*54*), whose unbalancing is co-responsible for the neurological symptoms of these diseases. In lower concentration KYNA is probably unable to inhibit NMDA receptors effectively and to prevent excitotoxicity arising from enhanced release of glutamate. On the other hand, increase in endogenous levels of KYNA is associated with reduced glutamate release (glutamatergic hypofunction) and consequently decreased extracellular dopamine levels (*54*), and therefore may significantly influence cognitive process leading to impaired cognitive capacity (*43*). In human post-mortem studies, the brain

concentration of KYNA was found to be elevated in the prefrontal cortex (PFC) of individuals with schizophrenia (*47, 50, 132*). Hypofunction of both NMDA-receptor and the α-7nACh-receptor are implicated in the pathophysiology of this disease, and especially in cognitive deficits and impairments in executive function (*25*). The discovery of increased cortical KYNA levels in the brain tissue of individuals with schizophrenia prompted the hypothesis that elevated KYNA concentration may be causally correlated to the cognitive dysfunction that has been attributed to altered glutamatergic and cholinergic transmission (*25*). Indeed, increases in brain KYNA levels, by virtue of the compound's ability to antagonize NMDARs and α7nAChRs, both of which are critically involved in physiological process underlying learning, memory and other manifestations of synaptic plasticity (*79, 80*), may cause or exacerbate cognitive impairments (*86, 133*). Behavioural studies in rats have demonstrated a causal link between increased cortical KYNA levels and neurocognitive deficits (*86, 87, 95, 133*). Animals with experimentally elevated KYNA levels exhibit performance deficits in behaviour task requiring cognitive process similar to those that are impaired in schizophrenia (*86, 87, 95, 133, 134*). These i*n vivo* studies on rats provided more substantive evidence favoring a pathophysiological role of increased levels of endogenous KYNA, as a consequence of altered KP metabolism, to the hypoglutamatergic and cholinergic tone in schizophrenia (*135*). Notably, in post mortem studies of schizophrenic patients brains, the upregulation of KYNA levels was accompanied by increases in the tissue levels of KYN, KYNA' s immediate bio precurosor (*132*). The increased cortical KYN content might be a direct consequence of enhanced synthesis catalyzed by either TDO or IDO (*102, 136*), or of a reduced KMO activity in the periphery and/or in the brain (*25, 137*).

In addition to being associated with schizophrenia, abnormally high KYNA levels have been observed in the brain and cerebrospinal fluids of Alzheimer's disease (AD) patients (*43*) and in the frontal and temporal cortices of Down's syndrome (DS) subjects (*127*). It can be hypothesized that inhibition of α7nAChRs by increased levels of KYNA contributes to the cognitive deficits in patients with AD and DS (*138*). Cortical KYNA is therefore considered an attractive new target for significant cognitive enhancement.

Modulation of KYNA synthesis as a future therapeutic strategy for cognitive enhancement

In view of the involvement of neuroactive KP metabolites in several neurodegenerative and psychiatric disorders, enzymes of the KP have long been considered interesting targets for rational therapeutic interventions to cure mental illness (*13*). In particular, the inhibition of kynurenine aminotransferse activity would result in lowering KYNA levels, with a concomitant relieve of glutamatergic inhibition. Decreased KYNA production in the brain is supposed to causes diminished inhibition of NMDA and α7 nicotinic acetylcholine receptors function, therefore enhancing glutamate and dopamine release and consequently cognitive processes (*139*). In line with accumulating evidence suggesting a role of altered KYNA function in mental illness and

cognitive impairment (*43, 49, 50, 133, 135*), recent years witnessed a growing interest in the study of mechanisms controlling KYNA synthesis in the CNS. The brain content of KYNA is governed by a delicate balance of interconnected factors: (i) the competition of the KP with alternative pathways using tryptophan to generate other bioactive metabolites (i.e. serotonine and melatonine) (*11*), (ii) the availability of the pivotal KP metabolite KYN for degradation through the KP, and (iii) the differential cellular uptake of KYN into various brain cells types (*13*). The optimal approach to limit the effects of elevated brain KYNA levels is by direct pharmacological manipulation of kynurenine pathway metabolism. In principle, such "kynurenergic" agents do not need to penetrate into the brain, but could be efficacious by reducing the pheripheral levels of circulating KYN. This would lower brain uptake of the precursor and decrease cerebral KYNA formation. Examples in these category includes inhibitors of TDO and/or IDO. Such compounds are available and, in the case of IDO inhibitors, are being developed for the treatment of a variety of diseases ranging from cancer to asthma and infectious diseases (*140, 141*), but they are yet to be adequately tested for possible applications in psychiatry.

Interventions resulting in the activation of KMO, too, might diminish peripheral and central KYN levels and consequently attenuate KYNA formation indirectly. However, the potential clinical merit of this approach will have to be weighed against possible detrimental consequences of inducing increased kynurenine pathway flux towards the neurotoxic compounds 3-hydroxykynurenine and quinolinic acid.

Therefore, the most prudent strategy to reduce brain KYNA is to target KATs, the enzymes responsible of KYNA synthesis. Although the mammalian brain contains at least four distinct KATs (*142*), it appears that KAT II accounts for the majority of KYNA formation in the human brain. Indeed, in contrast to the other three KATs, KAT II is distinguished by its substrate specificity to KYN and abundant common amino acids do not interfere with the enzyme's ability to convert KYN to KYNA. From the point of view of drug development, the existence in the human brain of at least four KYNA-synthesizing enzymes, combined with the necessity to fine-tune KYNA levels to avoid the potentially harmful effects caused by a drastic deficiency of this metabolite in the CNS, requires the design of isozymes-specific inhibitors. KAT II selective inhibitors could represent an effective way to sensibly lowering KYNA levels, whereas the potential harmful complete depletion of this neuroprotective compound would be prevented by the action of the other KAT isozymes. Selective inhibition of KAT II is therefore a rational pharmacological approach to attenuate KYNA formation in the brain with direct implications for the enhancement of cognitive process in disorders related to learning and memory deficits, such as schizophrenia and Alzheimer's diseases, where lowering the levels of brain KYNA is sought to counterbalance glutamatergic and cholinergic hypofunction.

The hypothesis that blockade of KAT II, causing a decrease in brain KYNA, may have cognition-enhancing effects, recently received strong support from *in vivo* studies in which mutant mice with a target deletion of KAT II displayed reduced brain KYNA levels concomitant with an increased

performance in cognitive tests (*25, 143, 144*). These functional changes were accompanied by increased extracellular glutamate. Moreover, recent studies were designed to probe the functional consequence of an acute disruption of cerebral KYNA synthesis using specific KAT II inhibitors. Early attempt to develop selective KAT II inhibitors were based on the structure of KYN and lead to the synthesis of the substrate analogue (S)-4-(ethylsulfonyl) benzoylalanine (S-ESBA); its intracerebral application in the rat brain caused a rapid decrease in KYNA formation, accompanied by an increase in extracellular dopamine levels (*15, 145*). Together with the demonstration of increased glutamatergic tone and enhanced cognitive abilities in KAT II deficient mice, these two complementary experimental tools provide further support for the concept that selective inhibition of KAT II is a rational approach to attenuate KYNA formation in the brain with direct implications for the enhancement of cognitive process.

A recent *in vivo* study on rats, (*21*) assessed the hypothesis whether KAT II inhibition may lead to elevated 3-HK and/or QUIN levels and possibly increased risk of neurotoxicity. As the two KP branches are functionally segregated, acute blockade of KYNA synthesis using a specific KAT II inhibitor, BFF122, did not lead to a compensatory up-regulation of the neurotoxic QUIN branch of the KP. This further result stimulates the development of KYNA synthesis inhibitors as cognition enhancers in patients with neurodegenerative disorders.

Despite its potential indication as a drug target in the treatment of schizophrenia and other neurological disorders, a through biochemical characterization of KAT II from human brain is still missing (*34*) and only a few compounds have been so far developed as KAT II selective inhibitors (*21, 146*).

KYNURENINE AMINOTRANSFERASES (KATs) FAMILY

Based on the demonstrated relationship between abnormal brain KYNA concentrations and neurodegenerative diseases and psychotic disorders, enzymes involved in brain KYNA synthesis have been considered as a potential drug target for regulating brain KYNA concentration (*13, 17, 42, 119, 120, 147-151*). A number of studies concerning the identification and functional characterization of KATs in rat, mouse and human have been undertaken. The relative importance of KATs *in vivo* appears to vary with species, tissue and developmental stage. In mammals, KAT activity is present in various tissues, such as liver, kidney, small intestine and brain (*152-154*). So far, in rat, mouse and human brain, four KATs have been reported to be implicated in KYNA biosynthesis in the central nervous system:

1) KAT I, glutamine transaminase K/cysteine conjugate beta-lyase 1 (KAT I/GTK/CCBL1), EC 2.6.1.64.
2) KAT II, α-aminoadipate aminotransferase (KAT II/AADAT), EC 2.6.1.7.
3) KAT III, cysteine conjugate beta-lyase 2 (KAT III/CCBL2), EC 4.4.1.13.

4) KAT IV, glutamic-oxaloacetic transaminase II/mitochondrial aspartate aminotransferase (KAT IV/GOTII/mitASAT), EC 2.6.1.1.

The genes of KAT I and KAT III are phylogenetically distant from those of KATII and KAT IV. Among the four human KATs, human KAT I and KAT III share the highest sequence identity (51.7%), whereas there is a significant sequence divergence between human KAT I and KAT II, as they share only 18% sequence identity (*142*). It is well established that KAT IV/mitonchondrial ASAT targets mitochondria (*155-157*). KAT II is also considered to be a mitochondrial protein (*158-160*), but further confirmation about the mechanism of export to mitochondria is needed (*142*).

Biochemical properties

All four mammalian KATs posses transamination activity towards KYN leading to the formation of KYNA. Like all known aminotransferases, KAT enzyme catalysis takes place with a ping-pong bi-bi mechanism from amino acid 1 and keto acid 2 to amino acid 2 and keto acid 1 (further details on reaction mechanism are described in the Section on Structural Properties). As revealed by substrate specificity studies, all KATs are multifunctional transaminase and share many amino acid and α-ketoacid substrates. In particular, all four KATs show activity with the aromatic amino acids phenylalanine, tyrosine and tryptophan and with the sulphur-containing amino acid methionine (*142*). On the other hand, they differ in substrate specificity and pH optimal range. Human KAT I and III display very similar amino acid substrate profiles, while hKAT II is the only one among KAT isoforms showing α- aminoadipate transaminase (AADAT) activity.

KAT II/AADAT

The enzyme was initially named aminoadipate aminotransferase (AADAT) when it was first partially purified from rat liver in 1969 (*161*) and its function in liver lysine degradation is well described (*162*). Later it was reported that the same aminotransferase from liver and kidney had both KAT activity and AADAT activity (*160, 163, 164*) and Tobes and Mason definitely confirmed that AADAT was identical to rat KAT II (*164*). Biochemical analysis of human KAT II (hKAT II) revealed that this enzyme has very broad substrate specificity (*34*). Indeed, recombinant hKAT II is able to catalyze the transamination reaction of a number of amino acids. In particular, kinetic analysis of hKAT II (Table 2) revealed that the enzyme is efficient in catalyzing the transamination of aminoadipate, KYN, methionine and glutamate, and is less efficient in catalyzing tyrosine, phenylalanine, tryptophane, leucine, 3-HK, glutamine, alanine and aminobutyrate. hKAT II can use many α-ketoacids as its amino group acceptors, but prefers α-ketoglutarate. The enzyme shows maximum activity around 50°C and has broad optimum pH range from 7-9 (*34*). Although hKAT II has a relatively high K_m for kynurenine (about 4.7 mM), its catalytic efficiency in KYN to KYNA pathway is enhanced by its relatively high turnover number (k_{cat} for L-KYN 585 min^{-1}) and also by the irreversible nature of the transamination reaction. The enzymatic product of kynurenine

transamination is an instable α-ketoacid intermediate that undergoes rapidly intramolecular cyclization to KYNA. Consequently, no direct enzymatic product will accumulate during KAT-catalyzed KYN transamination and the equilibrium always proceeds towards KYNA production. On the basis of its biochemical properties, KAT II has been considered the principal enzyme responsible for the synthesis of KYNA in the rodent and human brain (*13, 37*), as supported by *in vivo* studies. Indeed, mice in which KAT II was knocked out by genomic manipulation showed a substantial decrease in brain KYNA levels and presented phenotypic changes that were in line with this biochemical deficit (*139, 165*). The irreversible transamination of KYN to KYNA is one of the major functions of hKAT II (*34*). Furthemore, this enzyme is also involved in lysine catabolism by catalyzing the transamination of aminoadipate to α-ketoadipate (Scheme 2) (*34, 166-169*). Aminoadipate is a metabolic intermediate of the major route for the catabolism of lysine, an essential amino acid in humans, which is degraded when present in an excess beyond that required for protein synthesis. Aminoadipate occurs naturally in the brain (*170, 171*), where it is known to be a selective excitotoxin for astrocytes and related glial cells, as demonstrated by a number of *in vivo* and *in vitro* studies (*172-174*). High concentration of aminoadipate functions as a NMDA receptor agonist, inhibits glutamate transport, blocks glutamine synthetase and prevents the uptake of glutamate into synaptic vesicles. These effects can contribute to an increased excitatory tone because synaptic glutamate concentrations are elevated. High levels of aminoadipate in serum and/or urine have been observed in many cases with neurological and other disorders (*160, 175-184*). As demonstrated by a substrate specificity study on recombinant hKAT II, this enzyme has higher catalytic efficiency for aminoadipate than to kynurenine (k_{cat}/K_m aminoadipate 196.2 $min^{-1}mM^{-1}$, k_{cat}/K_m kynurenine 125.9 $min^{-1}mM^{-1}$)(*34*). Moreover, the fact that the affinity of hKAT II to aminoadipate (K_m = 0.9 mM) is much greater than its affinity for ketoadipate (K_m = 20.9 mM), suggests that the AADAT enzyme reaction does not tend to be reversible and prefers the direction from aminoadipate to α-ketoadipate, one of the reactions in lysine degradation. Accordingly, in addition to be responsible for the majority of KYNA formation in the adult mammalian brain, KAT II is considered primarily involved also in the neutralization of aminoadipate to α-ketoadipate across the lysine catabolism.

The character of multiple substrates transaminase of hKAT II suggested that this enzyme may play a role in metabolism of other ketoacids and amino acids. It also raised a fundamental question regarding the structural basis of its broad substrate specificity. Structural analysis of hKAT II in complex with α-ketoglutaric acid (*34*) revealed a conformational change of an N-terminal region, that is very flexible and able to adapt different conformations to bind different ligands. Basically, this N-terminal portion moves close to the active center when the protein binds small ligand and moves away from the center when the enzyme binds large ligand. This flexible N-terminal region therefore provides a structural basis for broad substrate specificity of hKAT II.

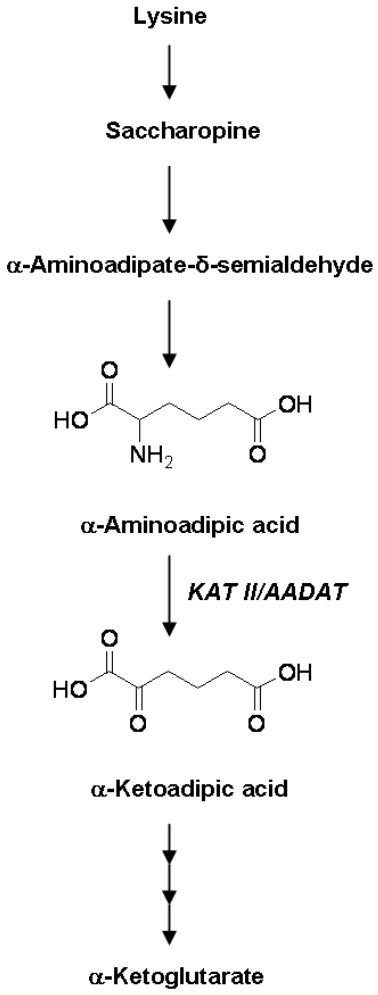

Scheme 2. Lysine catabolism pathway in mammals.

	K_m (mM)	k_{cat} (min^{-1})	k_{cat}/K_m (min^{-1}/mM^{-1})
Amino acid substrates			
Aminoadipate	0.9 ± 0.1	179.4 ± 5.7	196.2
Kynurenine	4.7 ± 0.8	585.3 ± 39.9	125.9
Methionine	1.7 ± 0.5	206.4 ± 17	123.8
Glutamate	1.6 ± 0.4	185.0 ± 14.8	118.7
Tyrosine	1.8 ± 0.2	131.5 ± 5.2	74.4
Phenylalanine	5.2 ± 1.7	327.1 ± 46.2	63.4
Tryptophan	4.3 ± 0.4	254.0 ± 8.6	58.7
Leucine	5.1 ± 3.0	285.0 ± 70.4	56.1
3-HK	3.8 ± 1.0	102.1 ± 12.2	26.8
Glutamine	8.1 ± 2.9	95.5 ± 16.6	11.8
Alanine	19.4 ± 9.2	173.6 ± 43.2	9.0
Aminobutyrate	17.8 ± 4.3	157.2 ± 19.4	8.8
Keto acid substrates			
α-ketoglutarate	1.2 ± 0.4	460.1 ± 49.8	374.5
α-ketocaproic acid	1.5 ± 0.1	289.7 ± 8.1	188.0
Phenylpyruvate	1.8 ± 0.2	284.0 ± 13	156.9
αKMB	2.4 ± 0.7	256.2 ± 31.9	105.2
Mercaptopyruvate	2.8 ± 0.5	215.5 ± 12.6	77.7
Indo-3-pyruvate	1.4 ± 1.2	89.1 ± 32.5	64.6
α-Ketovalerate	3.4 ± 0.3	159.3 ± 4.9	47.0
α-Ketoleucine	3.3 ± 0.8	150.5 ± 13.6	45.4
α-Ketobutyrate	12.7 ± 2.1	208.9 ± 12.5	16.4
Hydroxyphenylpyruvate	1.5 ± 1.1	23.6 ± 9.5	16.2
α-Ketoadipate	20.9 ± 5	290.3 ± 30	13.9
Glyoxylate	18.0 ± 3.7	218.4 ± 18.4	12.1
Oxaloacetate	16.8 ± 12.4	93.9 ± 51.6	5.6
α-Ketovaline	12.9 ± 2.9	55.1 ± 4.6	4.3
α-Ketoisoleucine	14.2 ± 3.8	55.2 ± 6.9	3.9
Pyruvate	9.7 ± 5.6	21.8 ± 6.4	2.3

Table 2: Kinetics parameters of recombinant hKAT II towards amino acid and α-keto acids (*34*).

KAT I/GTK/CCBL1

Analysis of substrate specificity revealed that hKAT I is a multifunctional PLP-dependent enzyme which possesses transaminase activity towards many amino acids and also cysteine conjugates β-lyase activity. As an aminotransferase, hKAT I has a broad amino acid specificity (*33, 36*) and can use many α-keto acids as its amino group acceptors. Unlike hKAT II, hKAT I is generally most active with large neutral, aromatic, sulphur-containing amino acids and prefers glyoxylate as amino group acceptor. hKAT I shows lower catalytic efficiency for KYN compared to hKAT II (hKAT II: K_{cat}/K_m 125.9 $min^{-1}mM^{-1}$, hKAT I: K_{cat}/K_m 42.8 $min^{-1}mM^{-}1$) (*33*). Moreover, hKAT I-mediated transamination of KYN is inhibited by physiologically abundant, competing amino acids (*30, 33*). The optimal pH range of human brain KAT I is 9.5-10 (*29, 37, 127, 185*). These biochemical properties led to the conclusion that hKAT I has a very limited contribution to brain KYNA production under physiological conditions (*13, 28, 37*). A further impediment to KYNA synthesis catalyzed by hKAT I could be the intrinsic enzyme's PLP-associated β-lyase activity (*35, 36*). This additional function not only underlines the intrinsic catalytic promiscuity of hKAT I, but also supports its role in mediating the toxicity of the sulphur-containing fragments released from halogenated alkene-derived cysteine S-conjugates (*186, 187*), that likely contributes to liver and kidney carcinogenesis (*188*). On the basis of these considerations, and in view of the biochemical properties of hKAT II (i.e., neutral pH optimum and insensitivity, at physiological KYN concentrations, to abundant amino acids), at a physiological concentration of KYN (i.e., in the low micromolar range), hKAT II is primarily responsible for the majority of KYNA formation in the adult mammalian brain (*30, 37*).

KAT III/CCBL2

Recently proposed as a novel member of the mammalian KAT family, KAT III has been identified in mouse, rat and human (*31*). The biochemical properties of KAT III have been further determined in mice (*32*). This enzyme showed activity towards a number of amino acids, including some aromatic amino acids (phenylalanine, KYN, tryptophan, 3-HK, tyrosine and hystidine) and sulphur-containing amino acids (methionine and cysteine). Human KAT I and mouse KAT III are highly similar in terms of both primary sequence and 3-dimensional structure, furthermore they also share a similar substrate profiles, but human KAT I favours certain hydrophobic substrates, while mouse KAT III prefers relatively hydrophilic substrates. Also the keto acid substrate profile of mouse KAT III is very similar to that of human KAT I (*32*). Moreover, mouse KAT III display optimal activity around pH 9.0-10.0 (*32*), which is close to the pH optimum reported for human brain KAT I (*29, 37, 127, 185*).

KAT IV/GOT2/mitASAT

The KAT activity of mit ASAT was first reported in *E. coli* (*189*) and later it was found that mit ASATs in mouse, rat and human posses KAT activity, therefore mammalian mit ASAT was named KAT IV (*30*). In addition to its KAT activity, mit ASAT, also called GOT2, catalyzes the reversible transamination of oxalacetate to aspartate in conjunction with conversion of glutamate to α-ketoglutarate (*142*). The enzymes is involved in a number of physiological process in astrocytes and neurons (*190-194*). Firstly, it as a role in the entry of glutamate into the tricarboxylic acid cycle, and in the re-synthesis of intra-mitochondrial glutamate from tricarboxylic acid cycle intermediates (*193, 195-199*); secondly, it has a key role in the synthesis of neurotransmitter glutamate in brains (*200, 201*); and at least it is an essential component of the malate-aspartate shuttle, which is considered the most important mechanism for transferring reducing equivalents from the cytosol into mitochondria in brain (*196, 202*). KAT IV was also reported to have cysteine conjugate beta-lyase activity (*203*). Mouse KAT IV has greatest activity at pH 8 (*142*).

Structural properties of hKAT II

Overall structure

Cristallographic studies of KATs from different organism, including human, have revealed that all of the functionally validated KATs whose structures have been experimentally determinated, namely human KAT I (*204*) and KAT II (*205, 206*), the KAT I orthologs of the mosquito *Aedes aegypti* (*207*), yeast *S.cerevisiae (208)*, and the archeobacterium *Pyrococcus horikoshii* (*209*), as well as 3-hydrokynurenine aminotransferase of A*nopheles gambiae* (*210*), belong to the α-family of pyridoxal-5'-phosphate (PLP)-dependent enzymes (*211*), and they are assigned to the fold type I group (*212-216*). As observed for the majority of others members of this group, KATs invariably function as homodimers, hosting two active sites at the inter-subunit interface (*126, 142*). Crystal structure analysis revealed that all KATs share an overall protein structure in which an N-terminal region, a small and a large domain can be distinguished (*126*). Comparisons of KATs crystal structures revealed a high degree of structural conservation in the PLP-bearing large domain, featured by an open α/β/α-fold that is conserved in all aminotransferases (*211*). On the other hand, peculiar structural traits characterize hKAT II (Figures 3 and 4). In particular, the functional hKAT II homodimer is featured by a strikingly swapped conformation of the catalytically essential N-terminal region encompassing residues 13-43, whose movements have been suggested to control substrate access into the enzyme active site during the catalysis (*34, 126, 142, 205*). In aminotransferases, the N-terminal region is a key structural component, which is involved in the enzyme's proper assembly and subcellular fate (*217*) and also plays a role in the catalysis by participating in substrate binding and structuring of the active site (*126*). The N-terminal region of hKAT II bears a substrate-recognition helix and an associated loop, which buds from the large domain of each subunit and protrudes toward the facing subunit, where it provides multiple inter-

subunits contacts and essential residues for shaping the PLP-binding site. While in the hKAT II dimer the N-terminal region of each subunit contributes to built up the active site of the symmetry mate, the N-terminal regions of KAT I, KAT III and KAT IV participate in building up the small domain and structuring the active site of the same subunit, that is, they do not show the swapping N-terminal observed in hKAT II. The topology observed for the hKAT II N-terminal motif has never been reported in the structure of any aminotransferase, and thus represents a distinct structural trait of hKAT II. Moreover, a unique strand/loop/strand motif (S2/S3) marks the boundary between the N-terminal element and the large domain (*206*). The latter is organized around a canonical PLP-binding inner core whose topology, consisting of a mainly parallel seven-stranded β-sheet sandwiched between α-helices, is strictly conserved through PLP-dependent aminotranferases (*211*). Furthemore in hKAT II structure, in contrast to what observed in the majority of aminotransferases, only residues of the C-terminal portion of the enzyme build up the small domain, with no contribution from the N-terminal region (*206*). Another striking structural element of hKAT II, critically contributing to the overall stability of the functional dimer, is represented by a four-stranded antiparallel flat β-sheet, formed by the unique S2/S3 motifs, that appears to sealing the two large domains together. Such an inter-subunit β-sheet has never been observed in the structure of any aminotransferase reported so far, therefore representing an element of novelty (*206*).

Interestingly, an ion binding site, located at the inter-subunit interface, was observed in the structure of hKAT II functional dimer, suggesting a possible contribution toward hKAT II dimer stability (*206*).

Fold type I aminotransferases are further classified into seven subgroups, Iα, Iβ, Iγ, Iδ, Iϕ, Iλ and Iω. KAT I and KAT IV have been assigned to Iγ and Iα respectively (*213*). KAT III is highly similar to KAT I in terms of primary sequence and crystal structure, therefore it can be assigned to Iγ, too (*32*). Because of its striking feature of the N-terminal tertiary structure, KAT II does not belong to any existing fold type I subgroups. Therefore it was proposed as a new subgroup in fold type I aminotransferase (*205*). A further sequence phylogenetic analysis revealed that KAT II and KAT II homologs form a separate lineage (*218*). This indicate that KAT II and its homologs form a new subgroup in fold type I aminotransferase, which has been designed as subgroup Iε (*142*).

The conformation adopted by the N-terminal region in KAT II is not unprecedented amongst PLP-depended enzymes and resembles what observed in the N-terminal sub-domain of members of PLP-dependent lyases, such as the cystathionine β-lyase from *E.coli* (*219*). Indeed, this β-lyase was identified as a far structural ortholog of hKAT II (*206*). Interestingly, hKAT II appears to contain structural elements that are typical of PLP-dependent enzymes belonging to functionally distinct subfamilies in the fold type I group. It can therefore not be excluded that hKAT II could catalyze, beside transamination of kynurenine and aminoadipate, additional PLP-dependent reactions (*126,*

206). An extensive functional characterization of hKAT II should be undertaken to assess this hypothesis.

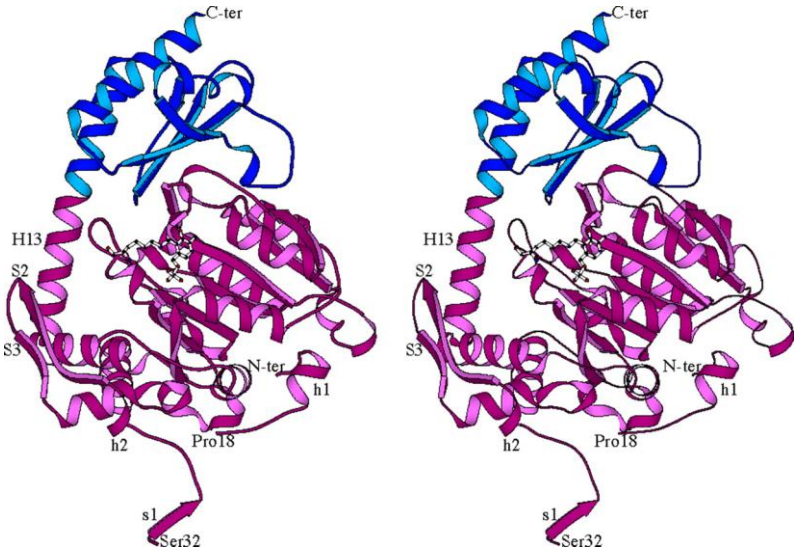

Figure 3. Stereo and ribbon representation of the hKAT II subunit. The N-terminal motif and the large domain are colored in magenta; the small domain and the C-termini are colored in blue. The enzyme active site can be observed at the domain interface where the PLP molecule, in its internal aldimine form, is shown in ball-and-stick. The S2/S3 motif and the secondary structural elements of the N-terminal motif as well as residues delimiting the disordered region are indicated (*206*).

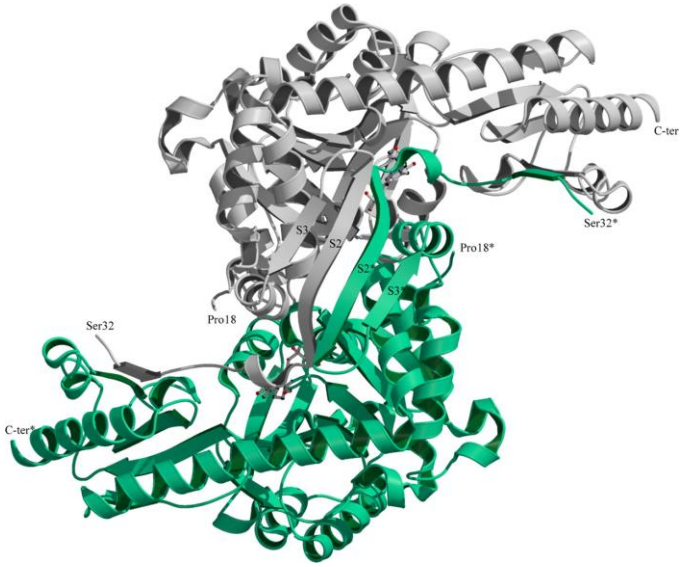

Figure 4. Ribbon representation of the functional dimer of hKAT II. The two sububits are differentially colored and the PLP molecules are shown as ball-and-sticks. The inter-subunit four-stranded antiparallel flat β-sheet, formed by the unique S2/S3 motifs of the two subunits and that seals the two large domains together is indicated (*206*).

Ligand-binding sites and substrate specificity

Each of the two active sites present in hKAT II functional dimers is located in a wide and deep cleft built up by residues of both domains of one subunit and by regions of the N-terminal motif and the large domain of the opposite one. Each active site hosts a PLP molecule, whose C4' atom, in the ligand-free form of the enzyme, is Schiff-base linked to the Nε atom of Lys263. Several residues are in direct contact with the PLP molecule and contribute to keep it in the proper orientation (Figure 5). In particular, the nitrogen atom in the PLP pyridine ring is in contact with the extremely conserved residue Asp230; the cofactor O3' atom is hydrogen bonded to the OH group of Tyr233, that points towards the PLP molecule from the bottom of the active site, and it is also in contact with Asn202 Nδ2. The resulting bonding network strongly affects the PLP plane orientation, resulting in the absence of a perfect π-stacking of its pyridine ring to the side chain of Tyr142, which is placed just above the cofactor molecule. The presence of a tyrosine residue in this position is uncommon in aminotransferases, where tryptophan or phenylalanine are the most frequently observed residues. Interestingly, a structural equivalent tyrosine residue characterizes a number of PLP-dependent enzymes involved in trans-sulphuration (*e.g* cystathionine γ-lyases and cystathionine β-lyases). Therefore, as already underlined when describing the N-terminal motif, hKAT II reveals intriguing structural determinants in common with PLP-dependent lyases. This observation suggests the possibility of a not yet investigated β-lyase activity of hKAT II. Interestingly, such activity has previously been reported for human KAT I (*36, 188*), even if this enzyme harbours a phenylalanine at the position equivalent to hKAT II Tyr142 (*204, 220*).

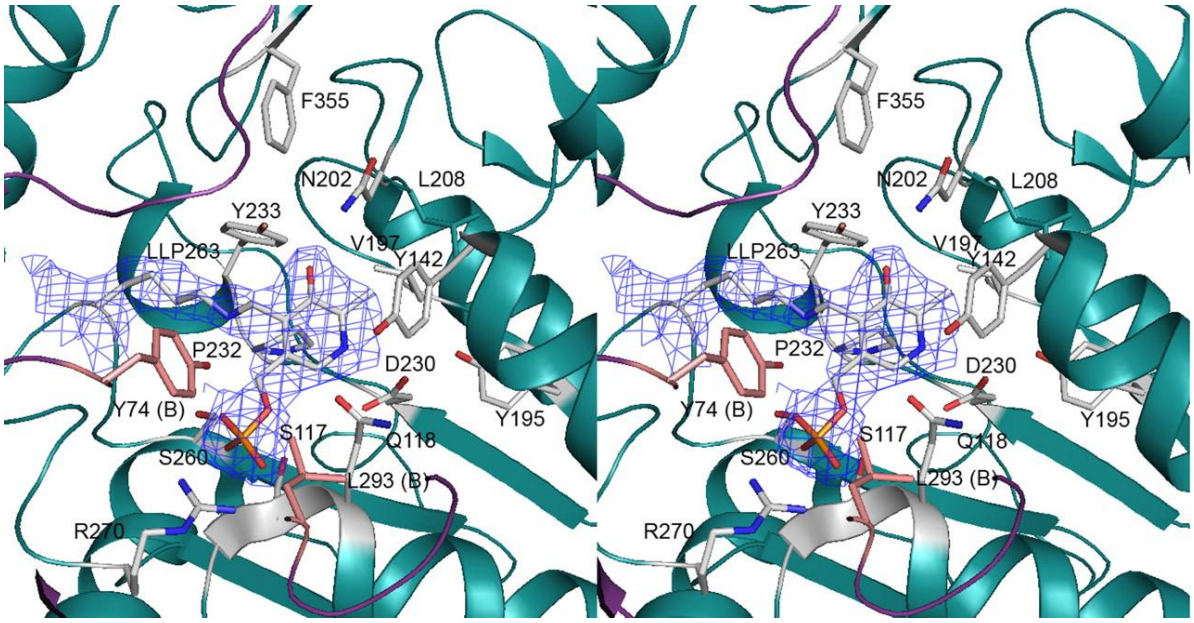

Figure 5. Stereo view of hKAT II active site with the PLP cofactor in its internal aldimine form. The protein portions building up the active site and contributed to by the two subunits of the functional homodimer are shown in a schematic representation and are colored in *deep teal* (subunit A) and

violet (subunit B). The PLP cofactor and the protein residues within a 5-Å distance of PLP are shown. The C4' atom of PLP is covalently attached to the Nε atom of Lys263, through the formation of an internal Shiff base, and the internal aldimine gives rise to the residue LLP263, represented as a stick. (*205*).

The structural homology among human KATs isoenzymes is restricted to high conserved subset of residues required for optimal PLP binding and to the C-terminal region of the small domain, while severe differences are observed for the rest of the molecule, including the unique hKAT II N-terminal region and S2/S3 motif. Consequently, the identification of the structural determinants that regulate substrate specificity in human KAT I and KAT II, can be obtained only by carefully inspecting the structures of the isoenzymes in their ligand-bound states. Indeed, the crystal structure of the Michaelis complex of human KAT I with L- phenyalanine or indole-3-acetate (*204, 220*), human KAT II with KYN (*205*), mouse KAT III with KYN (*32*), and chicken mitoshondrial ASAT (86% sequence identical to human KAT IV) structure (*221*), allowed the identification of residues that regulate substrate specificity and thus ligand binding in four KAT enzymes. In particular, the α-carboxylic group of KYN invariabily forms a salt bridge with the guanidinium group of Arg399, which drives the correct positioning of the substrate α-amino group just above the PLP C4' catalytic center. The presence of this Arg residue is a strictly conserved hallmark of all members of the aminotransferase superfamily and accounts for the anchoring of the amino acid group of KYN to the catalytic site of KAT (*213*). On the contrary, the recognition of the substrate side chain is achieved by different structural determinants in hKAT I and hKAT II (Figure 6). Specifically, the major molecular determinants responsible for substrate recognition in hKAT I consists of a hydrophobic pocket or a crown of aromatic residues in which the substrate side-chain is perfectly nested. Mouse KAT III has a similar aromatic crown. In contrast, the aromatic hydrophobic pocket observed in hKAT I and mKAT III is largely absent in the structure of hKAT II and chicken mitochondrial ASAT (human KAT II homolog), where the equivalent positions are occupied by polar or neutral amino acids. In addition, the substrate binding pocket in hKAT II appears sensibly wider, mainly owing to the absence of a residue equivalent to hKAT I Trp18 and to the substitution of KAT I Phe278 with Leu293 (*206*).

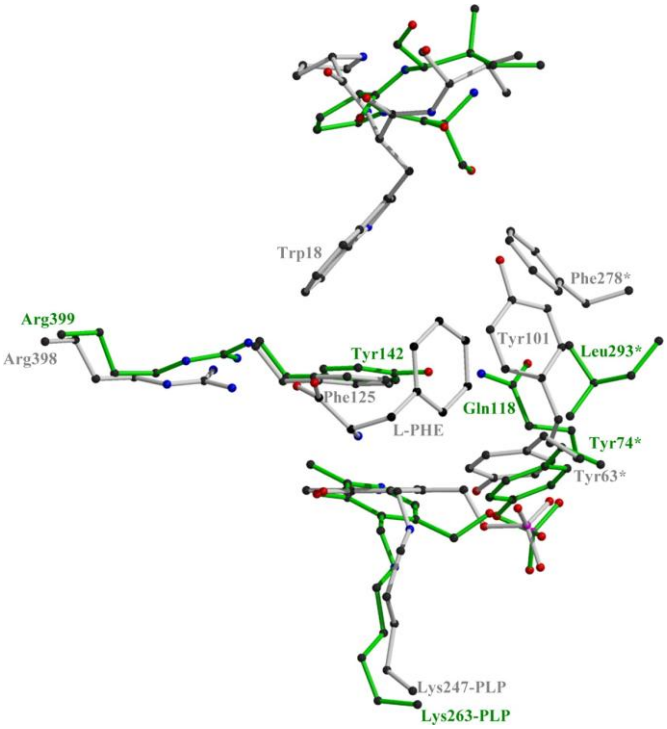

Figure 6. Representation of hKAT I and hKAT II active sites, after optimal superimposition of the two structures. The residues involved in L-Phe binding in hKAT I and their structurally equivalent residues in hKAT II are colored in white and green, respectively. The L-Phe sits above the PLP cofactor as observed in the structure of hKAT I: L-Phe complex (pdb code 1W7M) (*206*).

Conformational changes

It is well known that binding of substrates causes to aminotransferses a conformational change from the open to the closed form (*222-224*). However, similar conformational changes have not been observed in subgroup Iγ KATs (human KAT I and mouse KAT III) and in the new subgroup Iε aminotransferase (human KAT II). Another peculiar structural feature of human KAT II is a pronounced conformational change of the N-terminal region (residues 13-46) that affects the enzyme upon substrate binding, resulting in the correct structuring of the catalytic site (**Figure 7**). In particular, the loop encompassing residues 16-31 in hKAT II is subjected to a severe repositioning upon ligand binding. Indeed, it moves from one side of the active center to the other, becoming more exposed to the solvent and leaving space for the substrate aminophenyl side to bind. It also encapsulates the carboxylic side of the substrate within the center, thereby shielding the substrate binding pocket from bulk solvent (*205*). It has been proposed that the driving force of this conformational movement from a close conformation in the ligand-free form to an open conformation in the hKAT II/L-KYN complex, may be the interaction of Arg20 with the aromatic ring of L-KYN (*225*). Therefore, it was proposed that substrate specificity in human KAT II is achieved through an induced-fit mechanism, which, by properly structuring the active site of the enzyme, ultimately controls the recognition of substrates (*34, 126, 218*). In contrast, only limited

conformational changes take place during catalysis in human KAT I and mouse KAT III, which are characterized by a largely pre-formed active site that restricts the admission to the rigid enzyme's catalytic cavity to relatively small and hydrophobic molecules (*142*).

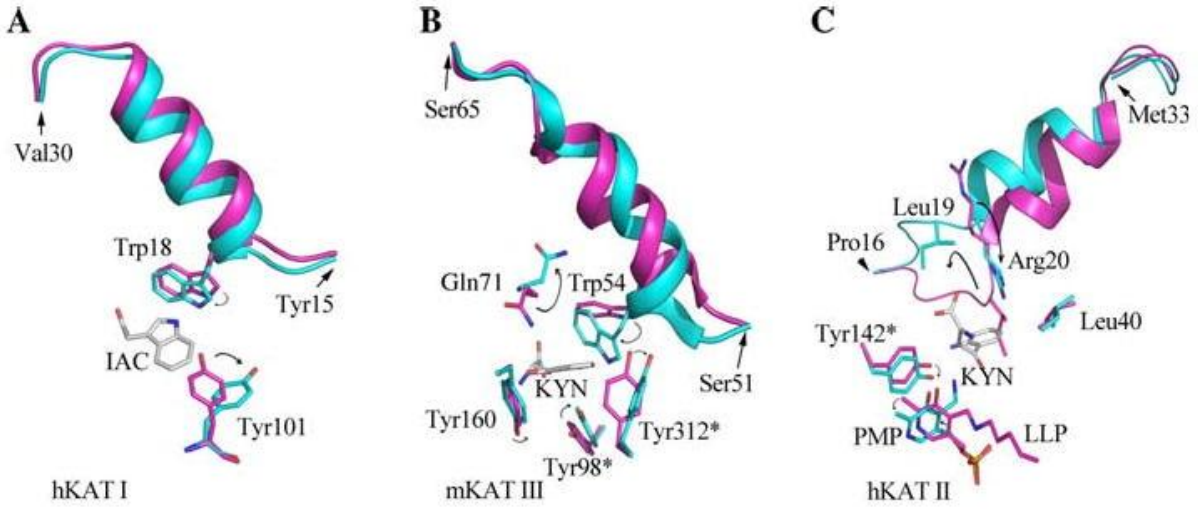

Figure 7. Conformational changes of KATs during catalysis. The structures of free (*magenta*) and ligand-bound (*cyan*) forms of each KAT structure are superposed upon each other. **A** human KAT I, **B** mouse KAT III, **C** human KAT II. The N-terminal α-helices are shown as *ribbons* and the other residues that show significant side chain repositioning are depicted as *sticks*. Residues with an *asterisk* are from the secondary subunit in each functional dimer. The *arrows* show the direction of the movement of the N-terminal α-helices and some crucial residues upon ligand binding (*142*).

KAT catalyzed transamination reaction

KATs irreversibly convert KYN to KYNA through a typical two-step transamination reaction, in which PLP acts as a coenzyme, alternating between the keto and amine forms in the two half-reactions that constitute a catalytic cycle (*225*). The transamination mechanism of KYN catalyzed by hKAT II has been theoretically determined in details performing combined quantum mechanical and molecular mechanical (QM/MM) simulations (*225*). A reliable model of the ternary complex hKAT II/KYN/H_20 system was built on the basis of the crystal structures of hKAT II recently released by Rizzi et al. (pdb code: 2vgz) (*206*), showing a ligand free enzyme co-crystallized with the cofactor in its PLP form, and by Han et al. (pdb code: 2r2n) (*205*), showing KYN bound to the enzyme with the cofactor in its PMP form.

The reaction mechanism (Scheme 3) begins with the PLP cofactor covalently bound in a Schiff-base linkage to the ε-amino group of a specific and highly conserved lysine residue (Lys263 according to hKAT II), forming an internal aldimmine. Consequently to substrate binding, the external aldimine intermediate is formed upon the nucleofilic attack of KYN to the internal aldimine

and the following displacement of Lys263. This reversible process then proceeds first through a hydrogen abstraction from the substrate Cα, leading to the ketimine intermediate. Following the electrophilic attack of the water molecule to the imine double bond, the covalent complex between the substrate and the cofactor is broken to give the cofactor in its PMP form and the ketoacid, namely 4-(2-aminophenyl)-2,4-dioxobutanoic acid, which quickly and spontaneously undergoes intramolecular cyclization leading the formation of KYNA. The intramolecular condensation leading KYNA is still poorly understood, but it is possible to envisage the formation of the pseudo-cyclic intermediate, as depicted in scheme 3. Moreover, it is not clear whether the intramolecualr cyclization of the keto acid 4-(2-aminophenyl)-2,4-dioxobutanoic acid may take place into the catalytic site of hKAT II or outside, in the external buffer. Computational evidence suggests that the formation of the cyclic product may take place directly into the catalytic site of hKAT II, and then it is released as final product from the catalytic centre (*225*).

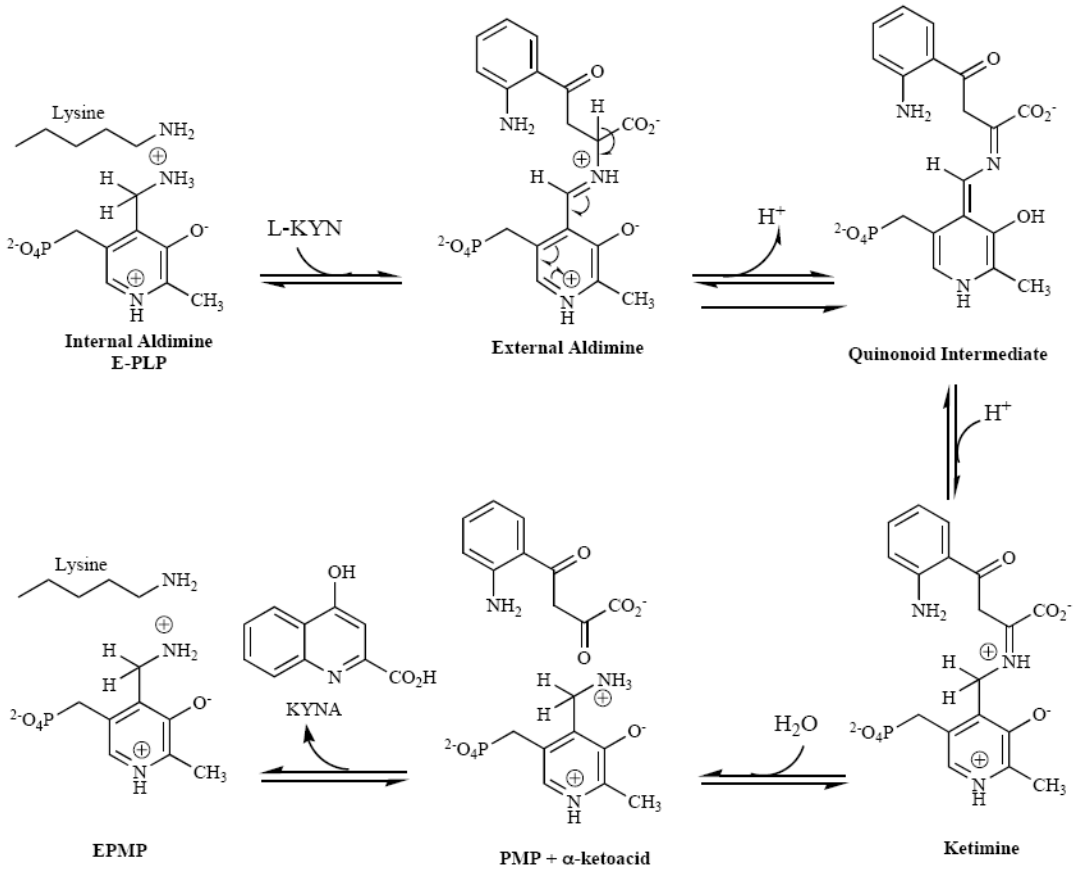

Scheme 3. Schematic representation of the first half-reaction catalyzed by KATs according to the standard catalytic mechanism adopted by PLP-dependent aminotransferases (*211*).

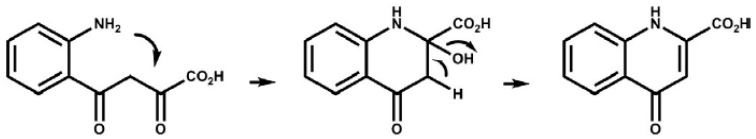

Scheme 4. Irreversible intramolecular condensation of the ketoacid intermediate to form KYNA (*225*).

Moreover, the QM/MM theoretical study of the transamination mechanism of KYN catalyzed by hKAT II pointed out a set of five basic and aromatic residues that differently contribute to the interactions with the substrate and the intermediates along the catalytic cycle of hKAT II. A peculiar feature of hKAT II is the pronounced conformational change of the N-terminal region, that is highly flexible and folds over the catalytic site upon the binding of the substrate, resulting in the correct structuring of the catalytic site. The residue Arg20 is located on this N-terminal loop and is critically involved in stabilizing the complexes between KYN, the ketimine, the keto acid and the enzyme through π-cation interaction with the anthranilic moiety of the substrates and intermediates. Another basic residue, Arg399, is involved in binding the substrate through salt bridge interactions between its guanidinium group and the α-carboxylic group of KYN. This basic residue is highly conserved across all aminotransferases and has a pivotal role in the recognition of the substrate in the active site. The salt bridge anchors the amino acid group of the substrate into the active site, allowing its correct binding pose along the catalysis. Lys263 is the catalytic base that performs the heterolytic cleavage of the Cα-H bond in order to promote the transition from the external aldimine to the ketimine intermediate. This residue also provides a general base assistance in the hydrolysis of the immine double bond by stabilizing the water molecule. Two aromatic residues are involved in mediating interactions between the substrate, the intermediates and the enzyme along the catalytic path. While Tyr74 is indirectly involved in the stabilization of the external aldimine by stabilizing the catalytic Lys263 with hydrogen bonds, Tyr142 has a direct role in favouring the substrate approaching to the cofactor.

Besides the roles of specific basic and aromatic residues, another interesting finding unveiled by this QM/MM theoretical study is the active role of the carbonyl group of KYN in driving a catalytic water molecule to adopt the correct pose over the imine bond for the hydrolysis. Indeed, the water molecule forms hydrogen bonds mainly with the carbonyl function of the substrate, with Lys263 being the only residue responsible for positioning the water molecule over the catalytic centre in the final step of the reaction. This finding may have important implications for the rational design of new hKAT II competitive inhibitors that may incorporate a water molecule in the structrure (*225*).

KATs structure – based drug design

From the point of view of drug development, the existence in the human brain of at least four KYNA-synthesizing enzymes, combined with the necessity of fine–tune KYNA levels to avoid the potentially harmful effects caused by a drastic deficiency of this neuroprotective metabolite in the CNS, requires the design of isozymes–specific inhibitors. This ambitious goal can be pursued only by defining the exquisite molecular traits governing substrates specificity in the different KATs isoforms. The different features of the ligand-biding pocket in KATs isoenzymes could be exploited for the rational design of highly specific hKAT II inhibitors. The structural informations about the steric requirement for KYN homing displayed by the active of hKAT I and hKAT II were exploited for the design of hKAT II specific inhibitors. Indeed, while in the human KAT I/KYN complex model the substrate anthranilic moiety perfectly fits the narrow and highly aromatic ligand binding site, some empty space is left in the structure of the human KAT II/KYN complex (*206*). Therefore the anthranilic moiety was proposed as hot spot for the chemical modification of substrate–like highly selective hKAT II inhibitors. In particular, increasing the steric hindrance of the anthranilic moiety would hamper binding to hKAT I, but would be tolerated by the wider hKAT II active site, as demonstrated by the synthesis of the first potent rat KAT II–specific inhibitor, (S)-4-ethylsulfonylbenzoylalanine (S-ESBA), that bears a bulky substituent on the anthranilc ring of L-KYN (*146*).

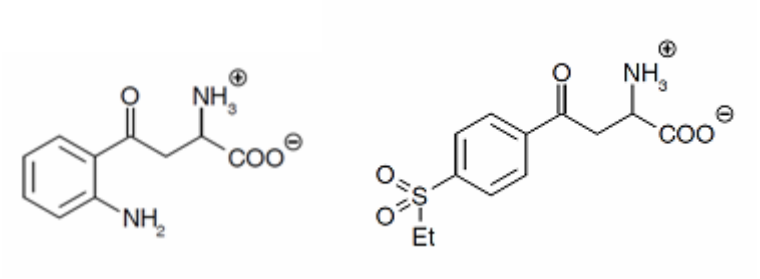

L-KYN S-ESBA

S-ESBA is an efficient and isoenzyme-selective inhibitor, as demonstrated by KYN transamination assay using either liver tissue homogenate or partially purified rat KAT II (IC_{50}= 6.1 μM)(*146*). Moreover, infusion of 5 mM ESBA in the rats hippocampus caused a decrease in extracellualr KYNA levels, which returned to normal values soon after the removal of the drug (*145*). However, the rat KAT II specific inhibitor S-ESBA is poorly active towards the human ortholog, as signalled by a 20-fold higher IC_{50} value (*146*). On the basis of the results of a molecular docking approach, two residues in KAT II amino acid sequence have been pointed out as the potential structural determinants responsible for the observed species-specificity of S-ESBA action (*226*). In particular, in the rat ortholog of KAT II, both the hydrophobic residues Leu 40 and pro 76 of human KAT II are substituted by polar serine residues. Since docking studies have proposed that these two residues may contribute to the different inhibitory activity exerted by ESBA, this hypothesis was further investigated by adopting a site-directed mutagenesis and a structural approach. A hKAT II double-

mutant harbouring at position 40 and 76 the serine residues characterizing the rat isoenzyme was generated and further assayed in the presence of S-ESBA to evaluate its inhibitor potency. Unexpectedly, S-ESBA potency was actually reduced rather than increased by the two amino acid substitutions that were engineered in the human KAT II active site. Therefore, factors other than the two non-conserved mutated amino acids need to be identified to explain the striking difference in S-ESBA inhibitory efficiencies toward rat and human KAT II.

REFERENCES

1. Smith, S. A., Carr, F. P., and Pogson, C. I. (1980) The metabolism of L-tryptophan by isolated rat liver cells. Quantification of the relative importance of, and the effect of nutritional status on, the individual pathways of tryptophan metabolism, *The Biochemical journal 192*, 673-686.
2. Beadle, G. W., Mitchell, H. K., and Nyc, J. F. (1947) Kynurenine as an Intermediate in the Formation of Nicotinic Acid from Tryptophane by Neurospora, *Proceedings of the National Academy of Sciences of the United States of America 33*, 155-158.
3. Reinhard, J. F., Jr. (2004) Pharmacological manipulation of brain kynurenine metabolism, *Annals of the New York Academy of Sciences 1035*, 335-349.
4. Hayaishi, O. (1976) Properties and function of indoleamine 2,3-dioxygenase, *J Biochem 79*, 13P-21P.
5. Hayaishi, O., Rothberg, S., Mehler, A. H., and Saito, Y. (1957) Studies on oxygenases; enzymatic formation of kynurenine from tryptophan, *The Journal of biological chemistry 229*, 889-896.
6. Dale, W. E., Dang, Y., and Brown, O. R. (2000) Tryptophan metabolism through the kynurenine pathway in rat brain and liver slices, *Free radical biology & medicine 29*, 191-198.
7. Comings, D. E., Muhleman, D., Dietz, G., Sherman, M., and Forest, G. L. (1995) Sequence of human tryptophan 2,3-dioxygenase (TDO2): presence of a glucocorticoid response-like element composed of a GTT repeat and an intronic CCCCT repeat, *Genomics 29*, 390-396.
8. Guillemin, G. J., Brew, B. J., Noonan, C. E., Takikawa, O., and Cullen, K. M. (2005) Indoleamine 2,3 dioxygenase and quinolinic acid immunoreactivity in Alzheimer's disease hippocampus, *Neuropathology and applied neurobiology 31*, 395-404.
9. Byrne, G. I., Lehmann, L. K., Kirschbaum, J. G., Borden, E. C., Lee, C. M., and Brown, R. R. (1986) Induction of tryptophan degradation in vitro and in vivo: a gamma-interferon-stimulated activity, *Journal of interferon research 6*, 389-396.
10. Mehler, A. H., and Knox, W. E. (1950) The conversion of tryptophan to kynurenine in liver. II. The enzymatic hydrolysis of formylkynurenine, *The Journal of biological chemistry 187*, 431-438.
11. Moroni, F. (1999) Tryptophan metabolism and brain function: focus on kynurenine and other indole metabolites, *European journal of pharmacology 375*, 87-100.
12. Guidetti, P., Eastman, C. L., and Schwarcz, R. (1995) Metabolism of [5-3H]kynurenine in the rat brain in vivo: evidence for the existence of a functional kynurenine pathway, *Journal of neurochemistry 65*, 2621-2632.

13. Schwarcz, R., and Pellicciari, R. (2002) Manipulation of brain kynurenines: glial targets, neuronal effects, and clinical opportunities, *The Journal of pharmacology and experimental therapeutics 303*, 1-10.
14. Stone, T. W. (1993) Neuropharmacology of quinolinic and kynurenic acids, *Pharmacological reviews 45*, 309-379.
15. Pellicciari, R., Natalini, B., Costantino, G., Mahmoud, M. R., Mattoli, L., Sadeghpour, B. M., Moroni, F., Chiarugi, A., and Carpenedo, R. (1994) Modulation of the kynurenine pathway in search for new neuroprotective agents. Synthesis and preliminary evaluation of (m-nitrobenzoyl)alanine, a potent inhibitor of kynurenine-3-hydroxylase, *Journal of medicinal chemistry 37*, 647-655.
16. Fukui, S., Schwarcz, R., Rapoport, S. I., Takada, Y., and Smith, Q. R. (1991) Blood-brain barrier transport of kynurenines: implications for brain synthesis and metabolism, *Journal of neurochemistry 56*, 2007-2017.
17. Nemeth, H., Toldi, J., and Vecsei, L. (2005) Role of kynurenines in the central and peripheral nervous systems, *Curr Neurovasc Res 2*, 249-260.
18. Heyes, M. P., Achim, C. L., Wiley, C. A., Major, E. O., Saito, K., and Markey, S. P. (1996) Human microglia convert l-tryptophan into the neurotoxin quinolinic acid, *The Biochemical journal 320 (Pt 2)*, 595-597.
19. Schwarcz, R., Ceresoli, G., and Guidetti, P. (1996) Kynurenine metabolism in the rat brain in vivo. Effect of acute excitotoxic insults, *Advances in experimental medicine and biology 398*, 211-219.
20. Guillemin, G. J., Kerr, S. J., Smythe, G. A., Smith, D. G., Kapoor, V., Armati, P. J., Croitoru, J., and Brew, B. J. (2001) Kynurenine pathway metabolism in human astrocytes: a paradox for neuronal protection, *Journal of neurochemistry 78*, 842-853.
21. Amori, L., Guidetti, P., Pellicciari, R., Kajii, Y., and Schwarcz, R. (2009) On the Relationship between the Two Branches of the Kynurenine Pathway in the Rat Brain in Vivo, *Journal of neurochemistry*.
22. Stone, T. W. (2001) Kynurenines in the CNS: from endogenous obscurity to therapeutic importance, *Prog Neurobiol 64*, 185-218.
23. Heyes, M. P., Saito, K., Milstien, S., and Schiff, S. J. (1995) Quinolinic acid in tumors, hemorrhage and bacterial infections of the central nervous system in children, *Journal of the neurological sciences 133*, 112-118.
24. Heyes, M. P., Saito, K., Lackner, A., Wiley, C. A., Achim, C. L., and Markey, S. P. (1998) Sources of the neurotoxin quinolinic acid in the brain of HIV-1-infected patients and retrovirus-infected macaques, *Faseb J 12*, 881-896.
25. Wonodi, I., and Schwarcz, R. Cortical kynurenine pathway metabolism: a novel target for cognitive enhancement in schizophrenia, *Schizophrenia bulletin 36*, 211-218.

26. Bender, D. A., and McCreanor, G. M. (1985) Kynurenine hydroxylase: a potential rate-limiting enzyme in tryptophan metabolism, *Biochemical Society transactions 13*, 441-443.
27. Okuno, E., and Kido, R. (1991) Kynureninase and kynurenine 3-hydroxylase in mammalian tissues, *Advances in experimental medicine and biology 294*, 167-176.
28. Okuno, E., Nakamura, M., and Schwarcz, R. (1991) Two kynurenine aminotransferases in human brain, *Brain research 542*, 307-312.
29. Schmidt, W., Guidetti, P., Okuno, E., and Schwarcz, R. (1993) Characterization of human brain kynurenine aminotransferases using [3H]kynurenine as a substrate, *Neuroscience 55*, 177-184.
30. Guidetti, P., Amori, L., Sapko, M. T., Okuno, E., and Schwarcz, R. (2007) Mitochondrial aspartate aminotransferase: a third kynurenate-producing enzyme in the mammalian brain, *Journal of neurochemistry 102*, 103-111.
31. Yu, P., Li, Z., Zhang, L., Tagle, D. A., and Cai, T. (2006) Characterization of kynurenine aminotransferase III, a novel member of a phylogenetically conserved KAT family, *Gene 365*, 111-118.
32. Han, Q., Robinson, H., Cai, T., Tagle, D. A., and Li, J. (2009) Biochemical and structural properties of mouse kynurenine aminotransferase III, *Mol Cell Biol 29*, 784-793.
33. Han, Q., Li, J., and Li, J. (2004) pH dependence, substrate specificity and inhibition of human kynurenine aminotransferase I, *Eur J Biochem 271*, 4804-4814.
34. Han, Q., Cai, T., Tagle, D. A., Robinson, H., and Li, J. (2008) Substrate specificity and structure of human aminoadipate aminotransferase/kynurenine aminotransferase II, *Biosci Rep 28*, 205-215.
35. Cooper, A. J., and Pinto, J. T. (2006) Cysteine S-conjugate beta-lyases, *Amino Acids 30*, 1-15.
36. Cooper, A. J., Pinto, J. T., Krasnikov, B. F., Niatsetskaya, Z. V., Han, Q., Li, J., Vauzour, D., and Spencer, J. P. (2008) Substrate specificity of human glutamine transaminase K as an aminotransferase and as a cysteine S-conjugate beta-lyase, *Archives of biochemistry and biophysics 474*, 72-81.
37. Guidetti, P., Okuno, E., and Schwarcz, R. (1997) Characterization of rat brain kynurenine aminotransferases I and II, *Journal of neuroscience research 50*, 457-465.
38. Lapin, I. P. (1978) Stimulant and convulsive effects of kynurenines injected into brain ventricles in mice, *J Neural Transm 42*, 37-43.
39. Stone, T. W., and Perkins, M. N. (1981) Quinolinic acid: a potent endogenous excitant at amino acid receptors in CNS, *European journal of pharmacology 72*, 411-412.
40. Schwarcz, R., and Kohler, C. (1983) Differential vulnerability of central neurons of the rat to quinolinic acid, *Neuroscience letters 38*, 85-90.

41. Schwarcz, R., Whetsell, W. O., Jr., and Mangano, R. M. (1983) Quinolinic acid: an endogenous metabolite that produces axon-sparing lesions in rat brain, *Science (New York, N.Y 219*, 316-318.
42. Stone, T. W., and Darlington, L. G. (2002) Endogenous kynurenines as targets for drug discovery and development, *Nat Rev Drug Discov 1*, 609-620.
43. Baran, H., Jellinger, K., and Deecke, L. (1999) Kynurenine metabolism in Alzheimer's disease, *J Neural Transm 106*, 165-181.
44. Ogawa, T., Matson, W. R., Beal, M. F., Myers, R. H., Bird, E. D., Milbury, P., and Saso, S. (1992) Kynurenine pathway abnormalities in Parkinson's disease, *Neurology 42*, 1702-1706.
45. Beal, M. F., Matson, W. R., Swartz, K. J., Gamache, P. H., and Bird, E. D. (1990) Kynurenine pathway measurements in Huntington's disease striatum: evidence for reduced formation of kynurenic acid, *Journal of neurochemistry 55*, 1327-1339.
46. Jauch, D., Urbanska, E. M., Guidetti, P., Bird, E. D., Vonsattel, J. P., Whetsell, W. O., Jr., and Schwarcz, R. (1995) Dysfunction of brain kynurenic acid metabolism in Huntington's disease: focus on kynurenine aminotransferases, *Journal of the neurological sciences 130*, 39-47.
47. Erhardt, S., Blennow, K., Nordin, C., Skogh, E., Lindstrom, L. H., and Engberg, G. (2001) Kynurenic acid levels are elevated in the cerebrospinal fluid of patients with schizophrenia, *Neuroscience letters 313*, 96-98.
48. Erhardt, S., Schwieler, L., and Engberg, G. (2003) Kynurenic acid and schizophrenia, *Advances in experimental medicine and biology 527*, 155-165.
49. Erhardt, S., Schwieler, L., Nilsson, L., Linderholm, K., and Engberg, G. (2007) The kynurenic acid hypothesis of schizophrenia, *Physiol Behav 92*, 203-209.
50. Nilsson, L. K., Linderholm, K. R., Engberg, G., Paulson, L., Blennow, K., Lindstrom, L. H., Nordin, C., Karanti, A., Persson, P., and Erhardt, S. (2005) Elevated levels of kynurenic acid in the cerebrospinal fluid of male patients with schizophrenia, *Schizophr Res 80*, 315-322.
51. Rejdak, K., Bartosik-Psujek, H., Dobosz, B., Kocki, T., Grieb, P., Giovannoni, G., Turski, W. A., and Stelmasiak, Z. (2002) Decreased level of kynurenic acid in cerebrospinal fluid of relapsing-onset multiple sclerosis patients, *Neuroscience letters 331*, 63-65.
52. Ilzecka, J., Kocki, T., Stelmasiak, Z., and Turski, W. A. (2003) Endogenous protectant kynurenic acid in amyotrophic lateral sclerosis, *Acta neurologica Scandinavica 107*, 412-418.
53. Carpenedo, R., Pittaluga, A., Cozzi, A., Attucci, S., Galli, A., Raiteri, M., and Moroni, F. (2001) Presynaptic kynurenate-sensitive receptors inhibit glutamate release, *Eur J Neurosci 13*, 2141-2147.

54. Wu, H. Q., Rassoulpour, A., and Schwarcz, R. (2007) Kynurenic acid leads, dopamine follows: a new case of volume transmission in the brain?, *J Neural Transm 114*, 33-41.
55. Dani, J. A., and Mayer, M. L. (1995) Structure and function of glutamate and nicotinic acetylcholine receptors, *Current opinion in neurobiology 5*, 310-317.
56. Daoudal, G., and Debanne, D. (2003) Long-term plasticity of intrinsic excitability: learning rules and mechanisms, *Learn Mem 10*, 456-465.
57. Whitlock, J. R., Heynen, A. J., Shuler, M. G., and Bear, M. F. (2006) Learning induces long-term potentiation in the hippocampus, *Science (New York, N.Y 313*, 1093-1097.
58. Ogura, A., Miyamoto, M., and Kudo, Y. (1988) Neuronal death in vitro: parallelism between survivability of hippocampal neurones and sustained elevation of cytosolic Ca2+ after exposure to glutamate receptor agonist, *Experimental brain research. Experimentelle Hirnforschung 73*, 447-458.
59. Vergun, O., Keelan, J., Khodorov, B. I., and Duchen, M. R. (1999) Glutamate-induced mitochondrial depolarisation and perturbation of calcium homeostasis in cultured rat hippocampal neurones, *J Physiol 519 Pt 2*, 451-466.
60. Mark, L. P., Prost, R. W., Ulmer, J. L., Smith, M. M., Daniels, D. L., Strottmann, J. M., Brown, W. D., and Hacein-Bey, L. (2001) Pictorial review of glutamate excitotoxicity: fundamental concepts for neuroimaging, *AJNR Am J Neuroradiol 22*, 1813-1824.
61. Danysz, W., and Parsons, C. G. (1998) Glycine and N-methyl-D-aspartate receptors: physiological significance and possible therapeutic applications, *Pharmacological reviews 50*, 597-664.
62. Yamazaki, M., Mori, H., Araki, K., Mori, K. J., and Mishina, M. (1992) Cloning, expression and modulation of a mouse NMDA receptor subunit, *FEBS letters 300*, 39-45.
63. Pereira, E. F., Hilmas, C., Santos, M. D., Alkondon, M., Maelicke, A., and Albuquerque, E. X. (2002) Unconventional ligands and modulators of nicotinic receptors, *J Neurobiol 53*, 479-500.
64. Clementi, F., Fornasari, D., and Gotti, C. (2000) Neuronal nicotinic receptors, important new players in brain function, *European journal of pharmacology 393*, 3-10.
65. Castro, N. G., and Albuquerque, E. X. (1995) alpha-Bungarotoxin-sensitive hippocampal nicotinic receptor channel has a high calcium permeability, *Biophysical journal 68*, 516-524.
66. Decker, E. R., and Dani, J. A. (1990) Calcium permeability of the nicotinic acetylcholine receptor: the single-channel calcium influx is significant, *J Neurosci 10*, 3413-3420.
67. Dani, J. A. (2001) Overview of nicotinic receptors and their roles in the central nervous system, *Biological psychiatry 49*, 166-174.
68. Albuquerque, E. X., Alkondon, M., Pereira, E. F., Castro, N. G., Schrattenholz, A., Barbosa, C. T., Bonfante-Cabarcas, R., Aracava, Y., Eisenberg, H. M., and Maelicke, A. (1997) Properties of neuronal nicotinic acetylcholine receptors: pharmacological characterization

and modulation of synaptic function, *The Journal of pharmacology and experimental therapeutics 280*, 1117-1136.

69. Levin, E. D., Bradley, A., Addy, N., and Sigurani, N. (2002) Hippocampal alpha 7 and alpha 4 beta 2 nicotinic receptors and working memory, *Neuroscience 109*, 757-765.
70. Broide, R. S., and Leslie, F. M. (1999) The alpha7 nicotinic acetylcholine receptor in neuronal plasticity, *Molecular neurobiology 20*, 1-16.
71. Nordberg, A. (1994) Human nicotinic receptors--their role in aging and dementia, *Neurochemistry international 25*, 93-97.
72. Perry, E. K., Morris, C. M., Court, J. A., Cheng, A., Fairbairn, A. F., McKeith, I. G., Irving, D., Brown, A., and Perry, R. H. (1995) Alteration in nicotine binding sites in Parkinson's disease, Lewy body dementia and Alzheimer's disease: possible index of early neuropathology, *Neuroscience 64*, 385-395.
73. Turski, W. A., Gramsbergen, J. B., Traitler, H., and Schwarcz, R. (1989) Rat brain slices produce and liberate kynurenic acid upon exposure to L-kynurenine, *Journal of neurochemistry 52*, 1629-1636.
74. Swartz, K. J., During, M. J., Freese, A., and Beal, M. F. (1990) Cerebral synthesis and release of kynurenic acid: an endogenous antagonist of excitatory amino acid receptors, *J Neurosci 10*, 2965-2973.
75. Moroni, F., Russi, P., Lombardi, G., Beni, M., and Carla, V. (1988) Presence of kynurenic acid in the mammalian brain, *Journal of neurochemistry 51*, 177-180.
76. Turski, W. A., and Schwarcz, R. (1988) On the disposition of intrahippocampally injected kynurenic acid in the rat, *Experimental brain research. Experimentelle Hirnforschung 71*, 563-567.
77. Turski, W. A., Nakamura, M., Todd, W. P., Carpenter, B. K., Whetsell, W. O., Jr., and Schwarcz, R. (1988) Identification and quantification of kynurenic acid in human brain tissue, *Brain research 454*, 164-169.
78. Moroni, F., Russi, P., Carla, V., and Lombardi, G. (1988) Kynurenic acid is present in the rat brain and its content increases during development and aging processes, *Neuroscience letters 94*, 145-150.
79. Kessler, M., Terramani, T., Lynch, G., and Baudry, M. (1989) A glycine site associated with N-methyl-D-aspartic acid receptors: characterization and identification of a new class of antagonists, *Journal of neurochemistry 52*, 1319-1328.
80. Hilmas, C., Pereira, E. F., Alkondon, M., Rassoulpour, A., Schwarcz, R., and Albuquerque, E. X. (2001) The brain metabolite kynurenic acid inhibits alpha7 nicotinic receptor activity and increases non-alpha7 nicotinic receptor expression: physiopathological implications, *J Neurosci 21*, 7463-7473.

81. Perkins, M. N., and Stone, T. W. (1982) An iontophoretic investigation of the actions of convulsant kynurenines and their interaction with the endogenous excitant quinolinic acid, *Brain research 247*, 184-187.
82. Kloog, Y., Lamdani-Itkin, H., and Sokolovsky, M. (1990) The glycine site of the N-methyl-D-aspartate receptor channel: differences between the binding of HA-966 and of 7-chlorokynurenic acid, *Journal of neurochemistry 54*, 1576-1583.
83. Mayer, M. L., Westbrook, G. L., and Vyklicky, L., Jr. (1988) Sites of antagonist action on N-methyl-D-aspartic acid receptors studied using fluctuation analysis and a rapid perfusion technique, *Journal of neurophysiology 60*, 645-663.
84. Birch, P. J., Grossman, C. J., and Hayes, A. G. (1988) Kynurenate and FG9041 have both competitive and non-competitive antagonist actions at excitatory amino acid receptors, *European journal of pharmacology 151*, 313-315.
85. Foster, A. C., Vezzani, A., French, E. D., and Schwarcz, R. (1984) Kynurenic acid blocks neurotoxicity and seizures induced in rats by the related brain metabolite quinolinic acid, *Neuroscience letters 48*, 273-278.
86. Chess, A. C., and Bucci, D. J. (2006) Increased concentration of cerebral kynurenic acid alters stimulus processing and conditioned responding, *Behavioural brain research 170*, 326-332.
87. Shepard, P. D., Joy, B., Clerkin, L., and Schwarcz, R. (2003) Micromolar brain levels of kynurenic acid are associated with a disruption of auditory sensory gating in the rat, *Neuropsychopharmacology 28*, 1454-1462.
88. Stone, T. W. (2007) Kynurenic acid blocks nicotinic synaptic transmission to hippocampal interneurons in young rats, *Eur J Neurosci 25*, 2656-2665.
89. Mansvelder, H. D., and McGehee, D. S. (2000) Long-term potentiation of excitatory inputs to brain reward areas by nicotine, *Neuron 27*, 349-357.
90. Zoli, M., Picciotto, M. R., Ferrari, R., Cocchi, D., and Changeux, J. P. (1999) Increased neurodegeneration during ageing in mice lacking high-affinity nicotine receptors, *The EMBO journal 18*, 1235-1244.
91. Kihara, T., Shimohama, S., Sawada, H., Honda, K., Nakamizo, T., Shibasaki, H., Kume, T., and Akaike, A. (2001) alpha 7 nicotinic receptor transduces signals to phosphatidylinositol 3-kinase to block A beta-amyloid-induced neurotoxicity, *The Journal of biological chemistry 276*, 13541-13546.
92. D'Angelo, E., Rossi, P., and Garthwaite, J. (1990) Dual-component NMDA receptor currents at a single central synapse, *Nature 346*, 467-470.
93. Singh, L., Oles, R. J., and Tricklebank, M. D. (1990) Modulation of seizure susceptibility in the mouse by the strychnine-insensitive glycine recognition site of the NMDA receptor/ion channel complex, *British journal of pharmacology 99*, 285-288.

94. Bergeron, R., Meyer, T. M., Coyle, J. T., and Greene, R. W. (1998) Modulation of N-methyl-D-aspartate receptor function by glycine transport, *Proceedings of the National Academy of Sciences of the United States of America 95*, 15730-15734.
95. Erhardt, S., Schwieler, L., Emanuelsson, C., and Geyer, M. (2004) Endogenous kynurenic acid disrupts prepulse inhibition, *Biological psychiatry 56*, 255-260.
96. Kiss, C., Ceresoli-Borroni, G., Guidetti, P., Zielke, C. L., Zielke, H. R., and Schwarcz, R. (2003) Kynurenate production by cultured human astrocytes, *J Neural Transm 110*, 1-14.
97. Roberts, R. C., McCarthy, K. E., Du, F., Ottersen, O. P., Okuno, E., and Schwarcz, R. (1995) 3-Hydroxyanthranilic acid oxygenase-containing astrocytic processes surround glutamate-containing axon terminals in the rat striatum, *J Neurosci 15*, 1150-1161.
98. Wang, J., Simonavicius, N., Wu, X., Swaminath, G., Reagan, J., Tian, H., and Ling, L. (2006) Kynurenic acid as a ligand for orphan G protein-coupled receptor GPR35, *The Journal of biological chemistry 281*, 22021-22028.
99. Kotani, M., Detheux, M., Vandenbogaerde, A., Communi, D., Vanderwinden, J. M., Le Poul, E., Brezillon, S., Tyldesley, R., Suarez-Huerta, N., Vandeput, F., Blanpain, C., Schiffmann, S. N., Vassart, G., and Parmentier, M. (2001) The metastasis suppressor gene KiSS-1 encodes kisspeptins, the natural ligands of the orphan G protein-coupled receptor GPR54, *The Journal of biological chemistry 276*, 34631-34636.
100. Lin, S. H., and Civelli, O. (2004) Orphan G protein-coupled receptors: targets for new therapeutic interventions, *Annals of medicine 36*, 204-214.
101. Mellor, A. L., and Munn, D. H. (2004) IDO expression by dendritic cells: tolerance and tryptophan catabolism, *Nature reviews 4*, 762-774.
102. Taylor, M. W., and Feng, G. S. (1991) Relationship between interferon-gamma, indoleamine 2,3-dioxygenase, and tryptophan catabolism, *Faseb J 5*, 2516-2522.
103. Ito, S., Komatsu, K., Tsukamoto, K., and Sved, A. F. (2000) Excitatory amino acids in the rostral ventrolateral medulla support blood pressure in spontaneously hypertensive rats, *Hypertension 35*, 413-417.
104. Kapoor, V., Kapoor, R., and Chalmers, J. (1994) Kynurenic acid, an endogenous glutamate antagonist, in SHR and WKY rats: possible role in central blood pressure regulation, *Clinical and experimental pharmacology & physiology 21*, 891-896.
105. Kiely, J. M., and Gordon, F. J. (1994) Role of rostral ventrolateral medulla in centrally mediated pressor responses, *The American journal of physiology 267*, H1549-1556.
106. Kapoor, V., Thuruthyil, S. J., and Human, B. (1998) Reduced kynurenine aminotransferase-I activity in SHR rats may be due to lack of KAT-Ib activity, *Neuroreport 9*, 1431-1434.
107. Mizutani, K., Sugimoto, K., Okuda, T., Katsuya, T., Miyata, T., Tanabe, T., Higaki, J., Ogihara, T., Yamori, Y., Tsujita, Y., Tago, N., and Iwai, N. (2002) Kynureninase is a novel

candidate gene for hypertension in spontaneously hypertensive rats, *Hypertens Res 25*, 135-140.

108. Smith, A. J., Stone, T. W., and Smith, R. A. (2007) Neurotoxicity of tryptophan metabolites, *Biochemical Society transactions 35*, 1287-1289.
109. Tavares, R. G., Schmidt, A. P., Abud, J., Tasca, C. I., and Souza, D. O. (2005) In vivo quinolinic acid increases synaptosomal glutamate release in rats: reversal by guanosine, *Neurochemical research 30*, 439-444.
110. Braidy, N., Grant, R., Adams, S., Brew, B. J., and Guillemin, G. J. (2009) Mechanism for quinolinic acid cytotoxicity in human astrocytes and neurons, *Neurotoxicity research 16*, 77-86.
111. Heyes, M. P., Swartz, K. J., Markey, S. P., and Beal, M. F. (1991) Regional brain and cerebrospinal fluid quinolinic acid concentrations in Huntington's disease, *Neuroscience letters 122*, 265-269.
112. Moroni, F., Russi, P., Gallo-Mezo, M. A., Moneti, G., and Pellicciari, R. (1991) Modulation of quinolinic and kynurenic acid content in the rat brain: effects of endotoxins and nicotinylalanine, *Journal of neurochemistry 57*, 1630-1635.
113. Saito, K., Markey, S. P., and Heyes, M. P. (1992) Effects of immune activation on quinolinic acid and neuroactive kynurenines in the mouse, *Neuroscience 51*, 25-39.
114. Rios, C., and Santamaria, A. (1991) Quinolinic acid is a potent lipid peroxidant in rat brain homogenates, *Neurochemical research 16*, 1139-1143.
115. Behan, W. M., McDonald, M., Darlington, L. G., and Stone, T. W. (1999) Oxidative stress as a mechanism for quinolinic acid-induced hippocampal damage: protection by melatonin and deprenyl, *British journal of pharmacology 128*, 1754-1760.
116. Eastman, C. L., and Guilarte, T. R. (1989) Cytotoxicity of 3-hydroxykynurenine in a neuronal hybrid cell line, *Brain research 495*, 225-231.
117. Jhamandas, K., Boegman, R. J., Beninger, R. J., and Bialik, M. (1990) Quinolinate-induced cortical cholinergic damage: modulation by tryptophan metabolites, *Brain research 529*, 185-191.
118. Goldstein, L. E., Leopold, M. C., Huang, X., Atwood, C. S., Saunders, A. J., Hartshorn, M., Lim, J. T., Faget, K. Y., Muffat, J. A., Scarpa, R. C., Chylack, L. T., Jr., Bowden, E. F., Tanzi, R. E., and Bush, A. I. (2000) 3-Hydroxykynurenine and 3-hydroxyanthranilic acid generate hydrogen peroxide and promote alpha-crystallin cross-linking by metal ion reduction, *Biochemistry 39*, 7266-7275.
119. Vamos, E., Pardutz, A., Klivenyi, P., Toldi, J., and Vecsei, L. (2009) The role of kynurenines in disorders of the central nervous system: possibilities for neuroprotection, *Journal of the neurological sciences 283*, 21-27.

120. Coyle, J. T. (2006) Glial metabolites of tryptophan and excitotoxicity: coming unglued, *Exp Neurol 197*, 4-7.
121. Gigler, G., Szenasi, G., Simo, A., Levay, G., Harsing, L. G., Jr., Sas, K., Vecsei, L., and Toldi, J. (2007) Neuroprotective effect of L-kynurenine sulfate administered before focal cerebral ischemia in mice and global cerebral ischemia in gerbils, *European journal of pharmacology 564*, 116-122.
122. Scharfman, H. E., Hodgkins, P. S., Lee, S. C., and Schwarcz, R. (1999) Quantitative differences in the effects of de novo produced and exogenous kynurenic acid in rat brain slices, *Neuroscience letters 274*, 111-114.
123. Cozzi, A., Carpenedo, R., and Moroni, F. (1999) Kynurenine hydroxylase inhibitors reduce ischemic brain damage: studies with (m-nitrobenzoyl)-alanine (mNBA) and 3,4-dimethoxy-[-N-4-(nitrophenyl)thiazol-2yl]-benzenesulfonamide (Ro 61-8048) in models of focal or global brain ischemia, *J Cereb Blood Flow Metab 19*, 771-777.
124. Zmarowski, A., Wu, H. Q., Brooks, J. M., Potter, M. C., Pellicciari, R., Schwarcz, R., and Bruno, J. P. (2009) Astrocyte-derived kynurenic acid modulates basal and evoked cortical acetylcholine release, *Eur J Neurosci 29*, 529-538.
125. Wu, H. Q., Pereira, E. F., Bruno, J. P., Pellicciari, R., Albuquerque, E. X., and Schwarcz, R. The astrocyte-derived alpha7 nicotinic receptor antagonist kynurenic acid controls extracellular glutamate levels in the prefrontal cortex, *J Mol Neurosci 40*, 204-210.
126. Rossi, F., Schwarcz, R., and Rizzi, M. (2008) Curiosity to kill the KAT (kynurenine aminotransferase): structural insights into brain kynurenic acid synthesis, *Curr Opin Struct Biol 18*, 748-755.
127. Baran, H., Cairns, N., Lubec, B., and Lubec, G. (1996) Increased kynurenic acid levels and decreased brain kynurenine aminotransferase I in patients with Down syndrome, *Life Sci 58*, 1891-1899.
128. Yamamoto, H., Shindo, I., Egawa, B., and Horiguchi, K. (1994) Kynurenic acid is decreased in cerebrospinal fluid of patients with infantile spasms, *Pediatr Neurol 10*, 9-12.
129. Medana, I. M., Day, N. P., Salahifar-Sabet, H., Stocker, R., Smythe, G., Bwanaisa, L., Njobvu, A., Kayira, K., Turner, G. D., Taylor, T. E., and Hunt, N. H. (2003) Metabolites of the kynurenine pathway of tryptophan metabolism in the cerebrospinal fluid of Malawian children with malaria, *J Infect Dis 188*, 844-849.
130. Heyes, M. P., Brew, B. J., Saito, K., Quearry, B. J., Price, R. W., Lee, K., Bhalla, R. B., Der, M., and Markey, S. P. (1992) Inter-relationships between quinolinic acid, neuroactive kynurenines, neopterin and beta 2-microglobulin in cerebrospinal fluid and serum of HIV-1-infected patients, *J Neuroimmunol 40*, 71-80.
131. Heyes, M. P., Saito, K., Crowley, J. S., Davis, L. E., Demitrack, M. A., Der, M., Dilling, L. A., Elia, J., Kruesi, M. J., Lackner, A., and et al. (1992) Quinolinic acid and kynurenine pathway

metabolism in inflammatory and non-inflammatory neurological disease, *Brain 115 (Pt 5)*, 1249-1273.

132. Linderholm, K. R., Skogh, E., Olsson, S. K., Dahl, M. L., Holtze, M., Engberg, G., Samuelsson, M., and Erhardt, S. Increased Levels of Kynurenine and Kynurenic Acid in the CSF of Patients With Schizophrenia, *Schizophrenia bulletin*.
133. Chess, A. C., Simoni, M. K., Alling, T. E., and Bucci, D. J. (2007) Elevations of endogenous kynurenic acid produce spatial working memory deficits, *Schizophrenia bulletin 33*, 797-804.
134. Chess, A. C., Landers, A. M., and Bucci, D. J. (2009) L-kynurenine treatment alters contextual fear conditioning and context discrimination but not cue-specific fear conditioning, *Behavioural brain research 201*, 325-331.
135. Schwarcz, R., Rassoulpour, A., Wu, H. Q., Medoff, D., Tamminga, C. A., and Roberts, R. C. (2001) Increased cortical kynurenate content in schizophrenia, *Biological psychiatry 50*, 521-530.
136. Zelante, T., Fallarino, F., Bistoni, F., Puccetti, P., and Romani, L. (2009) Indoleamine 2,3-dioxygenase in infection: the paradox of an evasive strategy that benefits the host, *Microbes and infection / Institut Pasteur 11*, 133-141.
137. Aoyama, N., Takahashi, N., Saito, S., Maeno, N., Ishihara, R., Ji, X., Miura, H., Ikeda, M., Suzuki, T., Kitajima, T., Yamanouchi, Y., Kinoshita, Y., Yoshida, K., Iwata, N., Inada, T., and Ozaki, N. (2006) Association study between kynurenine 3-monooxygenase gene and schizophrenia in the Japanese population, *Genes, brain, and behavior 5*, 364-368.
138. Court, J., Spurden, D., Lloyd, S., McKeith, I., Ballard, C., Cairns, N., Kerwin, R., Perry, R., and Perry, E. (1999) Neuronal nicotinic receptors in dementia with Lewy bodies and schizophrenia: alpha-bungarotoxin and nicotine binding in the thalamus, *Journal of neurochemistry 73*, 1590-1597.
139. Alkondon, M., Pereira, E. F., Yu, P., Arruda, E. Z., Almeida, L. E., Guidetti, P., Fawcett, W. P., Sapko, M. T., Randall, W. R., Schwarcz, R., Tagle, D. A., and Albuquerque, E. X. (2004) Targeted deletion of the kynurenine aminotransferase ii gene reveals a critical role of endogenous kynurenic acid in the regulation of synaptic transmission via alpha7 nicotinic receptors in the hippocampus, *J Neurosci 24*, 4635-4648.
140. Salter, M., Hazelwood, R., Pogson, C. I., Iyer, R., and Madge, D. J. (1995) The effects of a novel and selective inhibitor of tryptophan 2,3-dioxygenase on tryptophan and serotonin metabolism in the rat, *Biochemical pharmacology 49*, 1435-1442.
141. Tan, P. H., and Bharath, A. K. (2009) Manipulation of indoleamine 2,3 dioxygenase; a novel therapeutic target for treatment of diseases, *Expert opinion on therapeutic targets 13*, 987-1012.

142. Han, Q., Cai, T., Tagle, D. A., and Li, J. Structure, expression, and function of kynurenine aminotransferases in human and rodent brains, *Cell Mol Life Sci 67*, 353-368.

143. Yu, P., Di Prospero, N. A., Sapko, M. T., Cai, T., Chen, A., Melendez-Ferro, M., Du, F., Whetsell, W. O., Jr., Guidetti, P., Schwarcz, R., and Tagle, D. A. (2004) Biochemical and phenotypic abnormalities in kynurenine aminotransferase II-deficient mice, *Mol Cell Biol 24*, 6919-6930.

144. Potter, M. C., Elmer, G. I., Bergeron, R., Albuquerque, E. X., Guidetti, P., Wu, H. Q., and Schwarcz, R. Reduction of endogenous kynurenic acid formation enhances extracellular glutamate, hippocampal plasticity, and cognitive behavior, *Neuropsychopharmacology 35*, 1734-1742.

145. Amori, L., Wu, H. Q., Marinozzi, M., Pellicciari, R., Guidetti, P., and Schwarcz, R. (2009) Specific inhibition of kynurenate synthesis enhances extracellular dopamine levels in the rodent striatum, *Neuroscience 159*, 196-203.

146. Pellicciari, R., Rizzo, R. C., Costantino, G., Marinozzi, M., Amori, L., Guidetti, P., Wu, H. Q., and Schwarcz, R. (2006) Modulators of the kynurenine pathway of tryptophan metabolism: synthesis and preliminary biological evaluation of (S)-4-(ethylsulfonyl)benzoylalanine, a potent and selective kynurenine aminotransferase II (KAT II) inhibitor, *ChemMedChem 1*, 528-531.

147. Schwarcz, R. (2004) The kynurenine pathway of tryptophan degradation as a drug target, *Curr Opin Pharmacol 4*, 12-17.

148. Stone, T. W., Mackay, G. M., Forrest, C. M., Clark, C. J., and Darlington, L. G. (2003) Tryptophan metabolites and brain disorders, *Clin Chem Lab Med 41*, 852-859.

149. Costantino, G. (2009) New promises for manipulation of kynurenine pathway in cancer and neurological diseases, *Expert opinion on therapeutic targets 13*, 247-258.

150. Erhardt, S., Olsson, S. K., and Engberg, G. (2009) Pharmacological manipulation of kynurenic Acid: potential in the treatment of psychiatric disorders, *CNS Drugs 23*, 91-101.

151. Nemeth, H., Toldi, J., and Vecsei, L. (2006) Kynurenines, Parkinson's disease and other neurodegenerative disorders: preclinical and clinical studies, *J Neural Transm Suppl*, 285-304.

152. Noguchi, T., Minatogawa, Y., Okuno, E., Nakatani, M., and Morimoto, M. (1975) Purification and characterization of kynurenine--2-oxoglutarate aminotransferase from the liver, brain and small intestine of rats, *The Biochemical journal 151*, 399-406.

153. Okuno, E., Minatogawa, Y., Nakamura, M., Kamoda, N., Nakanishi, J., Makino, M., and Kido, R. (1980) Crystallization and characterization of human liver kynurenine--glyoxylate aminotransferase. Identity with alanine--glyoxylate aminotransferase and serine--pyruvate aminotransferase, *The Biochemical journal 189*, 581-590.

154. Okuno, E., Schmidt, W., Parks, D. A., Nakamura, M., and Schwarcz, R. (1991) Measurement of rat brain kynurenine aminotransferase at physiological kynurenine concentrations, *Journal of neurochemistry 57*, 533-540.
155. Papadimitriou, J. M., and van Duijn, P. (1970) The ultrastructural localization of the isozymes of aspartate aminotransferase in murine tissues, *The Journal of cell biology 47*, 84-98.
156. Cechetto, J. D., Sadacharan, S. K., Berk, P. D., and Gupta, R. S. (2002) Immunogold localization of mitochondrial aspartate aminotransferase in mitochondria and on the cell surface in normal rat tissues, *Histology and histopathology 17*, 353-364.
157. Tanaka, M., Takeda, N., Tohyama, M., and Matsunaga, T. (1990) Immunocytochemical localization of mitochondrial and cytosolic aspartate aminotransferase isozymes in the vestibular end-organs of rats, *Eur Arch Otorhinolaryngol 247*, 119-121.
158. Goh, D. L., Patel, A., Thomas, G. H., Salomons, G. S., Schor, D. S., Jakobs, C., and Geraghty, M. T. (2002) Characterization of the human gene encoding alpha-aminoadipate aminotransferase (AADAT), *Molecular genetics and metabolism 76*, 172-180.
159. Mawal, M. R., Mukhopadhyay, A., and Deshmukh, D. R. (1991) Purification and properties of kynurenine aminotransferase from rat kidney, *The Biochemical journal 279 (Pt 2)*, 595-599.
160. Takeuchi, F., Otsuka, H., and Shibata, Y. (1983) Purification, characterization and identification of rat liver mitochondrial kynurenine aminotransferase with alpha-aminoadipate aminotransferase, *Biochimica et biophysica acta 743*, 323-330.
161. Nakatani, Y., Fujioka, M., and Higashino, K. (1970) Alpha-aminoadipate aminotransferase of rat liver mitochondria, *Biochimica et biophysica acta 198*, 219-228.
162. Higashino, K., Fujioka, M., and Yamamura, Y. (1971) The conversion of L-lysine to saccharopine and alpha-aminoadipate in mouse, *Archives of biochemistry and biophysics 142*, 606-614.
163. Tobes, M. C., and Mason, M. (1975) L-kynurenine aminotransferase and L-alpha-aminoadipate aminotransferase. I. Evidence for identity, *Biochemical and biophysical research communications 62*, 390-397.
164. Tobes, M. C., and Mason, M. (1977) Alpha-Aminoadipate aminotransferase and kynurenine aminotransferase. Purification, characterization, and further evidence for identity, *The Journal of biological chemistry 252*, 4591-4599.
165. Sapko, M. T., Guidetti, P., Yu, P., Tagle, D. A., Pellicciari, R., and Schwarcz, R. (2006) Endogenous kynurenate controls the vulnerability of striatal neurons to quinolinate: Implications for Huntington's disease, *Exp Neurol 197*, 31-40.

166. Miyazaki, T., Miyazaki, J., Yamane, H., and Nishiyama, M. (2004) alpha-Aminoadipate aminotransferase from an extremely thermophilic bacterium, Thermus thermophilus, *Microbiology (Reading, England) 150*, 2327-2334.
167. Xu, H., Andi, B., Qian, J., West, A. H., and Cook, P. F. (2006) The alpha-aminoadipate pathway for lysine biosynthesis in fungi, *Cell biochemistry and biophysics 46*, 43-64.
168. Zabriskie, T. M., and Jackson, M. D. (2000) Lysine biosynthesis and metabolism in fungi, *Natural product reports 17*, 85-97.
169. Matsuda, M., and Ogur, M. (1969) Separation and specificity of the yeast glutamate-alpha-ketoadipate transaminase, *The Journal of biological chemistry 244*, 3352-3358.
170. Chang, Y. E. (1978) Lysine metabolism in the rat brain: the pipecolic acid-forming pathway, *Journal of neurochemistry 30*, 347-354.
171. Chang, Y. F. (1982) Lysine metabolism in the human and the monkey: demonstration of pipecolic acid formation in the brain and other organs, *Neurochemical research 7*, 577-588.
172. Brown, D. R., and Kretzschmar, H. A. (1998) The glio-toxic mechanism of alpha-aminoadipic acid on cultured astrocytes, *Journal of neurocytology 27*, 109-118.
173. Nishimura, R. N., Santos, D., Fu, S. T., and Dwyer, B. E. (2000) Induction of cell death by L-alpha-aminoadipic acid exposure in cultured rat astrocytes: relationship to protein synthesis, *Neurotoxicology 21*, 313-320.
174. Takada, M., and Hattori, T. (1986) Fine structural changes in the rat brain after local injections of gliotoxin, alpha-aminoadipic acid, *Histology and histopathology 1*, 271-275.
175. Candito, M., Richelme, C., Parvy, P., Dageville, C., Appert, A., Bekri, S., Rabier, D., Chambon, P., Mariani, R., and Kamoun, P. (1995) Abnormal alpha-aminoadipic acid excretion in a newborn with a defect in platelet aggregation and antenatal cerebral haemorrhage, *Journal of inherited metabolic disease 18*, 56-60.
176. Casey, R. E., Zaleski, W. A., Philp, M., Mendelson, I. S., and MacKenzie, S. L. (1978) Biochemical and clinical studies of a new case of alpha-aminoadipic aciduria, *Journal of inherited metabolic disease 1*, 129-135.
177. Duran, M., Beemer, F. A., Wadman, S. K., Wendel, U., and Janssen, B. (1984) A patient with alpha-ketoadipic and alpha-aminoadipic aciduria, *Journal of inherited metabolic disease 7*, 61.
178. Fischer, M. H., and Brown, R. R. (1980) Tryptophan and lysine metabolism in alpha-aminoadipic aciduria, *American journal of medical genetics 5*, 35-41.
179. Gray, R. G., O'Neill, E. M., and Pollitt, R. J. (1980) Alpha-aminoadipic aciduria: chemical and enzymatic studies, *Journal of inherited metabolic disease 2*, 89-92.
180. Jakobs, C., and de Grauw, A. J. (1992) A fatal case of 2-keto-, 2-hydroxy- and 2-aminoadipic aciduria: relation of organic aciduria to phenotype?, *Journal of inherited metabolic disease 15*, 279-280.

181. Lee, J. S., Yoon, H. R., and Coe, C. J. (2001) A Korean girl with alpha-aminoadipic and alpha-ketoadipic aciduria accompanied with elevation of 2-hydroxyglutarate and glutarate, *Journal of inherited metabolic disease 24*, 509-510.
182. Manders, A. J., von Oostrom, C. G., Trijbels, J. M., Rutten, F. J., and Kleijer, W. J. (1981) alpha-Aminoadipic aciduria and persistence of fetal haemoglobin in an oligophrenic child, *European journal of pediatrics 136*, 51-55.
183. Sela, B. A., Massos, T., Fogel, D., and Zlotnik, J. (1999) [Alpha-amino adipic aciduria: a rare psychomotor syndrome], *Harefuah 137*, 451-453, 511.
184. Vianey-Liaud, C., Divry, P., Cotte, J., and Teyssier, G. (1985) alpha-Aminoadipic and alpha-ketoadipic aciduria: detection of a new case by a screening program using two-dimensional thin layer chromatography of amino acids, *Journal of inherited metabolic disease 8 Suppl 2*, 133-134.
185. Baran, H., Okuno, E., Kido, R., and Schwarcz, R. (1994) Purification and characterization of kynurenine aminotransferase I from human brain, *Journal of neurochemistry 62*, 730-738.
186. Dekant, W., Vamvakas, S., and Anders, M. W. (1994) Formation and fate of nephrotoxic and cytotoxic glutathione S-conjugates: cysteine conjugate beta-lyase pathway, *Advances in pharmacology (San Diego, Calif 27*, 115-162.
187. McGoldrick, T. A., Lock, E. A., Rodilla, V., and Hawksworth, G. M. (2003) Renal cysteine conjugate C-S lyase mediated toxicity of halogenated alkenes in primary cultures of human and rat proximal tubular cells, *Archives of toxicology 77*, 365-370.
188. Cooper, A. J. (2004) The role of glutamine transaminase K (GTK) in sulfur and alpha-keto acid metabolism in the brain, and in the possible bioactivation of neurotoxicants, *Neurochemistry international 44*, 557-577.
189. Han, Q., Fang, J., and Li, J. (2001) Kynurenine aminotransferase and glutamine transaminase K of Escherichia coli: identity with aspartate aminotransferase, *The Biochemical journal 360*, 617-623.
190. Faff-Michalak, L., and Albrecht, J. (1991) Aspartate aminotransferase, malate dehydrogenase, and pyruvate carboxylase activities in rat cerebral synaptic and nonsynaptic mitochondria: effects of in vitro treatment with ammonia, hyperammonemia and hepatic encephalopathy, *Metabolic brain disease 6*, 187-197.
191. Moran, J., Alavez, S., Rivera-Gaxiola, M., Valencia, A., and Hurtado, S. (1999) Effect of NMDA antagonists on the activity of glutaminase and aspartate aminotransferase in the developing rat cerebellum, *Int J Dev Neurosci 17*, 57-65.
192. Moran, J., and Rivera-Gaxiola, M. (1992) Effect of potassium and N-methyl-D-aspartate on the aspartate aminotransferase activity in cultured cerebellar granule cells, *Journal of neuroscience research 33*, 239-247.

193. Westergaard, N., Drejer, J., Schousboe, A., and Sonnewald, U. (1996) Evaluation of the importance of transamination versus deamination in astrocytic metabolism of [U-13C]glutamate, *Glia 17*, 160-168.

194. Yudkoff, M., Daikhin, Y., Nissim, I., Horyn, O., Lazarow, A., Luhovyy, B., Wehrli, S., and Nissim, I. (2005) Response of brain amino acid metabolism to ketosis, *Neurochemistry international 47*, 119-128.

195. Hertz, L., Drejer, J., and Schousboe, A. (1988) Energy metabolism in glutamatergic neurons, GABAergic neurons and astrocytes in primary cultures, *Neurochemical research 13*, 605-610.

196. McKenna, M. C., Tildon, J. T., Stevenson, J. H., Boatright, R., and Huang, S. (1993) Regulation of energy metabolism in synaptic terminals and cultured rat brain astrocytes: differences revealed using aminooxyacetate, *Developmental neuroscience 15*, 320-329.

197. McKenna, M. C., Tildon, J. T., Stevenson, J. H., and Huang, X. (1996) New insights into the compartmentation of glutamate and glutamine in cultured rat brain astrocytes, *Developmental neuroscience 18*, 380-390.

198. Schousboe, A., Westergaard, N., Sonnewald, U., Petersen, S. B., Huang, R., Peng, L., and Hertz, L. (1993) Glutamate and glutamine metabolism and compartmentation in astrocytes, *Developmental neuroscience 15*, 359-366.

199. Sonnewald, U., Westergaard, N., and Schousboe, A. (1997) Glutamate transport and metabolism in astrocytes, *Glia 21*, 56-63.

200. Palaiologos, G., Hertz, L., and Schousboe, A. (1988) Evidence that aspartate aminotransferase activity and ketodicarboxylate carrier function are essential for biosynthesis of transmitter glutamate, *Journal of neurochemistry 51*, 317-320.

201. Palaiologos, G., Hertz, L., and Schousboe, A. (1989) Role of aspartate aminotransferase and mitochondrial dicarboxylate transport for release of endogenously and exogenously supplied neurotransmitter in glutamatergic neurons, *Neurochemical research 14*, 359-366.

202. McKenna, M. C., Stevenson, J. H., Huang, X., and Hopkins, I. B. (2000) Differential distribution of the enzymes glutamate dehydrogenase and aspartate aminotransferase in cortical synaptic mitochondria contributes to metabolic compartmentation in cortical synaptic terminals, *Neurochemistry international 37*, 229-241.

203. Cooper, A. J., Bruschi, S. A., Iriarte, A., and Martinez-Carrion, M. (2002) Mitochondrial aspartate aminotransferase catalyses cysteine S-conjugate beta-lyase reactions, *The Biochemical journal 368*, 253-261.

204. Rossi, F., Han, Q., Li, J., Li, J., and Rizzi, M. (2004) Crystal Structure of Human Kynurenine Aminotransferase I, *J. Biol. Chem. 279*, 50214-50220.

205. Han, Q., Robinson, H., and Li, J. (2008) Crystal structure of human kynurenine aminotransferase II, *The Journal of biological chemistry 283*, 3567-3573.

206. Rossi, F., Garavaglia, S., Montalbano, V., Walsh, M. A., and Rizzi, M. (2008) Crystal structure of human kynurenine aminotransferase II, a drug target for the treatment of schizophrenia, *The Journal of biological chemistry 283*, 3559-3566.
207. Han, Q., Gao, Y. G., Robinson, H., Ding, H., Wilson, S., and Li, J. (2005) Crystal structures of Aedes aegypti kynurenine aminotransferase, *The FEBS journal 272*, 2198-2206.
208. Wogulis, M., Chew, E. R., Donohoue, P. D., and Wilson, D. K. (2008) Identification of formyl kynurenine formamidase and kynurenine aminotransferase from Saccharomyces cerevisiae using crystallographic, bioinformatic and biochemical evidence, *Biochemistry 47*, 1608-1621.
209. Chon, H., Matsumura, H., Koga, Y., Takano, K., and Kanaya, S. (2005) Crystal structure of a human kynurenine aminotransferase II homologue from Pyrococcus horikoshii OT3 at 2.20 A resolution, *Proteins 61*, 685-688.
210. Rossi, F., Garavaglia, S., Giovenzana, G. B., Arca, B., Li, J., and Rizzi, M. (2006) Crystal structure of the Anopheles gambiae 3-hydroxykynurenine transaminase, *Proceedings of the National Academy of Sciences of the United States of America 103*, 5711-5716.
211. Jansonius, J. N. (1998) Structure, evolution and action of vitamin B6-dependent enzymes, *Curr Opin Struct Biol 8*, 759-769.
212. Alexander, F. W., Sandmeier, E., Mehta, P. K., and Christen, P. (1994) Evolutionary relationships among pyridoxal-5'-phosphate-dependent enzymes. Regio-specific alpha, beta and gamma families, *Eur J Biochem 219*, 953-960.
213. Jensen, R. A., and Gu, W. (1996) Evolutionary recruitment of biochemically specialized subdivisions of Family I within the protein superfamily of aminotransferases, *J Bacteriol 178*, 2161-2171.
214. Schneider, G., Kack, H., and Lindqvist, Y. (2000) The manifold of vitamin B6 dependent enzymes, *Structure 8*, R1-6.
215. Christen, P., and Mehta, P. K. (2001) From cofactor to enzymes. The molecular evolution of pyridoxal-5'-phosphate-dependent enzymes, *Chemical record (New York, N.Y 1*, 436-447.
216. Percudani, R., and Peracchi, A. (2003) A genomic overview of pyridoxal-phosphate-dependent enzymes, *EMBO Rep 4*, 850-854.
217. Zhang, X., Roe, S. M., Hou, Y., Bartlam, M., Rao, Z., Pearl, L. H., and Danpure, C. J. (2003) Crystal structure of alanine:glyoxylate aminotransferase and the relationship between genotype and enzymatic phenotype in primary hyperoxaluria type 1, *Journal of molecular biology 331*, 643-652.
218. Tomita, T., Miyagawa, T., Miyazaki, T., Fushinobu, S., Kuzuyama, T., and Nishiyama, M. (2008) Mechanism for multiple-substrates recognition of alpha-aminoadipate aminotransferase from Thermus thermophilus, *Proteins*.

219. Clausen, T., Huber, R., Laber, B., Pohlenz, H. D., and Messerschmidt, A. (1996) Crystal structure of the pyridoxal-5'-phosphate dependent cystathionine beta-lyase from Escherichia coli at 1.83 A, *Journal of molecular biology 262*, 202-224.

220. Han, Q., Robinson, H., Cai, T., Tagle, D. A., and Li, J. (2009) Structural insight into the inhibition of human kynurenine aminotransferase I/glutamine transaminase K, *Journal of medicinal chemistry 52*, 2786-2793.

221. McPhalen, C. A., Vincent, M. G., and Jansonius, J. N. (1992) X-ray structure refinement and comparison of three forms of mitochondrial aspartate aminotransferase, *Journal of molecular biology 225*, 495-517.

222. Goto, M., Omi, R., Miyahara, I., Hosono, A., Mizuguchi, H., Hayashi, H., Kagamiyama, H., and Hirotsu, K. (2004) Crystal structures of glutamine:phenylpyruvate aminotransferase from Thermus thermophilus HB8: induced fit and substrate recognition, *The Journal of biological chemistry 279*, 16518-16525.

223. Hirotsu, K., Goto, M., Okamoto, A., and Miyahara, I. (2005) Dual substrate recognition of aminotransferases, *Chemical record (New York, N.Y 5*, 160-172.

224. Okamoto, A., Nakai, Y., Hayashi, H., Hirotsu, K., and Kagamiyama, H. (1998) Crystal structures of Paracoccus denitrificans aromatic amino acid aminotransferase: a substrate recognition site constructed by rearrangement of hydrogen bond network, *Journal of molecular biology 280*, 443-461.

225. Bellocchi, D., Macchiarulo, A., Carotti, A., and Pellicciari, R. (2009) Quantum mechanics/molecular mechanics (QM/MM) modeling of the irreversible transamination of L-kynurenine to kynurenic acid: the round dance of kynurenine aminotransferase II, *Biochimica et biophysica acta 1794*, 1802-1812.

226. Pellicciari, R., Venturoni, F., Bellocchi, D., Carotti, A., Marinozzi, M., Macchiarulo, A., Amori, L., and Schwarcz, R. (2008) Sequence variants in kynurenine aminotransferase II (KAT II) orthologs determine different potencies of the inhibitor S-ESBA, *ChemMedChem 3*, 1199-1202.

CHAPTER 2

SPECTROSCOPIC CHARACTERIZATION OF HKAT II

Introduction and aim of the work

Aminotransferases contain pyridoxal-5'-phosphate (PLP) as coenzyme, which provides characteristic absorption spectra in the wavelength range of 300-500 nm. Free PLP and pyridoxamine phosphate (PMP) show absorption bands in the near ultraviolet, at 388 nm and 330 nm respectively. When covalently bound to the enzyme active site, the Schiff's base of cofactor with the catalytic Lys residue can exist in several different tautomeric forms, depending on their protonation equilibria. In aminotransferases the deprotonated species is in equilibrium with a protonated form that can be present as either the enolimine tautomer, that absorbs at about 330 or the ketoenamine tautomer, characterized by an unprotonated phenolic oxygen and a protonated imino group absorbing at 420 nm (Scheme 1, species 1a and 1b). Accordingly, aminotransferases absorb at a specific wavelength depending on the the predominant form of these species. Furthermore, the complete process of enzymatic transamination involves at least five kinetically distinguishable steps (see Scheme 3 in chapter 1). The different covalent intermediates formed during PLP-dependent catalysis exhibit characteristic UV-visible spectra, as shown in Scheme 1. The quinonoid intermediate formed upon α-proton removal can follow two pathways: protonation on the imine nitrogen to form the ketimine (transamination pathway) or elimination of the β-substituent to form the α-aminoacrylate Schiff's base (β-elimination pathway) that spontaneously hydrolyzes to pyruvate and ammonia. It is well assessed that transaminases, due to the chemistry of the catalyzed reaction, are prone, in the presence of substrates with good leaving groups, to carry out β-elimination as a side reaction (1-5). Since the tautomeric species of the enzyme-bound cofactor as well as certain PLP-derived reaction intermediates have distinctive UV-visible absorption maxima, their spectrophotometric detection provides a convenient means for monitoring the binding of substrates, substrate analogs and inhibitors, as well as the formation of catalytic intermediates (6-9). There is a multitude of examples in literature that capitalize the spectroscopic properties of the cofactor to study the catalytic mechanism and the substrate specificity of PLP-dependent enzymes.

Although hKAT II is considered a potential drug target for cognition enhancement, a detailed spectroscopic analysis regarding its native form and reaction intermediates has never been addresses so far. The analysis of spectral changes that accompany substrate interaction is essential not only for the understanding of the catalytic mechanism of this enzyme, but also for the investigation of the interaction mechanisms with inhibitors. Therefore, a detailed spectral analysis of the enzyme was carried out. The reactivity of hKAT II with its natural substrates α-aminoadipate

(AAD) and glutamine was investigated either in solution or in the crystalline state by spectrophotometry and spectrofluorimetry, and polarized absorption microspectrophotometry, respectively. We also report the spectroscopic characterization of the mutant hKAT II Tyr142Phe, expected, on the basis of structural considerations (10), to exhibit a decrease propensity for β-elimination, a side reaction common to transaminases (5).

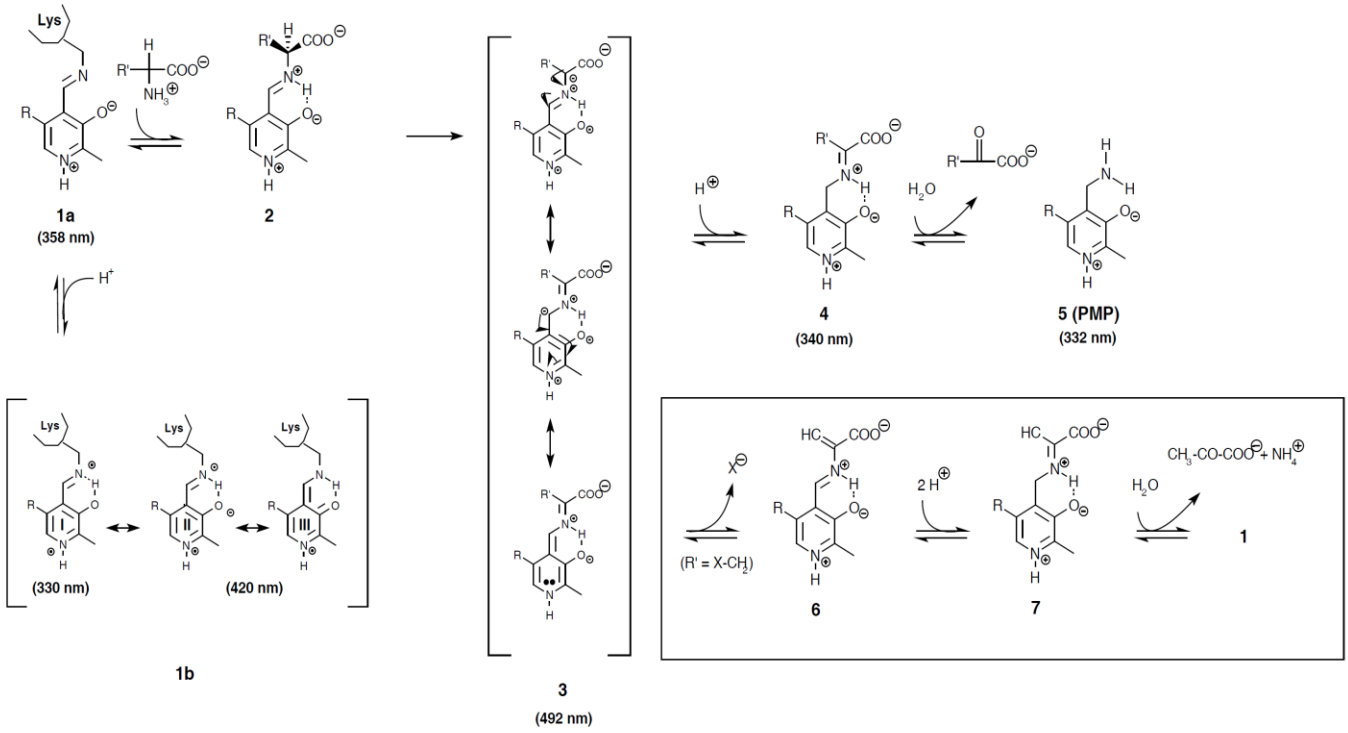

Scheme 1. General reaction mechanism of aminotransferases, including tautomeric and protonation equilibria. The absorption maxima for the catalytic intermediates are reported. The β-elimination side reaction is boxed. Adapted from (*3, 11, 12*).

Materials and methods

Chemicals. All chemicals were purchased from Sigma-Aldrich (St. Louis, MO) and were used as received. Experiments, unless otherwise specified, were carried out in 50 mM Hepes buffer, pH 7.5 at 25 °C.

Protein expression and purification. Human KAT II and the mutant Tyr142Phe were expressed and purified as previously described (10). The expression and purification procedures were kindly carried out by Proff. Menico Rizzi and Franca Rossi, Università Piemonte Orientale. The purified enzyme was fully saturated with PLP by addition of a ten fold molar excess cofactor, followed by overnight dialysis against a solution containing 20 mM Hepes, 50 mM NaCl, pH 8.0. The purified recombinant hKAT II was concentrated to 10 mg/ml using a Vivaspin 10,000 concentrator (Sartorius), and stored at -80°C in aliquots of 30 μL.

Determination of hKAT II extinction coefficient. The extinction coefficient of hKAT II was calculated by the amount of PLP released upon alkali denaturation by the method of Peterson (13). An absorption spectra of 25 μM hKAT II in water was collected and corrected for water contribution. Then, 10 N NaOH was added to a final concentration of 1 N and the solution was incubated at 25°C for 20 minutes. A final absorption spectra was collected, to verify the presence in the visible region of a single band centered at 388 nm, indicating that all PLP molecules were released from enzyme active sites. hKAT II extinction coefficient was calculated using the following formula:

$$\varepsilon_{358nm} = n * \varepsilon_{388nm\ PLP} * \frac{A_{358nm\ protein}}{A_{388nm\ PLP*f.d}}$$

where:

n is the stechiometric ratio between PLP and protein, equal to 1 for hKAT II

f.d. is the dilution factor after the addition of NaOH

A_{358} nm is the absorption at 358 nm of olo-hKAT II

A_{388} nm is the absorption at 388 nm of free PLP, $\varepsilon_{388\ nm}$ PLP = 6,600 $M^{-1} \cdot cm^{-1}$at basic pH.

Spectroscopic measurements in solution. Absorption spectra were collected in 50 mM Hepes, pH 7.5, using a Cary 400 Scan spectrophotometer (Varian Inc.). Cuvette holders were thermostated at 25°C. Spectra were corrected for buffer contribution.

Fluorescence emission spectra were collected in 50 mM Hepes, pH 7.5, 25°C, using a Spex Fluoromax-2 fluorimeter (Jobin-Yvon) by exciting at 298 nm the emission of tryptophan residues or by exciting at 330, 360 and 420 nm the emission of the cofactor. Excitation and emission slits were set at 1,5 nm (λ_{exc} = 298 nm), 3,5 nm (λ_{exc} = 330 nm and 360 nm) and 4 nm (λ_{exc} = 420 nm). Spectra were corrected for buffer contribution.

Single-crystal polarized absorption microspectrophotometric measurements. Crystals of recombinant hKAT II were kindly provided by Proff. Menico Rizzi and Franca Rossi. They were obtained as previously described (10) by mixing 1 μL of a protein solution at 16 mg/ml with an equal volume of a reservoir solution containing 22% (w/v) polyethylene glycol (PEG) 3350, 0.3 M potassium iodide, 0.1 M Tris HCl pH 8.0, and equilibrating the resulting drop against 500 μL of the reservoir solution, at 20°C. Needle-shaped yellow crystals grew in about three weeks. Crystals obtained under the same conditions were used to X-ray crystallographic structure determination (pdb code 2VGZ) (10). For polarized microspectrophotometric measurements single crystals were resuspended at least six times in a solution containing 26% (w/v) PEG 3350, 0.3 M potassium iodide, 0.1 M Tris HCl pH 8.0. Individual crystals were placed within a quartz observation cell,

located on the microscope stage. The cell upper window can be easily removed for mounting or handling the crystal. The replacement of the suspending medium for the different experiments was carried out by flowing solution through the cell. Channels through the cell allow the suspending medium to be quickly replace without causing appreciable crystal movements. The cell was mounted on the stage of a Zeiss MPM03 microspectrophotometer, equipped with a thermostatic apparatus. Polarized absorption spectra were recorded in the range between 250 and 600 nm, with the electric vector of linearly polarized light parallel to crystal edges that coincide with crystal extinction directions. Single crystal polarized absorption spectra were usually recorded on one flat face of the crystal. All the experiments were carried out at 25°C.

Results

hKAT II extinction coefficient

The accurate measurement of protein concentration by spectroscopic methods requires the knowledge of its extinction coefficient. As hKAT II extinction coefficient has never been reported so far in the literature, it was calculated following cofactor release by alkali denaturation. For a PLP-dependent enzyme the calculation of protein concentration using the extinction coefficient of the cofactor calculated by this method is the most accurate and allow reproducible results also with different enzymes preparation. hKAT II extinction coefficients at 280 and 360 nm were found to be 47,575 and 9,510 $M^{-1}\cdot cm^{-1}$, respectively. For the mutant Tyr142Phe KAT II the calculated values are 47,000 and 9400 $M^{-1}\cdot cm^{-1}$ at 280 and 360 nm, respectively.

Absorption spectroscopy

The absorption spectrum of native hKAT II (Figure 1A) exhibits two main bands at 280 nm and 360 nm, attributed to the aromatic residues and to the deprotonated internal aldimine of the cofactor with the catalytic Lys263, respectively. The observed ratio A_{280}/A_{360} for the enzyme fully saturated with PLP is 5. The absorption spectrum of hKAT II also shows a shoulder at about 420 nm, likely the ketoenamine tautomer of the protonated internal aldimine. KATII instability below pH 6 precludes the determination of the pKa of the cofactor (Fig. 1B).

In the presence of the natural and non-cromophoric substrate α-amino adipate (AAD) (14) the band at 360 nm rapidly disappears with the concomitant formation of a new species absorbing maximally at 325 nm, likely the pyridoxamine form of the cofactor (Figure 1C; Scheme 1, species 5). The shoulder at 420 nm corresponds to a species that does not react with AAD. Addition of 2 mM KG ($\varepsilon_{320\ nm}$ = 32 $M^{-1}\cdot cm^{-1}$) to the reaction mixture does not lead to appreciable changes in the spectrum of the cofactor, an indication that, at equilibrium, the most stable species is the PMP form of the enzyme, i.e. the rate of the first half reaction is significantly faster than the rate of the second half reaction.

Tyr142Phe KAT II exhibits an absorption spectrum almost superimposable with that of the wild type enzyme with an invariant A_{280}/A_{360} (Figure 1A). This finding can be attributed to a decrease in both the extinction coefficient at 280 nm due to the Y→F substitution and the extinction coefficient of the cofactor at 360 nm, which is 9,400 $M^{-1}\cdot cm^{-1}$. The addition of AAD and KG causes similar spectroscopic changes as those observed for the wt enzyme (data not shown).

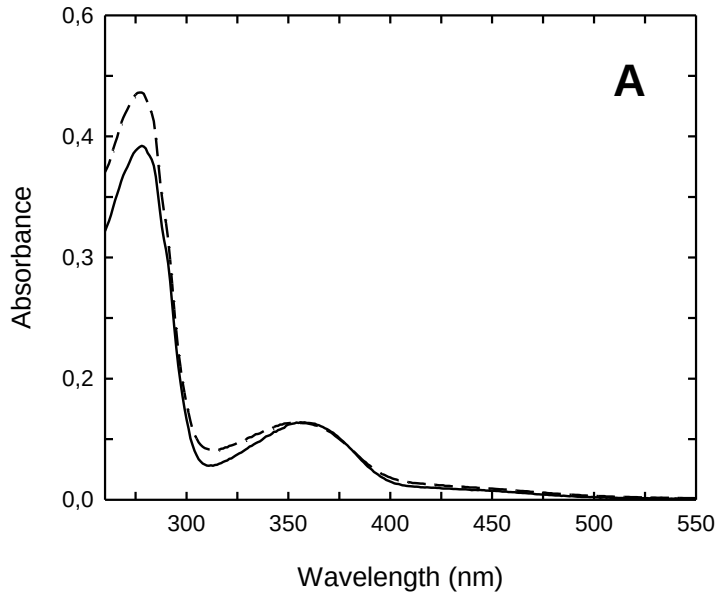
A
Absorbance
Wavelength (nm)
0,0
0,2
0,3
0,4
0,6
300
350
400
450
500
550

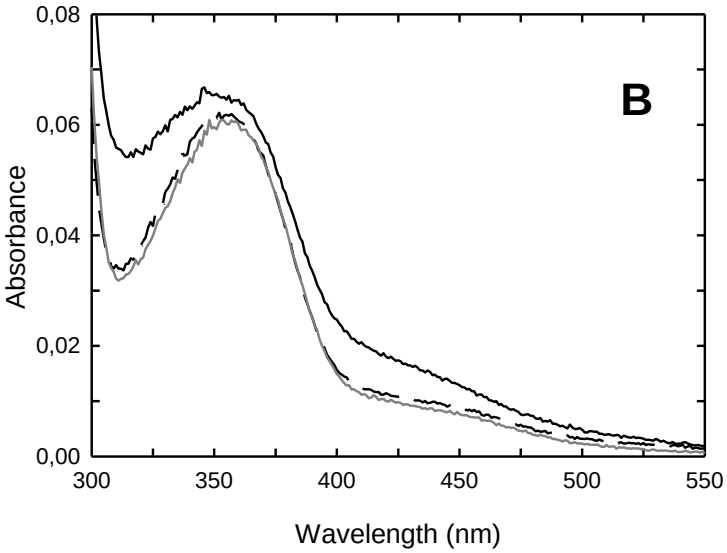
B
Absorbance
Wavelength (nm)
0,00
0,02
0,04
0,06
0,08
300
350
400
450
500
550

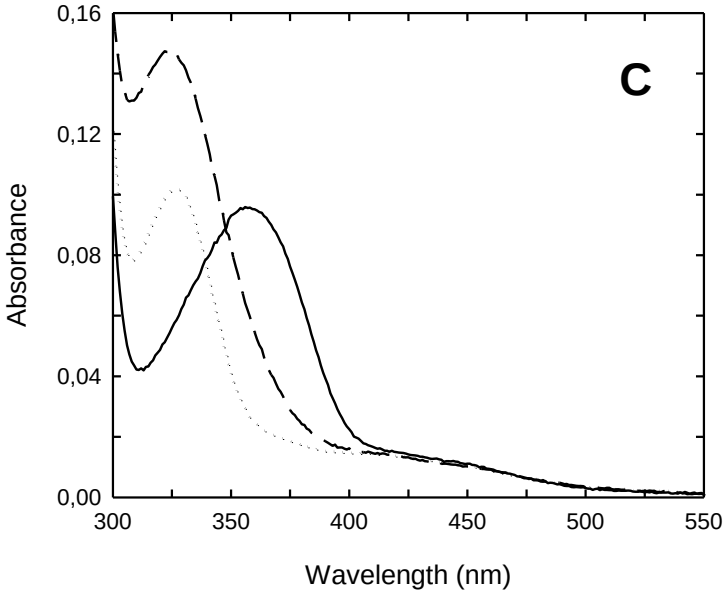
C
Absorbance
Wavelength (nm)
0,00
0,04
0,08
0,12
0,16
300
350
400
450
500
550

Figure 1. Absorption spectra of hKAT II and Tyr142Phe KAT II in the absence and in the presence of the natural substrate α-aminoadipate.

A Absorption spectra of 10 μM hKAT II (solid line) and Tyr142Phe KAT II (dashed line) in 50 mM Hepes, pH 7.5, at 25°C.

B Absorption spectra of 6 μM hKAT II in 200 mM potassium phosphate, pH 8.0 (solid grey line), pH 7.5 (dashed line) and pH 6.0 (solid black line), at 25°C.

C The reaction mixture contained 10 μM of hKAT II in the absence (solid line) and in the presence of 10 mM α-aminoadipate (dotted line) in 50 mM Hepes, pH 7.5, at 25°C. 2 mM KG was added to the reaction mixture (dashed line).

Fluorescence spectroscopy

hKAT II contains three tryptophan residues that can be selectively excited at 298 nm. The emission spectrum upon excitation at 298 nm shows a band centred at 345 nm, indicative of tryptophan residues exposed to the solvent. No energy transfer occurs between tryptophan and PLP, as indicated by the absence of peaks centred at either 420 or 500 nm (Figure 2A), in contrast with observations on fold type II enzymes, such as tryptophan synthase (15) and *O*-acetylserine sulfhydrylase (16). Direct excitation of PLP at the absorbance maximum, i.e. 360 nm, gives a structured emission with a maximum at 417 nm and a shoulder at 520 nm (Figure 2B). The emission at 520 is typical of the ketoenamine tautomer of the internal aldimine of the cofactor, whereas the emission at 415 nm is typical of the enolimine tautomer. In fact, direct excitation of the enolimine tautomer at 330 nm gives an emission with a main peak centred at about 415 nm, whereas direct excitation of the ketoenamine tautomer at 420 nm gives an emission centred at about 520 nm. The fluorescence emission spectra of Tyr142Phe KAT II is indistinguishable from that of wt KAT II and the addition of α-KG to both enzyme variants does not lead to any appreciable change in the emission properties (data not shown).

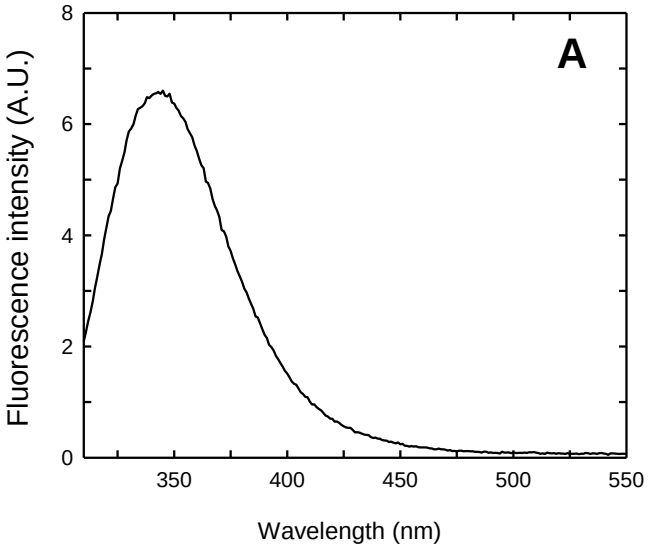

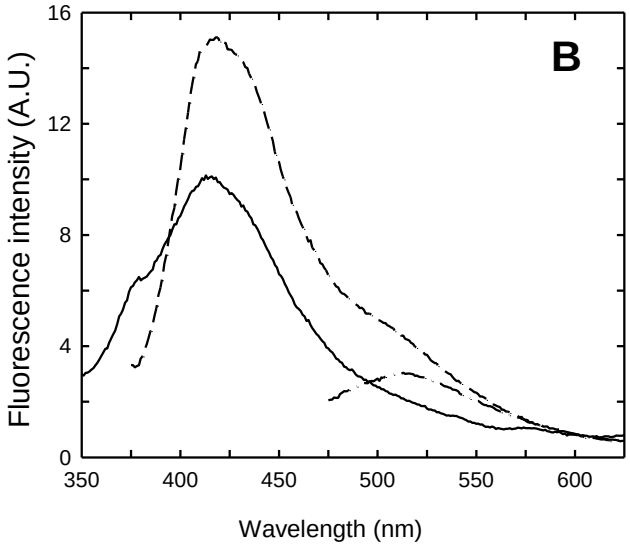

Figure 2. Spectrofluorimetric properties of KATII.

A Emission spectrum of a solution containing 26 μM KAT II in 50 mM Hepes, pH 7.5, at 25 °C, excited at 298 nm.

B Emission spectra of a solution containing 26 μM KAT II in 50 mM Hepes, pH 7.5, at 25 °C, excited at 330 nm (continuous line), 360 nm (dotted line) and 420 nm (dash-dotted line).

Microspectrophotometric study on single crystals of hKAT II

Polarized absorption spectra of hKAT II single crystal in 26% (w/v) PEG 3350, 0.3 M potassium iodide, 0.1 M Tris HCl pH 8.0 exhibits a mean peak centered at about 332 nm, a shoulder at 360 nm and a broad band at 400-500 nm (Figure 3, grey line). The positions of cofactor absorption maxima differ from those of the enzyme in solution (Figure 1A). In the latter case, absorption maxima is situated at 360 nm, corresponding to the deprotonated form of the internal pyridoxal 5'-phosphate-lysine aldimine. In the spectrum of hKAT II crystal, the 360 nm band is blue-shifted to about 332 nm. This shift might be caused by the formation of a covalent adduct between enzyme-bound cofactor and Tris buffer during the long crystallization period. Indeed, although Tris has been used as a standard buffer in biochemical research for over 40 years, its use with systems containing pyridoxal 5'-phosphate can result in complications from the non-enzymatic reaction of the primary amine function of Tris buffer that is capable of forming a Schiff's base with the aldehyde moiety of the coenzyme (*17, 18*). Indeed, when hKAT II crystals were resuspended in potassium phosphate a decrease of the band at 332 nm was observed, likely due to the partial removal of the Tris-pyridoxal 5'-phosphate Schiff's base from the enzyme active site (Figure 3, dotted line). Soaking of the crystals in a phosphate solution containing PLP led to a spectrum peaked at 360 nm, indicating the recovery of the deprotonated internal aldimine with the cofactor (Figure 3, dashed line). This species is the reactive one, as demonstrated by its fast disappearance after soaking of the crystal in a solution containing 20 mM glutamine, the natural substrate (Figure 3, black line). However, the spectral changes brought about by the addition of the glutamine do not correspond to those observed in solution (Figure 3, inset). The absence of the appearance of the pyridoxamine species absorbing at about 330 nm might be due to the diffusion of the PMP species out of the crystal. Further studies are required to fully understand these events and the nature of the band at about 400 nm. Nevertheless, polarized absorption spectra of hKAT II single crystal indicate that hKAT II is catalytically competent in the crystalline state.

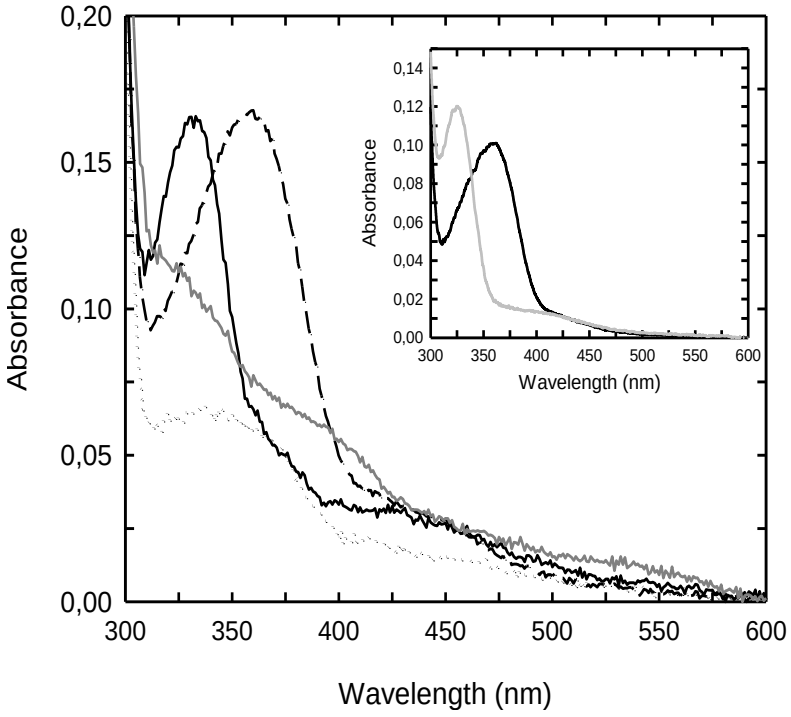

Figure 3. Polarized absorption spectra of hKAT II

Polarized absorption spectra of hKAT II crystals were recorded in solutions containing 26% (w/v) PEG 3350, 0.3 M potassium iodide, 0.1 M Tris HCl pH 8.0 (grey line), 26% (w/v) PEG 3350, 0.1 M potassium phosphate at pH 8.0 (dotted line), 26% (w/v) PEG 3350, 50 μM PLP, 0.1 M potassium phosphate pH 8.0 (dashed line), and 26% (w/v) PEG 3350, 20 mM glutamine, 0.1 M potassium phosphate pH 8.0 (black line).

Inset: Absorption spectra of a solution containing 10 μM hKAT II in the absence (black line) and in the presence of 20 mM glutamine (grey line) about 5 minutes after addition of the amino acid. Temperature was maintained constant at 25°C.

Discussion

The absorption spectrum of KAT II shows a band at 360 nm that, based on previous reports on aminotransferases (*19-21*), can be attributed to a Schiff base of the active site lysine (in KATII, K263) with a deprotonated imine nitrogen (Figure 1A; Scheme 1, species 1a). Interestingly, a previous work on bovine and rat KAT II reported absorption spectra with two main peaks at 320-330 and 400 nm (*22*). Furthermore, hKAT I shows a completely different absorption spectrum with two bands attributable to the cofactor: a band centered at 335 nm and a band centered at 422 nm, probably indicative of a mixture of the PLP and PMP forms of the enzyme (*23*), with PLP protonated at the imine nitrogen. PLP is a probe of the active site environment and thus the distribution of its tautomers is an indication of the active site polarity and amino acidic composition. The deprotonated form of the internal aldimine of PLP is quite typical of aminotransferases, as in aspartate aminotransferase (AAT) (*24*). It is well assessed that the deprotonated form of PLP in

transaminases is stabilized by a hydrogen bond with the hydroxyl group of a tyrosine that lowers the pKa of the imine nitrogen by two orders of magnitude (*24-26*). Based on crystallographic studies, a conserved tyrosine residue in hKAT II, Y233, is suggested to play this stabilizing role *(10)*. Curiously, a structurally corresponding residue, i.e. Y216, is also present in hKAT I, although the predominant form of the cofactor at pH 7.5 is the protonated ketimine. In aminotransferases the deprotonated species is in equilibrium with a protonated form that can be present as either the enolimine tautomer, absorbing at about 330 or the ketoenamine tautomer that absorbs at 420 nm (Scheme 1, species 1a and 1b). The pK_a for the equilibrium is 6.3 for glutamate aminotransferase GAT (*20*). The pK_a for the equilibrium of protonation of the internal aldimine of hKAT II could not be determined due to the instability of the enzyme below pH 6 and is estimated to be lower than 6.

As already observed for other aminotransferases (*20, 27*), the species that absorbs at 360 nm is the reactive one, whereas the species absorbing at 420 nm is unreactive (*20*). In agreement, the addition of AAD (Figure 1C) leads to the decrease in the peak at 360 nm with no changes in the shoulder at 420 nm. This finding also suggests that the 420 nm band is not a tautomeric form but a covalent modification of PLP. KAT II was previously indicated as ADD aminotransferase. Indeed, the catalytic efficiency of the enzyme towards AAD is slightly higher than that towards KYN (14). Reaction of hKAT II with AAD in the absence of ketoacids leads to the transamination of PLP to form PMP (Figure 1C), that stably accumulates also in the presence of KG. Thus, at equilibrium, the PMP form of KATII is the most stable enzyme form, i.e. the rate of its formation is higher than the rate of its consumption. The high absorbance of KYN in the spectral range where also PLP and PMP intermediates absorb hampers to carry out the same analysis on the reaction between KYN, KG and hKAT II.

PLP is an intrinsic fluorescent probe often exploited in vitamin B_6-dependent enzymes spectroscopy due to its sensitivity to the environment surrounding the cofactor and thus to changes in the conformation and ligation state of the active site (*28-30*). However, very few studies have investigated the fluorescence in aminotransferases (*31-40*). Often, fluorescence was exploited to monitor the release of PMP from the enzyme active site, binding of the cofactor and protein folding (*32-36, 38*). Differently from other PLP-dependent enzymes (*29*), the emission spectrum of hKAT II does not show any energy transfer between tryptophan residues and the cofactor (Figure 2A). The analysis of hKAT II three-dimensional structure (10) reveals that three tryptophan residues are within a 30 Å distance from the cofactor, thus the absence of energy transfer is an indication of an unfavourable orientation between tryptophan and PLP. The deprotonated internal aldimine, absorbing at 360 nm, is fluorescent with a structured emission showing a maximum at 420 nm and a shoulder at about 500 nm (Figure 2B). This is in agreement with findings on PLP Schiff bases and AspAT (*40*). Only the emission at 420 nm is directly attributed to the excitation of the deprotonated internal aldimine, whereas the band at 500 nm is due to the spurious excitation of the 420 nm band. This is confirmed by the emission spectra upon excitation at 420 nm. Excitation at

330 nm gives a structured emission with a shoulder at about 380 nm that could originate from the excitation of some residual PMP (*40*) and a band centred at about 420 nm that is likely originated from the excitation of the deprotonated internal aldimine band. Despite the reported conformational change induced by α-KG on the N-terminal stretch of KATII (*14, 41*), no spectral changes are observed in the emission spectrum of the protein upon binding of the substrate.

The mutation Tyr142Phe does not change the absorption (Figure 1A) and emission properties of KAT II (data not shown), its reactivity towards AAD and its activity with KYN and KG as substrates (data not shown). These findings indicate that the mutation does not have significant effects on the overall structure and function of the enzyme.

The spectral properties of the crystalline enzyme differ in some respect with those observed in solution. The absorption band of the enzyme-bind cofactor is blue-shifted as compared to the spectra in solution, where the main band is the peak of the deprotonated internal aldimine at 360 nm. This spectral differences could be attributed to the effect of Tris buffer. Its primary amine function breaks the imine bond between pyridoxal 5'-phosphate and the Lys263 residue to form a Tris-pyridoxal 5'-phosphate Schiff base in the enzyme active site. The effect of Tris on the polarized-light spectrum of hKAT II crystals is of interest as it confirms what already observed for other PLP-dependent enzymes. For example, in human mitochondrial branched-chain aminotransferase, Tris was found to bind the cofactor PLP and form a Schiff base in the protein structure (*42*). Spectral shift of PLP cofactor in the presence of Tris was also observed in hKAT I, suggesting that Tris can interact with the enzyme-associated PLP (*43*). Inspection of the crystal structure of the hKATI-Tris complex revealed that Tris is located in the enzyme active center and that its amine does not form an external aldimine with PLP. In this case Tris interacts with protein residues through a hydrogen-bonding network in the active center (*44*). Interactions with Tris molecules in the enzyme active site could interfere with the substrate binding and internal aldimine formation, therefore affecting the enzyme activity. The results of the experiments carried out on crystal of hKAT II suggest that the use of primary or secondary amine buffers should be avoided when inhibitors are being tested with hKAT II or aminotransferases in general. Moreover, single-crystal spectrophotometric study of hKAT II shown that, after replacement of Tris buffer with phosphate, the enzyme in the crystalline state is catalitically competent. Indeed, the natural substrate glutamine rapidly diffused through crystals of hKAT II and reacted at the active site causing spectral changes.

The detailed information obtained from the spectroscopic analysis of hKAT II both in solution and in the crystalline state, allowed to compare the spectroscopic properties of hKAT II to the well-defined spectroscopic properties of other aminotransferases. Furthermore, it was essential to establish the conditions for the enzyme functional characterization and investigation of the interaction mechanisms with inhibitors, which are discussed in the following chapters.

REFERENCES

1. Cooper, A. J., Bruschi, S. A., Iriarte, A., and Martinez-Carrion, M. (2002) Mitochondrial aspartate aminotransferase catalyses cysteine S-conjugate beta-lyase reactions, *The Biochemical journal 368*, 253-261.
2. Cooper, A. J., Pinto, J. T., Krasnikov, B. F., Niatsetskaya, Z. V., Han, Q., Li, J., Vauzour, D., and Spencer, J. P. (2008) Substrate specificity of human glutamine transaminase K as an aminotransferase and as a cysteine S-conjugate beta-lyase, *Archives of biochemistry and biophysics 474*, 72-81.
3. Graber, R., Kasper, P., Malashkevich, V. N., Strop, P., Gehring, H., Jansonius, J. N., and Christen, P. (1999) Conversion of aspartate aminotransferase into an L-aspartate beta-decarboxylase by a triple active-site mutation, *The Journal of biological chemistry 274*, 31203-31208.
4. Morino, Y., Kojima, H., and Tanase, S. (1979) Affinity labeling of alanine aminotransferase by 3-chloro-L-alanine, *The Journal of biological chemistry 254*, 279-285.
5. Cooper, A. J., and Pinto, J. T. (2006) Cysteine S-conjugate beta-lyases, *Amino acids 30*, 1-15.
6. Karsten, W. E., and Cook, P. F. (2002) Detection of intermediates in reactions catalyzed by PLP-dependent enzymes: O-acetylserine sulfhydrylase and serine-glyoxalate aminotransferase, *Methods in enzymology 354*, 223-237.
7. Laber, B., Gerbling, K. P., Harde, C., Neff, K. H., Nordhoff, E., and Pohlenz, H. D. (1994) Mechanisms of interaction of Escherichia coli threonine synthase with substrates and inhibitors, *Biochemistry 33*, 3413-3423.
8. Mozzarelli, A., Peracchi, A., Rossi, G. L., Ahmed, S. A., and Miles, E. W. (1989) Microspectrophotometric studies on single crystals of the tryptophan synthase alpha 2 beta 2 complex demonstrate formation of enzyme-substrate intermediates, *The Journal of biological chemistry 264*, 15774-15780.
9. Sterk, M., and Gehring, H. (1991) Spectroscopic characterization of true enzyme-substrate intermediates of aspartate aminotransferase trapped at subzero temperatures, *European journal of biochemistry / FEBS 201*, 703-707.
10. Rossi, F., Garavaglia, S., Montalbano, V., Walsh, M. A., and Rizzi, M. (2008) Crystal structure of human kynurenine aminotransferase II, a drug target for the treatment of schizophrenia, *The Journal of biological chemistry 283*, 3559-3566.
11. Jansonius, J. N. (1998) Structure, evolution and action of vitamin B6-dependent enzymes, *Current opinion in structural biology 8*, 759-769.
12. Metzler, D. E. (1979) Tautomerism in pyridoxal phosphate and in enzymatic catalysis, *Advances in enzymology and related areas of molecular biology 50*, 1-40.

13. Peterson, E. A., and Sober, H. A. (1954) Preparation of crystalline phosphorylated derivatives of vitamin B6, *J. Amer. Chem. Soc. 76*, 169-175.
14. Han, Q., Cai, T., Tagle, D. A., Robinson, H., and Li, J. (2008) Substrate specificity and structure of human aminoadipate aminotransferase/kynurenine aminotransferase II, *Biosci Rep 28*, 205-215.
15. Raboni, S., Bettati, S., and Mozzarelli, A. (2009) Tryptophan synthase: a mine for enzymologists, *Cell Mol Life Sci 66*, 2391-2403.
16. Campanini, B., Speroni, F., Salsi, E., Cook, P. F., Roderick, S. L., Huang, B., Bettati, S., and Mozzarelli, A. (2005) Interaction of serine acetyltransferase with O-acetylserine sulfhydrylase active site: evidence from fluorescence spectroscopy, *Protein Sci 14*, 2115-2124.
17. Hopkins, M. H., Bichler, K. A., Su, T., Chamberlain, C. L., and Silverman, R. B. (1992) Inactivation of gamma-aminobutyric acid aminotransferase by various amine buffers, *Journal of enzyme inhibition 6*, 195-199.
18. Rej, R., and Vanderlinde, R. E. (1975) Effects of buffers on aspartate aminotransferase activity and association of the enzyme with pyridoxal phosphate, *Clinical chemistry 21*, 1585-1591.
19. Makarov, V. L., Kochkina, V. M., and Torchinsky, Y. M. (1981) Reorientations of coenzyme in aspartate transaminase studied on single crystals of the enzyme by polarized-light spectrophotometry, *Biochim Biophys Acta 659*, 219-228.
20. Jenkins, W. T., Yphantis, D. A., and Sizer, I. W. (1959) Glutamic aspartic transaminase. I. Assay, purification, and general properties, *J Biol Chem 234*, 51-57.
21. Morino, Y., Osman, A. M., and Okamoto, M. (1974) Formate-induced labeling of the active site of aspartate aminotransferase by beta-chloro-L-alanine, *J Biol Chem 249*, 6684-6692.
22. Deshmukh, D. R., and Mungre, S. M. (1989) Purification and properties of 2-aminoadipate: 2-oxoglutarate aminotransferase from bovine kidney, *Biochem J 261*, 761-768.
23. Han, Q., Li, J., and Li, J. (2004) pH dependence, substrate specificity and inhibition of human kynurenine aminotransferase I, *Eur J Biochem 271*, 4804-4814.
24. Morino, Y., Shimada, K., and Kagamiyama, H. (1990) Mammalian aspartate aminotransferase isozymes. From DNA to protein, *Ann N Y Acad Sci 585*, 32-47.
25. Goldberg, J. M., Swanson, R. V., Goodman, H. S., and Kirsch, J. F. (1991) The tyrosine-225 to phenylalanine mutation of Escherichia coli aspartate aminotransferase results in an alkaline transition in the spectrophotometric and kinetic pKa values and reduced values of both kcat and Km, *Biochemistry 30*, 305-312.
26. Kirsch, J. F., Eichele, G., Ford, G. C., Vincent, M. G., Jansonius, J. N., Gehring, H., and Christen, P. (1984) Mechanism of action of aspartate aminotransferase proposed on the basis of its spatial structure, *Journal of Molecular Biology 174*, 497-525.

27. Jenkins, W. T., and Sizer, I. W. (1959) Glutamic aspartic transaminase. II. The influence of pH on absorption spectrum and enzymatic activity, *J Biol Chem 234*, 1179-1181.
28. Vaccari, S., Benci, S., Peracchi, A., and Mozzarelli, A. (1996) Time-resolved fluorescence of tryptophan synthase, *Biophysical chemistry 61*, 9-22.
29. Benci, S., Vaccari, S., Mozzarelli, A., and Cook, P. F. (1999) Time-resolved fluorescence of O-acetylserine sulfhydrylase, *Biochimica et biophysica acta 1429*, 317-330.
30. Benci, S., Vaccari, S., Mozzarelli, A., and Cook, P. F. (1997) Time-resolved fluorescence of O-acetylserine sulfhydrylase catalytic intermediates, *Biochemistry 36*, 15419-15427.
31. Salerno, C., Churchich, J. E., and Fasella, P. M. (1975) Fluorescence polarization studies on the binding between glutamate dehydrogenase and cytoplasmic aspartate aminotransferase, *The Italian journal of biochemistry 24*, 351-359.
32. Herold, M., and Leistler, B. (1992) Coenzyme binding of a folding intermediate of aspartate aminotransferase detected by HPLC fluorescence measurements, *FEBS letters 308*, 26-29.
33. Evans, R. W., and Holbrook, J. J. (1974) Studies on the changes in protein fluorescence and enzymic activity of aspartate aminotransferase on binding of pyridoxal 5'-phosphate, *The Biochemical journal 143*, 643-649.
34. Churchich, J. E., and Harpring, L. (1965) The effect of 8 M urea on fluorescence and activity properties of aspartate aminotransferase, *Biochimica et biophysica acta 105*, 575-582.
35. Churchich, J. E., and Farrelly, J. G. (1969) Mechanism of binding of pyridoxamine 5-phosphate to the apoenzyme aspartate aminotransferase. Fluorescence studies, *The Journal of biological chemistry 244*, 3685-3690.
36. Churchich, J. E. (1969) The binding of pyridoxamine 5-phosphate to alanine aminotransferase as measured by fluorescence spectroscopy, *Biochimica et biophysica acta 178*, 480-490.
37. Berezov, A., McNeill, M. J., Iriarte, A., and Martinez-Carrion, M. (2005) Electron paramagnetic resonance and fluorescence studies of the conformation of aspartate aminotransferase bound to GroEL, *The protein journal 24*, 465-478.
38. Beeler, T., and Churchich, J. E. (1978) 4-Aminobutyrate aminotransferase fluorescence studies, *European journal of biochemistry / FEBS 85*, 365-371.
39. Arrio-Dupont, M. (1978) Fluorescence of aromatic amino acids in a pyridoxal phosphate enzyme: aspartate aminotransferase, *European journal of biochemistry / FEBS 91*, 369-378.
40. Arrio-Dupont, M. (1970) [Fluorescence study of Schiff bases of pyridoxal. Comparison with L-aspartate aminotransferase], *Photochemistry and photobiology 12*, 297-315.

41. Tomita, T., Miyagawa, T., Miyazaki, T., Fushinobu, S., Kuzuyama, T., and Nishiyama, M. (2008) Mechanism for multiple-substrates recognition of alpha-aminoadipate aminotransferase from Thermus thermophilus, *Proteins*.
42. Yennawar, N., Dunbar, J., Conway, M., Hutson, S., and Farber, G. (2001) The structure of human mitochondrial branched-chain aminotransferase, *Acta crystallographica 57*, 506-515.
43. Han, Q., and Li, J. (2004) Cysteine and keto acids modulate mosquito kynurenine aminotransferase catalyzed kynurenic acid production, *FEBS letters 577*, 381-385.
44. Han, Q., Robinson, H., Cai, T., Tagle, D. A., and Li, J. (2009) Structural insight into the inhibition of human kynurenine aminotransferase I/glutamine transaminase K, *Journal of medicinal chemistry 52*, 2786-2793.

CHAPTER 3

FUNCTIONAL CHARACTERIZATION OF hKAT II

Development of new spectrophotometric assays for hKAT II activity

Introduction and aim of the work

Despite the number of works present in the literature dealing with KATs, no reliable continuous method has been so far developed (based on data present on Brenda and from a survey of the literature). The activity assays for this enzyme rely on a cumbersome discontinuous assay coupled to a HPLC determination or liquid scintillation spectrometry of KYNA (*1*-*5*). Briefly, a typical reaction mixture of 50 μL, containing 10 mM KYN, 5 mM α-KG, 40 μM PLP and 2 μg of protein sample, is prepared in 100 mM phosphate buffer pH 7.5. The mixture is incubated for 15 minutes at 37°C, the reaction is then stopped by adding an equal volume of 0.8 M formic acid. The supernatant of the reaction mixture, obtained by centrifugation at 15,000 *g* for 10 minutes at 4°C, is analyzed by HPLC for KYNA detection (3,4). Exiting HPLC-based methods for the quantification of KYNA as a product of KAT enzymatic activity are based on the chromatographic separation of KYNA on a HPLC column, followed by its detection based on either its electrochemical properties or the fluorescent properties as a complex with Zn^{2+} (λex = 344, λem = 398 nm) nm (6,7). An assay in which the reaction is stopped by addition of an acid and then protein is removed by centrifugation is complicated, time consuming and presents a high degree of variability. Moreover, this discontinuous assay require specific equipment and instrumental set up, and is difficult to apply to large-scale screenings for inhibitors. Obviously, the search for specific hKAT II inhibitors must rely on a continuous assay that allow for the determination of K_I values and, more importantly, of the mechanisms of inhibition. Furthermore, the high-throughput screening of inhibitors needs the careful optimization of a 96-wells plate suited assay, i.e. a spectrophotometric assay adapted to an end-point determination.

The development of a continuous spectrophotometric assay for hKAT II using KYN as a substrate has been hampered by its non-optimal spectrophotometric properties. In facts, KYN strongly absorbs at 361 nm (ε = 4,350 M^{-1} cm^{-1}) (8) and does not thus allow for assays at concentrations higher than 2 mM, being the estimated K_M of the enzyme about 5 mM (*3*). In a recent study on KAT from yeast *Saccharomyces cerevisiae* (9), a continuous spectrophotometric assay was used to monitor KYNA production by measuring the increase in absorbance at 285 nm over time. Unfortunately, this method was unreliable as data were not convincingly fitted with a standard Michaelis-Menten curve. Moreover, both KYNA and KYN have significant absorbance at this wavelength (8), thus the loss of KYN has a substantial effect on the absorbance at 285 nm.

Continuous coupled assays based on dehydrogenases are very convenient to study the kinetics of a specific transamination reaction and can be easily employed in large-scale screenings. Moreover, these assays are specific, since detection of different keto acid products requires the use of different coupling enzymes, i.e. malate dehydrogenase to monitor the formation of oxaloacetate from aspartate (ASP) aminotransferase activity. hKAT II can use many α-keto acids as amino group acceptors, but prefers α-ketoglutarate (KG) (3). This substrate preference can be exploited to set up an enzymatic coupled assay based on the consumption, by a specific enzyme, of the glutamate produced during the transamination of KYN, or other substrates, in the presence of KG. In general, the main enzymatic systems employed for the determination of L-glutamate are the glutamate dehydrogenase (GDH) and glutamate decarboxylase (GDC) assays (10,11). However, these enzymatic methods have some drawbacks due to the poor substrate specificity and the requirement for NAD^+ coenzyme. L-glutamate oxidase (GOX) holds excellent potentials for the use in the determination of L-glutamate due to the relatively high substrate specificity comparing to GDH and GDC and no requirement of additional coenzyme. GOX specifically catalyzes the oxidative deamination of L-glutamate in the presence of water and oxygen with the formation of α-ketoglutarate, ammonia and hydrogen peroxide (12). The hydrogen peroxide formed in this reaction can be easily detected by a chromogenic peroxidase reaction (13). Peroxidase readily combines with hydrogen peroxide and the resultant peroxidase-H_2O_2 complex can oxidize a wide variety of hydrogen donors, generating a chromogenic, chemilumnescent or fluorogenic signal depending on the substrate used. Although the productivities of the GOX enzyme from microbiological sources are still low and the commercially available GOX is very expensive, this enzyme attracted attention because of its biotechnological applications. Indeed, it is used as a diagnostic tool for the determination of L-glutamic acid in physiological fluids, and as an analytical reagent for the evaluation of food quality (14). Furthermore, an important application of GOX is in the diagnosis of liver function, as it is used in the determination of serum glutamate oxaloacetate transaminase (GOT) and glutamate pyruvate transaminase (GPT) levels in the clinical laboratories (12). Moreover, the immobilization of this enzyme to solid supports and membranes for the assay of glutamate has been reported (14).

Great advantages in the discovery of hKAT II inhibitors would arise from the development of new KAT activity assays which allow first the rapid screening of potential inhibitors and then further characterization of the inhibition mechanisms of selected compounds. We reasoned that two options for the activity assay of KATII are available: the exploitation of any significant difference in the absorption spectrum of KYN with respect to KYNA or the coupling of the reaction to a reporter assay with a product absorbing in the red side of the visible spectrum. The first option has been exploited for the development of a continuous assay based on the large difference in the extinction coefficient of KYN and KYNA at 310 nm, which allows rapid measurement of hKAT II activity and analysis of inhibition mechanisms. The second option has been exploited for the development of

an end-point assay to measure the concentration of glutamate formed by transamination activity in the presence of the amino group acceptor α-KG. This assay was further optimized to a 96-wells plate format for high-throughput screening of hKAT II transamination substrates and inhibitors, as discussed in chapter 5.

Materials and methods

Materials. L-Kynurenine (K8625), L-aspartate (A6558), glutamate oxidase from Streptomyces sp. (G5921), peroxidase from horseradish (P8375), *o*-dianisidine (D9143), glutamate dehydrogenase from bovine liver (G2626) and malate dehydrogenase from porcine heart (M7383) were purchased from Sigma-Aldrich (St.Louis, MO).

KAT activity measured by a continuous spectrophotometric assay. A continuous assay for the measurement of transamination of KYN by hKAT II using KG as the acceptor was developed (see Results). KYN and KYNA concentrations were calculated from the absorbance in the UV-visible range using published extinction coefficients at pH 7.3 (8) (for KYN ε_{257} = 6,750 $M^{-1} \cdot cm^{-1}$, ε_{361} = 4,350 $M^{-1} \cdot cm^{-1}$; for KYNA ε_{332} = 9,800 $M^{-1} \cdot cm^{-1}$, ε_{344} = 7,920 $M^{-1} \cdot cm^{-1}$).

Data fitting. Data fitting was carried out using Sigma Plot software, release 9.0. Plots of initial velocity as a function of KYN concentration at a constant KG concentration (10 mM) were fitted to a hyperbolic equation:

$$V_0 = \frac{V'_{max} \cdot [KYN]}{K' + [KYN]} \quad [1]$$

where:

$$V'_{max} = \frac{V_{max} \cdot [KG]}{K_M^{KG} + [KG]} \quad [2]$$

and

$$K' = \frac{\alpha K_M^{KYN} \cdot [KG]}{K_M^{KG} + [KG]} \quad [3]$$

V'_{max} and K' are apparent K_M and V_{max}, K_M^{KYN} and K_M^{KG} are Michaelis constants for KYN and KG, respectively (15).

KAT transamination activity measured by a coupled glutamate oxidase-peroxidase assay (GOX-peroxidase coupled assay). The amounts of glutamate produced by transamination activity in the presence of KG were determined by an end-point assay based on the use of GOX and peroxidase. A reaction mixture containing 10 mM KG, 40 μM PLP and 10 mM KYN was equilibrated at the desired reaction temperature (25°C) in 50 mM Hepes, pH 7.5, before starting the reaction with addition of 2 μM KATII. Aliquots (20 μL each) were removed after 30 minutes, and stopped by mixing with 2 μL of 1.14 M phosphoric acid (final concentration 14 mM). Each aliquot was subsequently mixed with a solution containing 0.02 units of glutamate oxidase (GOX-Sigma G5921), 3 units of peroxidase (perox-Sigma P8375), 1 mM *o*-dianisidine and 50 mM Hepes pH 7.5, in a final volume of 200 μL. The mixture was incubated at 37 °C for 30 minutes. Finally, the mixture was supplemented with 50 μL sulphuric acid (final concentration 3.36 mM) to dissolve the occasional precipitates of oxidized *o*-dianisidine and to increase the assay sensitivity (13), before measuring the absorbance at 530 nm to quantify the extent of *o*-dianisidine oxidation. A calibration curve was prepared, using known concentrations of glutamate, ranging from 10 to 800 μM in the presence of 10 mM KG, 40 μM PLP, 14 mM phosphoric acid, 1 mM *o*-dianisidine, 0.02 units of glutamate oxidase (GOX-Sigma G5921), 3 units of peroxidase (Perox-Sigma P8375) and 50 mM Hepes pH 7.5, in a final volume of 200 μL. The reaction mixtures were incubated and treated as above, and the absorbance at 530 nm was plotted against the initial amount of glutamate to generate a calibration curve. Blanks (control reactions) were set up using the same reagents as for the assay except for hKAT II that was replaced by the same volume of buffer.

KAT activity measured by a coupled malate dehydrogenase assay (MDH assay). A continuous spectrophotometric assay for the measurement of transamination rate between aspartate (ASP) and KG by hKAT II was developed (see Results). Reactions (200 μL final volume) containing 50 mM Hepes pH 7.5, 5 mM KG, 10 μM PLP, 1.35 mM NADH, 6 U MDH and variable concentrations of ASP (1-40 mM) were incubated at 37°C. The reaction was started by the addition of 1.6 μM hKAT II and carried out at 37 °C in a 0.1 cm optical path cuvette. The disappearance of NADH was monitored at 340 nm (ε = 6,220 $M^{-1} \cdot cm^{-1}$).

KAT activity measured by a coupled glutamate dehydrogenase assay (GDH assay). The rate of transamination reaction between α-aminoadipate (AAD) and KG by hKAT II was determined spectrophotometrically by an assay coupled with glutamate dehydrogense (GDH). A reaction mixture (200 μL final volume) containing 10 mm AAD, 10 mM KG, 10 μM PLP, 1.5 mM $NADP^+$ and 1 U GDH, in 50 mM Hepes pH 7.5 was incubated at 25°C. The reaction was started by the addiction of 62 nM hKAT II and carried out at 25 °C in a 0.1 cm optical path cuvette. The accumulation of NADPH was monitored at 340 nm (ε = 6,220 $M^{-1} \cdot cm^{-1}$).

Results

A new continuous spectrophotometric assay for hKAT II activity

To overcome the limitations of the discontinuous KAT assay (2-5,16,17), an assay for the continuous monitoring of KYN transamination was developed. The absorption spectrum of a solution containing 900 μM KYN, 10 mM KG and 40 μM PLP, in 50 mM Hepes pH 7.5, at 37°C, exhibits a maximum at 361 nm, typical of KYN at neutral pH. The spectrum obtained when hKAT II is added to the reaction mixture and reaction reaches equilibrium is blue shifted with a peak at 332 and a shoulder at approximately 344 nm (Figure 1A), typical of KYNA (8). The difference spectra (Figure 1A, inset) shows a positive peak at about 340 nm and a negative peak at 360 nm. At wavelengths lower than 352 nm it is possible to follow the accumulation of KYNA and thus to develop an assay with a good sensitivity for product formation. Nonetheless, the extinction coefficient of KYN at 340 nm is too high (3,290 M^{-1} cm^{-1}) to allow for initial velocities determinations at KYN concentrations higher than 8 mM, being the published K_M for KYN about 5 mM (*3*). We thus chose to carry out the assays at 310 nm, a wavelength that represents a good compromise between high sensitivity and an extinction coefficient of KYN low enough to monitor kinetics up to about 3 times the expected K_M. Extinction coefficients at 310 nm of 1049 $M^{-1} \cdot cm^{-1}$ and 4674 $M^{-1} \cdot cm^{-1}$ were calculated for KYN and KYNA, respectively. Thus, a $\Delta\varepsilon$ at 310 nm of 3625 $M^{-1} \cdot cm^{-1}$ was used to calculate the initial velocities from kinetic traces at 310 nm. A series of reactions were carried out as a function KYN concentration from 2 mM to 23 mM KYN, at constant KG concentration (10 mM), that, based on a previously determined K_M for KG of 1.2 mM, should be saturating (*3*). We found that V_0 values are independent of KG concentration down to 200 μM. From a typical Michaelis Menten plot (Figure 1B) K' of 10 ± 1 mM, V'_{max} of 0.022 ± 0.001 mM/min and k_{cat} of 25 min^{-1} were calculated.

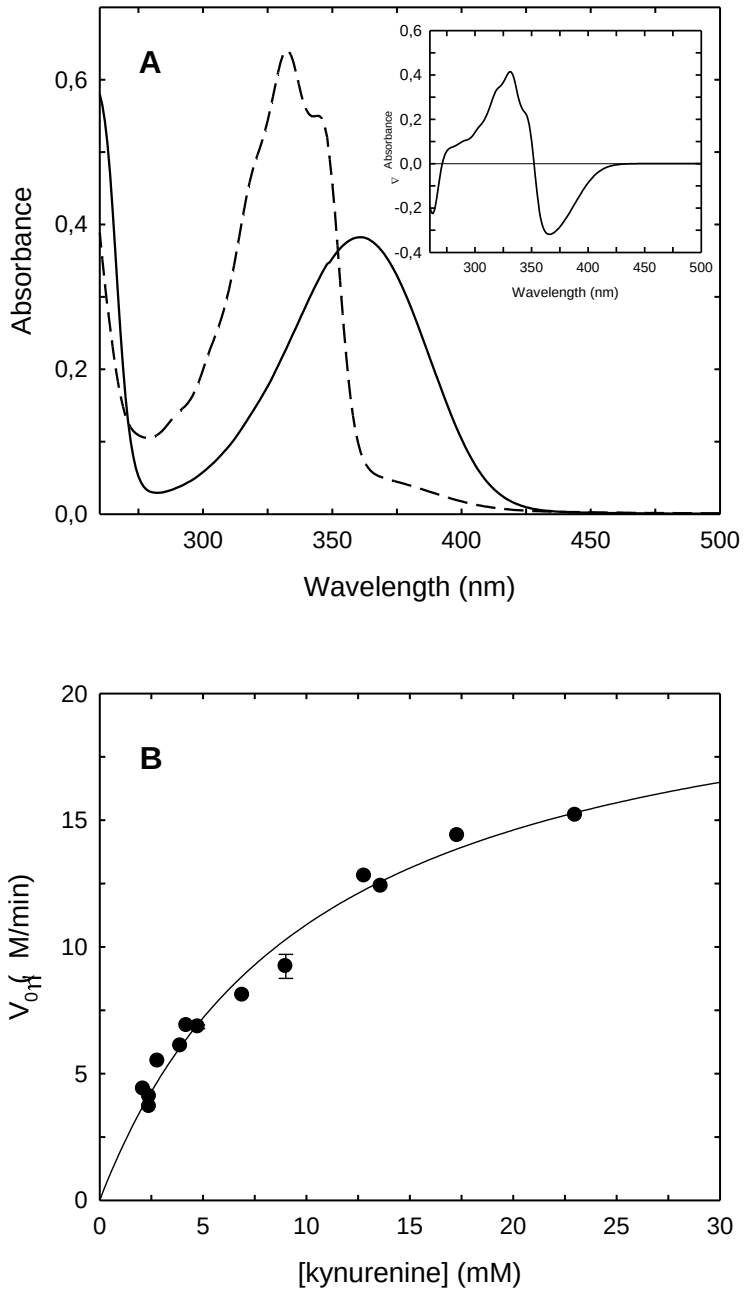

Figure 1. Reactivity of KATII towards KYN

A *Absorption spectra of KYN and its reaction products in the presence of hKAT II and KG*

The reaction mixture contained 10 mM KG, 40 μM PLP and 900 μM KYN in 50 mM Hepes pH 7.5, at 37 °C (solid line). The reaction, carried out in 0.1 cm optical path cuvettes, was started by the addition of 9.4 μM hKAT II. A spectrum was collected at equilibrium about 150' upon enzyme addition (dashed line). **Inset:** difference spectrum.

B *Dependence of the rate of reaction of hKAT II on KYN in the presence of KG*

The reaction mixture contained 870 nM hKAT II in 50 mM Hepes pH 7.5 in the presence of 10 mM KG, 40 μM PLP and variable concentrations of KYN. The reaction was carried out at 25 °C in a 0.1

cm optical path cuvette. The solid line through data points represents the fitting to the Michaelis-Menten equation with V_{max} = 0.022 ± 0.001 mM/min and K_M = 10 ± 1 mM.

Development and validation of an end-point assay using GOX and peroxidase as coupling enzymes.

A GOX-peroxidase coupling end-point assay was developed to assess the concentration of glutamate produced by hKAT II transamination activity in the presence of KG. The principle of the assay is illustrated in Scheme 1. Glutamate is deaminated to ketoglutaric acid and hydrogen peroxide by glutamate oxidase. Hydrogen peroxide reacts with *O*-dianisidine in the presence of peroxidase to form a coloured product. Oxidized *O*-dianisidine reacts with sulfuric acid to form a stable coloured product. The intensity of the absorbance measured at 530 nm is proportional to the glutamate concentration. This method is simple and advantageous for routine usage. Moreover, its accuracy and precision are excellent, compared to more commonly used non enzymatic methods (13). As references (13,18) mention the use of strong acid for optimal colour development, we employed a final sulphuric acid concentration of 3.36 mM, which gives an intense and stable pink colour with maximum absorbance at 415 and 530 nm (Figure 2A).

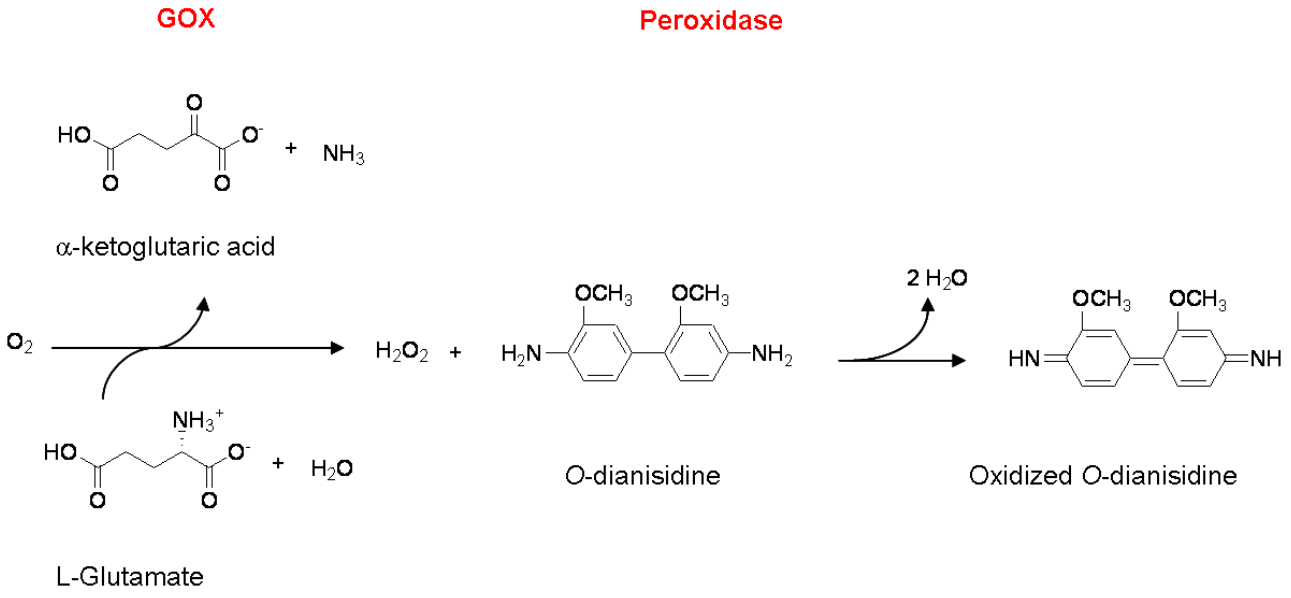

Scheme 1. The principle of the GOX-peroxidase assay for glutamate quantification

First, GOX oxidizes glutamate, yielding hydrogen peroxide, which is then used by peroxidase to convert *o*-dianisidine into a coloured product. This oxidized *O*-dianisidine turns deep pink in the presence of concentrated sulfuric acid.

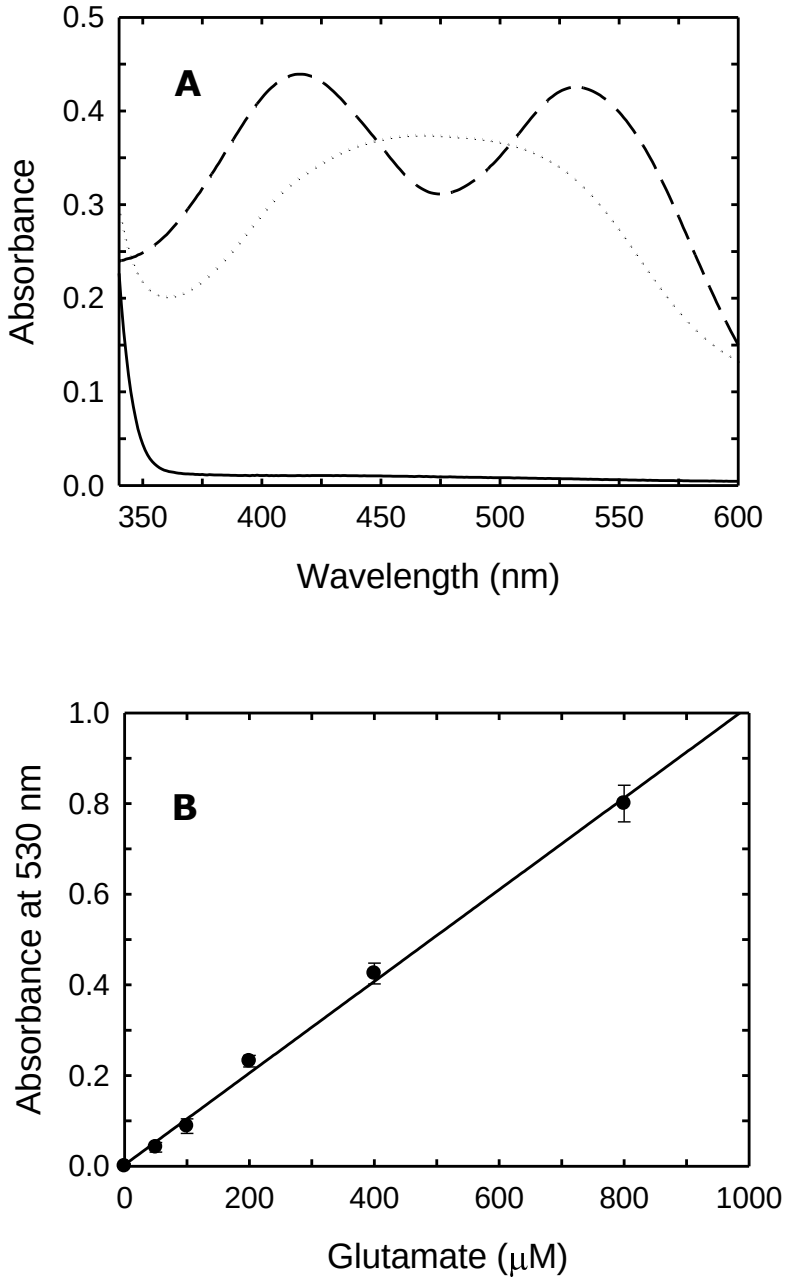

Figure 2. GOX-peroxidase coupled assay

A *Absorption spectra of the chromogen used in the enzymatic procedure.*

Absorption spectra of a solution containing 400 μM *O*-dianisidine in 50 mM Hepes at 25°C in the reduced (solid line), oxidized form in the absence of sulphuric acid (dotted line) and oxidized form in the presence of 3.36 mM sulphuric acid (dashed line).

B *Calibration curve for GOX-peroxidase end-point assay*.

Reactions were prepared as described in Materials and Methods, using known concentrations of glutamate, ranging from 10 to 800 μM. Each reaction was repeated in triplicate. The solid line through data points represents the fitting to linear equation with slope $0.001 \pm 2.92 \cdot 10^{-5}$.

The optimization procedure for GOX-peroxidase endpoint assay was performed with the following conditions held constant: i) the buffer was 50 mM Hepes pH 7.5 containing 40 μM PLP; ii) the final volume of the solution containing *O*-dianisidine, GOX and peroxidase as mentioned in the literature, was 200 μL (18); iii) the reaction mixture was incubated for 30 minutes at 37°C and then stopped with a final sulphuric acid concentration of 3.36 mM.

Incubation time and concentrations of hKAT II and substrates (KYN and KG) were optimized to ensure steady-state conditions of the endpoint readings, preventing equilibrium achievement and therefore consumption of glutamate by hKAT II. Moreover, as this coupled endpoint assay was designed also to assess the inhibition of transamination activity brought about by screened compounds, it should be possible to evaluate even low decreases in absorbance intensity in the presence of inhibitors. Therefore, the conditions of hAKTII reaction were optimized to obtain the highest possible absorbance intensity (about 800 μM glutamate). Optimized concentrations were found to be 2 μM for hKAT II and 10 mM for both KYN and KG. These concentrations ensure a linear substrate consumption over a period of 30 minutes, with minimal enzyme amount. After this time period, only approximately 8% of the total substrate amount was consumed, therefore ensuring steady state conditions and a constant substrate turnover rate. Furthermore, the resulting signal provided the desired assay sensitivity. Termination of hKAT II reaction was tested with either phosphoric acid or TCA. The absorbance intensity generated in the latter was lower, indicating a possible inhibition of one or both the coupled enzymes. Therefore, phosphoric acid in a final concentration of 14 mM was used.

An assay validation for the endpoint system was performed. For comparison, the amounts of KYNA and glutamate produced by hKAT II in the presence of 10 mM KYN and 10 mM KG, were determined through the continuous assay based on the absorbance increase at 310 nm and the GOX-peroxidase end-point assay, respectively, using the same substrate concentrations and reaction conditions. The reaction mixture contained 10 mM KYN, 10 mM KG, and 40 μM PLP in 50 mM Hepes pH 7.5. The reaction, carried out at 25°C in 0.1 cm optical path cuvettes, was started by the addition of 2 μM hKAT II. The transamination of 10 mM KYN leads to the accumulation of 814 μM KYNA (specific activity 0.27 μmol/μg·min), as determined spectroscopically using the $\Delta\varepsilon$ at 310 nm (3625 $M^{-1} \cdot cm^{-1}$) for KYNA. The amount of glutamate produced by the same reaction was 701 ± 67 μM (specific activity 0.24 μmol/μg·min), as detected by the GOX-peroxidase end-point assay. The concentrations of transamination products (KYNA and glutamate) obtained through the two methods are enough similar to validate the application of the GOX-based assay for measuring the amounts of enzymatic glutamate production.

Discussion

KAT activity has been usually assayed by a cumbersome discontinuous method coupled to a HPLC determination or liquid scintillation spectrometry of KYNA (2-5,16). The spectral properties of

KYN have hindered the development of a continuous assay for KATII activity using KYN as substrate. As KYN strongly absorbs at 361 nm (ε = 4,350 $M^{-1}\cdot cm^{-1}$) (8), activity assays could not be performed at concentrations higher than 2 mM, a value below the estimated K_M of the enzyme (about 5 mM). Our strategy towards the development of a continuous assay was the observation that only at 310 nm the absorbance of KYN is low enough to allow assays at up to 23 mM KYN in cuvettes with 0.1 cm optical path. At the same time, at 310 nm there is a significant absorbance difference between KYN and KYNA to make easily detectable transamination time courses. Kinetic traces collected at 310 nm were linear over the time needed to calculate initial velocities (about 10 minutes) and showed no lag or burst phases. The extinction coefficient used to calculate V_0 was 3625 $M^{-1} \cdot cm^{-1}$, i.e. for each molecule of KYN consumed in the reaction (1049 $M^{-1} \cdot cm^{-1}$) one molecule of KYNA (4674 $M^{-1} \cdot cm^{-1}$) is produced. The amount of KYN consumed during the linear portion of the kinetics is less than 5 %, thus fulfilling the requirements for steady state. Furthermore, this assay allows for the determination of V_0 in a range of substrate concentrations from 0.3 to more than 2.5 K_M, that is acceptable for an accurate determination of V_{max} and K_M (15). The assay was intended for use in conjunction with the 96-well plate assay for the characterization of the mechanism of action of selected inhibitors. We thus checked that the concentration of KG was saturating under our experimental conditions. We estimated K_M^{KG} to be lower than 20 μM. At saturating KG concentrations V'_{max} is equal to V_{max} that exhibits a value of 0.022 mM/min, and K' is equal to αK_M^{KYN} that has a value of 10 mM, where $\alpha = k_4/k_2$.

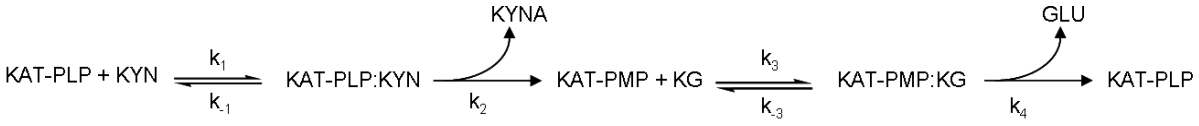

In many cases (19) the rate-limiting step for transaminases is the α-proton abstraction (see scheme 1 in chapter 2), thus $k_4 > k_2$ and *K'* represents an upper limit to K_M^{KYN}. Consequently, K_M^{KYN} is in the mM range, in agreement with a previous work on KATII (*3*), where a value of about 5 mM was reported. On the contrary, the k_{cat} value, that we found to be about 25 min^{-1}, does not agree with the value previously reported, about 580 min^{-1}. The discrepancy can be due to the use of a discontinuous assay and the intrinsic heterogeneity in different enzyme preparations. Furthermore, an inaccurate determination of enzyme concentration leads to significant errors in the determination of k_{cat}. In this work, the enzyme concentration was evaluated following cofactor release by alkali denaturation, a method that is accepted to be the most accurate for PLP-

dependent enzymes. Notably, the continuous assay allows the rapid measurement of enzyme activity, and more importantly, the fast determination of K_I values and inhibition mechanisms, as discussed in chapter 4. As a further advantage, the amount of enzyme needed for each assay is low, about 9 μg, compatible with the low yields of KAT II expression.

A colorimetric end-point assay was developed to quantify the amount of glutamate produced by hKAT II transamination activity in the presence of KG. The GOX-peroxidase coupling system is very efficient and sensitive in converting the enzymatic production of glutamate into an intense chromogenic signal. GOX catalyses the conversion of glutamate into KG and H_2O_2. The latter is then used by peroxidase to oxidize *o*-dianisidine, yielding an intensely coloured product (13). The method was optimized to fulfill the requirements of steady state conditions for hAKT II catalyzed reaction and to enhance the assay sensitivity. This assay was validated using the natural substrate KYN and allows to test the transamination activity on a variety of other substrates. Moreover, it can be adapted for use with different members of the KAT superfamily, thus allowing the comparison of substrate preferences among the different isoforms. In principle, the use of GOX and peroxidase as indicator enzymes could allow monitoring of glutamate formation in real time by means of continuous assay. However, in continuous coupled assay, the reaction catalyzed by the indicator enzyme must not be rate-limiting to the overall kinetics. This requisite is difficult to meet with GOX, which is a slow enzyme ($k_{cat} \approx 86\ min^{-1}$) (20). Moreover, commercially available GOX is very expensive. Hence, we developed a discontinuos method, which, despite being more cumbersome, is not limited by the rate of the coupled reaction, affords an improved reliability of the assay and provides a much greater flexibility in terms of the kinetics conditions that can be explored. More importantly, this assay was designed and optimized to be further implemented on a 96-wells plate format to rapidly monitor the transamination of potential substrates and the inhibitory activity brought about by screened compounds, as discussed in chapter 5.

In summary, two new useful assays for KAT II activity were developed. Both are advantageous in terms of specificity and reliability. More interestingly, they were intended for use in conjunction: the GOX-peroxidase end-point assay was adapted to a 96-wells plate assay for the fast evaluation of libraries of compounds as potential hKAT II inhibitors *via* an initial visual inspection, subsequently the continuous spectrophotometric assay at 310 nm allows the rapid determination of K_I values and the characterization of mechanisms of action of selected inhibitors.

As a part of the activities carried out during the thesis, we report here the unsuccessful attempts to develop a continuous spectrophotometric assays for hKAT II activity, based on coupled enzyme reactions different from above. To develop a continuous spectrophotometric assay for hKAT II activity other two methods were first examined.

MDH coupled assay

The ability of hKAT II to use L-aspartate (ASP) as an amino group donor was first assessed spectroscopically. In the presence of 10 mM ASP, the internal aldimine band disappears with the concomitant appearance of a peak centred at 325-330 nm, indicating the formation of PMP that accumulates in the absence of keto acids (Figure 3). The aspartate aminotransferase activity of hKAT was exploited to developed a continuous spectrophotometric assay coupled with NADH-dependent malate dehydrogenase (MDH). The oxaloacetate produced by the transamination of aspartate serves as a substrate for malate dehydrogenase, that reduces oxaloacetate to malate in the presence of dihydronicotinamide-adenine dinucleotide (NADH), which is simultaneously oxidized (Scheme 2). NADH has an absorption peak at 340 nm (ε = 6,220 $M^{-1}\cdot cm^{-1}$) whereas NAD does not shown any absorption. The absorbance decrease at this wavelength provides a means for the measurement of the rate of transaminase activity (21-23). A series of reactions were carried out as a function ASP concentration from 1 mM to 40 mM, at constant KG concentration (5 mM), that, based on a previously determined K_M for KG of 1.2 mM, should be saturating (*3*). From a typical Michaelis Menten plot (Figure 4), K_M of 27 ± 6 mM, V_{max} of 0.029 ± 0.003 mM/min, k_{cat} of 18 min^{-1} and k_{cat}/K_M of 0.67 mM^{-1} min^{-1} were calculated.

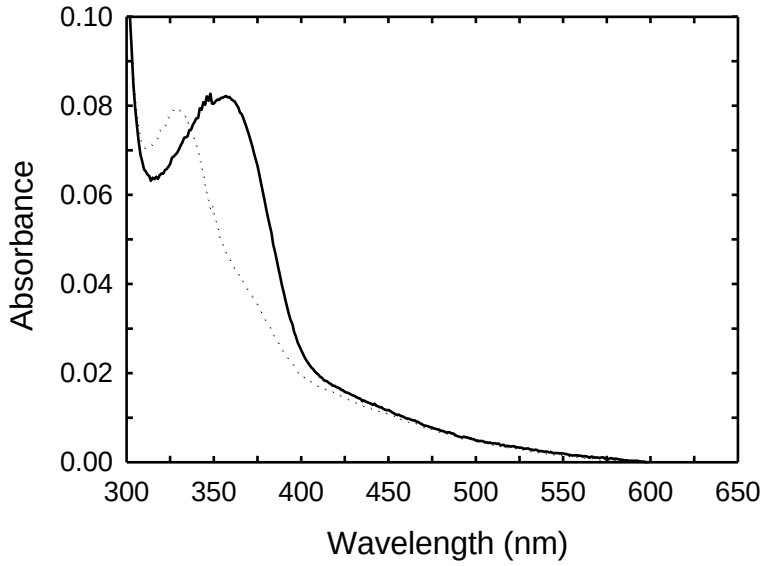

Figure 3. Absorption spectra of hKAT II in the presence of ASP

Absorption spectra of 8 μM hKATI, 50 mM Hepes pH 7.5 at 25 °C, in the absence (solid line) and in the presence of 10 mM ASP, about 10' upon addition (dotted line).

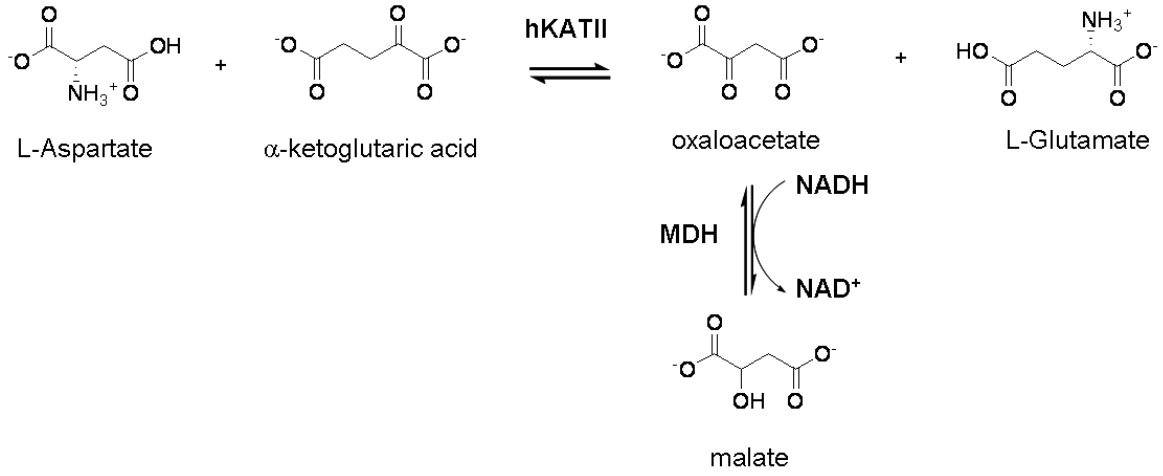

Scheme 2. **The principle of MDH coupled assay for aspartate aminotransferase activity.**

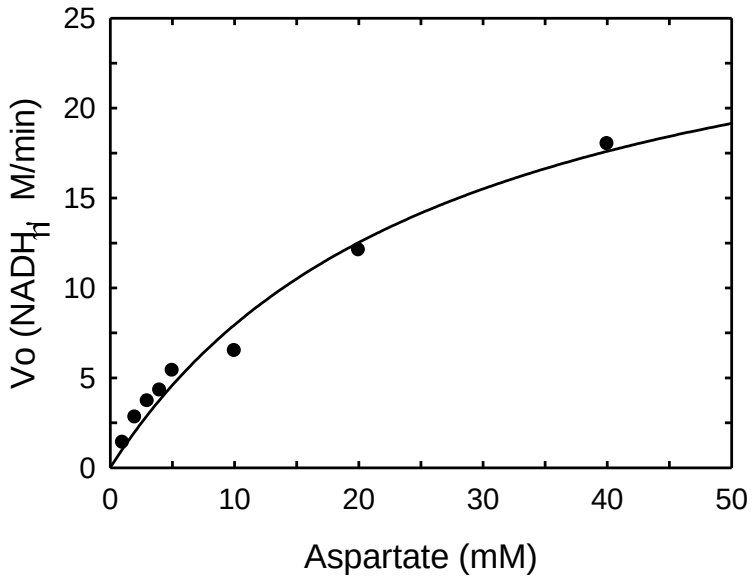

Figure 4. Dependence of the rate of reaction of hKAT II on ASP in the presence of KG

The reaction mixture (200 μL final volume) contained 1.6 μM hKAT II in 50 mM Hepes pH 7.5 in the presence of 5 mM KG, 10 μM PLP, 1.35 mM NADH, 6 U MDH and variable concentrations of ASP (1-40 mM). The reaction was carried out at 37 °C in a 0.1 cm optical path cuvette. The disappearance of NADH was monitored at 340 nm. The solid line through data points represents the fitting to the Michaelis-Menten equation with V_{max} = 0.029 ± 0.003 mM/min and K_M = 27 ± 6 mM.

The MDH coupled assay has been optimized to fulfill the kinetic requirements for a continuous coupled enzymatic assay. The reaction catalyzed by the indicator enzyme, in this case MDH, was

not rate-limiting to the overall kinetic, whereas initial rate measurements were linearly dependent to hKAT II concentration. Kinetic traces collected at 340 nm were linear over the time needed to calculate initial velocities (about 10 minutes) and showed no lag or burst phases. The amount of ASP consumed during the linear portion of the kinetics was less than 10 %, thus fulfilling the requirements for steady state conditions. Unfortunately, the estimate of the catalytic efficiency of hKAT II to ASP indicates that ASP is a poor substrate for transamination reaction. Moreover, MDH coupled assay is not a specific method for the detection of hKAT II activity. Indeed, little amounts of contaminant aminotransferases present in the enzymatic preparation may exert aspartate aminotransferase activity, thereby interfering with KATII activity measurement. This represents a significant drawback in the determination of inhibition mechanisms and inhibition constants measurement. Therefore, we focused to developed a specific KAT activity assay based on the use of KYN as substrate.

GDH coupled assay

In principle, the kinetic of the transamination reaction between aminoadipate (AAD) and KG could be monitored spectrophotometrically by an assay coupled with glutamate dehydrogenase (GDH). This enzyme catalyzes the reversible oxidative deamination of glutamate to KG and ammonia (24). As the enzymatic oxidation of glutamate is coupled to the reduction of $NAD^+/NADP^+$ to NADH/NADPH, the absorbance increase at 340 nm provides a useful mean for the measurement of the transaminase activity. Mammalian forms of GDH, including the bovine form, can use either NADP(H) or NAD(H) as coezymes with comparable efficacy (25).

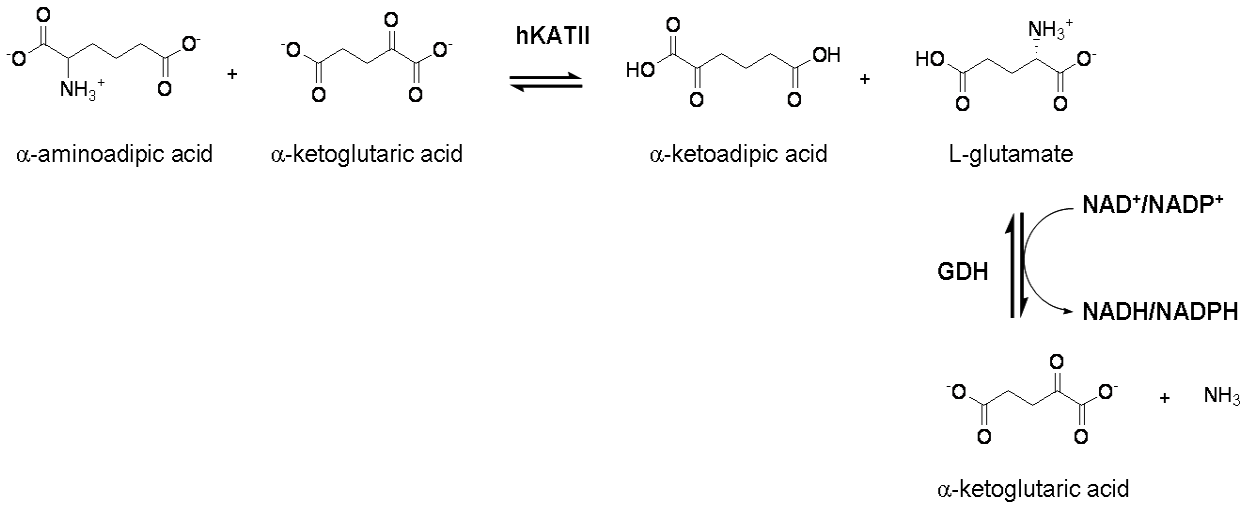

Scheme 3. **The principle of GDH coupled assay for AAD aminotransferase activity.**

A reaction mixture (200 μL final volume) containing 10 mm AAD, 10 mM KG, 10 μM PLP, 1.5 mM $NADP^+$ and 1 U GDH, in 50 mM Hepes pH 7.5 was incubated at 25°C. The reaction was started by the addiction of 62 nM hKAT II and the reduction of the coenzyme was monitored at 340 nm. The initial rate was 2.4 μM/min, corresponding to a k_{cat} of 39 min-1, which is well below the rate measured on AAD with glyoxylate as an acceptor of amino groups, 179 min^{-1} (3). A possible reason for this discrepancy is the fact that the oxidative deamination of glutamate to KG and ammonia actually is not favored. The equilibrium is in favor of the reverse reaction to form glutamate. It is well assessed that KG exhibits feed-back inhibition on GDH (26,27). Studies of steady-state kinetics of the oxidative deamination of glutamate by GDH and $NADP^+$ revealed that the product KG is a potent competitive inhibitor of L-glutamate oxidation (28). It behaves as a tightly bound substrate analogue competing with glutamate in the formation of complexes at the enzyme active site. In particular, stopped-flow studies showed that both binary enzyme-KG and ternary enzyme-$NADP^+$-KG complexes are inhibitory in the burst phase of the enzyme-catalyzed reaction (29). Dissociation constants of 2.5 ± 0.4 mM (30) and 1.7 ± 0.3 mM (29) for the enzyme-KG complex have been reported. We also found a considerable (about 60%) inhibition of bovine GDH activity by 10 mM KG. On the basis of these observations, coupled assay with GDH could not be considered a reliable method for continuous measuring of hKAT II transamination activity.

Investigation on beta-lyase activity of wild type hKAT II and the mutant Tyr142Phe

Introduction and aim of the work

Pyridoxal-5'-phosphate (PLP)-dependent enzymes are unrivalled in the diversity of reactions that they catalyze (31). The catalytic versatility of PLP-dependent enzymes arises from the ability of the cofactor pyridoxal-5'-phosphate to covalently bind the substrate and then to function as an electron sink, thereby stabilizing different types of carbanionic reaction intermediates (32,33). PLP-catalyzed reactions can be divided according to the position at which the net reaction occurs. Reaction at the α position include transamination, decarboxylation, racemization, and elimination and replacement of an electrophilic R group. Those at the β or γ position include elimination and replacement (31). As many of the reaction pathways share common intermediates, PLP-dependent enzymes often show "catalytic promiscuity", that is, the ability of a single enzyme to catalyze different chemical reactions (34,35). In addition, PLP-dependent enzyme may exhibit a promiscuous reaction specificity (36). Indeed, it is known that many PLP-dependent enzymes, including tryptophan synthase (37), DOPA decarboxylase (38), aspartate aminotransferase (39) and serine racemase (40,41) can catalyze side reactions with substrates analogues or even with their natural substrates, some of which have been suggested to play a physiological role (40,41). In particular, it is well assessed that transaminases, due to the chemistry of the catalyzed reaction, are prone, in the presence of substrates with good leaving groups at the β position, to carry out β-elimination as a side reaction (42-45), with the formation of α-aminoacrylate that spontaneously hydrolyzes to pyruvate and ammonia (see Scheme 1 in chapter 2).

KAT I was initially identified as glutamine transaminase K (GTK) and later was shown to be identical to cysteine S-conjugate β-lyase 1 (CCBL1). KAT I/GTK/CCBL1 from both human and rat is one of the several PLP-depending enzymes that catalyze non-physiological β-elimination reactions with cysteine S-conjugates that possess an electron-withdrawing group attached at the sulphur (43,46). Cysteine S-conjugates are intermediates in the "mercapturate pathway", a mechanism by which potentially dangerous electrophilic xenobiotics, that enter in mammalian tissues as environmental pollutants from industrial and commercial use, are detoxified. However, this pathway may sometimes generate metabolites more toxic than the parent unmodified electrophile. Toxicity may results from the action of cysteine S-conjugates β-lyases. If a cysteine S-conjugate contains a good leaving groups in the β position, it may be diverted away from the mercapturate pathway by the action of cysteine S-conjugate β-lyases. These enzymes convert the cysteine S-conjugate to aminoacrylate, which is non-enzymatically hydrolyzed to pyruvate and ammonia, and a sulphur-containing fragment. The thiol released can be highly toxic or pharmacologically active depending on its structure (47). If the sulphur-containing fragment eliminated by the cysteine S-conjugate β-lyase reaction is chemically reactive, the parent cysteine S-conjugate may be toxic, particularly to kidney mitochondria, liver, brain and possibly other

organs. The toxicity of most halogenated cysteine S-conjugates is associated with the formation of reactive thioacylating agents, which thioacylate macromolecules, particularly at the ε-amino group of lysine residues in proteins (48-50). Halogenates xenobiotics that are present in the environment and are metabolized, at least in part, to toxic cysteine S-conjugates, include tetrafluoroethylene, which is used in industry as precursor of Teflon, trichloroethylene, used in industry as solvent and degreasing agent, and tetrachloroethylene. The corresponding toxic cysteine S-conjugates are S-(1,1,2,2-tetrafluoroethyl)-L-cysteine (TFEC), (S-(1,2-dichlorovinyl)-L-cysteine (DVDC) and S-(1,2,2-trichlorovinyl)-L-cysteine, respectively (44). DVDC is nephro- and hepatotoxic/carcinogenic in experimental animals (51). Toxicity of DVDC is associated in part with covalent modification of macromolecules and initiation of lipid peroxidation (52). Both human and rat KAT I/GTK/CCBL1 efficiently catalyze β-lyase reactions with TFEC and DCVC, therefore they can potentially contribute to the bioactivation of these toxic cysteine S-conjugates (43,46). Conversely, when the sulphur-containing fragment eliminated in a cysteine S-conjugate β-lyase reaction is not reactive, the parent cysteine S-conjugate is not particularly toxic (53).

On the other hand, cysteine S-conjugates β-lyase side reactions can also have beneficial physiological consequences (53). Indeed, the ability of cysteine S-conjugate β-lyase to cleave a C-S bond has been exploited in the design of cysteine S-conjugate prodrugs of sulphur-containing anti-cancer agents. Studies (53-56) show the potential pharmacological application in cancer therapy for some designed cysteine S-conjugates prodrugs, that release active anti-proliferative and pro-apoptotic agents in target tumor tissues by the β-lyase-dependent bioactivation.

Considerable effort has been devoted in last years to identify mammalian cysteine S-conjugates β-lyases that might contribute to this bioactivation process. Mammalian tissues are known to contain at least eleven PLP-dependent enzymes capable of catalyzing cysteine S-conjugates β-lyase reactions (53), they include the cytosolic enzymes kynureninase (57), GTK/KAT I/CCBL1 (43,46), cytosolic aspartate aminotransferase (cytAspAT) (58), alanine aminotransferase(AlaAT) (58-60) and cytosolic branched- chain aminotransferase (BCATc) (61) and the mitochondrial enzymes mitochondrial aspartate aminotransferase (mitAspAT) (44), mitochondrial branched-chain aminotransferase (BCATm) (61), alanine glyoxylate aminotransferase II (62) and GABA aminotransferase (53). Most of the cysteine S-conjugate β-lyases discovered so far are aminotransferases. Thus an aminotransferase reaction may compete with the β-elimination reaction. Interestingly, most of the cysteine S-conjugate β-lyases identified to date, including kynureninase, cytAspAT, mitAspAT, AlaAT and cytosolic BCAT, but not cytosolic GTK/KAT I, are syncatatalitically inactivated by end-products (63). Aminoacrylate eliminated from the β-lyase active site is known to inactivate pig heart cytAspAT by reacting with the PLP-coenzyme to generate a PLP-pyruvate aldol condensation product that remains attached to the active site (64). Moreover, the sulphur-containing fragment released from the halogenated cysteine S-conjugate may react with a lysine residue leading to self-inactivation (53).

Because the ability to catalyze non-physiological β-lyase reactions appears to be a common feature among many aminotransferases (62), and in particularly human GTK/KAT I like its rat counterpart, has the potential to bioactivate halogenated cysteine S-conjugates (43), the exploration of the β-lyase activity for hKAT II is particularly intriguing. Furthermore, it is worth noting that hKAT II contains structural elements which are typical of members of PLP-dependent lyases, such as the conformation of the N-terminal region and a tyrosine residue in position 142, which is normally occupied by a tryptophan or a phenylalanine in most AT (65). On the basis of these interesting observations, we decided to investigate the possible β-lyase activity of hKAT II and a variant carrying the Tyr142Phe mutation, expected, on the basis of structural evaluation (65), to exhibit a decrease propensity for β-elimination.

Materials and methods

β-lytic activity. β-elimination reactions carried out by aminotransferases involve formation of an α-aminoacrylate intermediate that, being unstable, rapidly decomposes to pyruvate and ammonia. The rates of β-elimination of β-chloro-L-alanine (BCA) by KATII and Tyr142Phe KATII were measured by monitoring the the absorbance increase at 220 nm associated with the formation of pyruvate ($\varepsilon_{220\ nm}$ pyruvate = 1050 M^{-1} cm^{-1}) (62,66). Kinetics were collected at 25 °C using a 0.1 cm path length cuvette. The reaction was initiated by adding 64 nM KATII or Tyr142Phe KATII. The assay was carried out in 100 mM phosphate buffer pH 7.5 to minimize background signal at 220 nm.

When the substrate tested for β-elimination reaction heavy interfered with the spectroscopic signal used to monitor pyruvate formation, as in the case of S-phenylcysteine, KYN and ESBA, the β-lytic activity of KATII was evaluated by measuring the accumulation of ammonia by the Nessler's method.

Nessler's assay. Reaction mixtures containing ammonia produced by β-elimination were tested with the Nessler's assay (67) using a ready-to-use solution (Fluka, code 72190). At pH 7.5 98% of ammonia is in the NH_4^+ form and the solubility of NH_3 in water at 25 °C is about 50 % (w/w), thus no significant loss of ammonia by evaporation is expected under our experimental conditions. A standard curve was built using ammonium sulfate concentrations in the range 1-20 mM. 40 μl of a solution containing ammonia were diluted with 860 μl of water. 100 μl of Nessler's reagent were added to the mixture and the absorbance of the solution immediately recorded at 436 nm.

Results

The propensity of hKAT II for β-elimination was first evaluated on β-chloro-L-alanine (BCA), a substrate that contains chloride as a good β-leaving group (68). Transamination of BCA in the presence of 10 mM KG was found to be negligible, as measured by the GOX coupled assay that monitors the formation of glutamate. On the contrary, a series of spectra recorded as a function of

time for a reaction of 15 μM hKAT II in the presence of 5 mM BCA exhibited the immediate decrease of the deprotonated internal aldimine band at 360 nm and the concomitant accumulation of a species absorbing maximally at 330 nm (Figure 5A), that progressively shifted to about 315-320 nm, indicating the accumulation of pyruvate (69). Upon reaction completion, the concentration of pyruvate was estimated on the basis of its absorbance at 315 nm ($\varepsilon_{315\ nm}$ pyruvate = 23 $M^{-1}\ cm^{-1}$) and found to be 3.7 mM. An equivalent amount of ammonia (3.8 mM) was produced, as determined by the Nessler's assay. This indicates that a significant amount of BCA has undergone a β-elimination reaction with formation of β-aminoacrylate that decomposes to pyruvate and ammonia. The same assay, carried out on Tyr142Phe KATII, indicated a reduced efficiency of the mutant in the β-elimination of chloride from BCA. In fact, at equilibrium only about 1.8 mM ammonia was produced from 5 mM BCA under the same conditions.

The initial rates of pyruvate formation catalyzed by KATII and Tyr142Phe KATII in the presence of 5 mM BCA were measured by monitoring pyruvate accumulation at 220 nm. (Figure 5B). Specific activities of 5 nmol/μg·min and 0.22 nmol/μg·min, were determined, respectively. The formation of pyruvate was characterized by a fast linear phase (Figure 5B), followed by a slow establishment of the chemical equilibrium. Deviation from linearity in the reaction took place at a concentration of pyruvate that was less than 1% of the total substrate concentration. This deviation, hardly attributable to lack of adherence to steady state conditions, is strongly suggestive of an inactivation process that is taking place as a consequence of the β-elimination reaction. Two possible mechanisms can be invoked to explain enzyme inhibition: covalent modification of the enzyme and product inhibition. In the latter case, removal of the products from the reaction mixture should lead to the recovery of enzymatic activity, whereas covalent modification causes a permanent inactivation of the enzyme. It is known that some aminotransferases during β-lytic reactions become covalently inactivated by a syncatalytic mechanism involving the cofactor and a basic residue in the active site (42,70). To test if this is the case also for KATII, the residual activity of the enzyme was measured upon reaction with BCA. KATII (174μM), incubated with 50 mM BCA for 20 minutes at 25 °C, was assayed upon 200-fold dilution using 10 mM KYN and 10 mM KG. The initial rate was compared to the value obtained for KATII incubated for 20 minutes at 25°C, in the absence of BCA. The activity of the enzyme reacted with BCA was found to be only 3 % compared to the activity of the unreacted enzyme, indicating that a significant amount of the enzyme has been covalently inactivated as a consequence of the occurrence of the β-elimination reaction. Therefore, the observed decreased in the rate of β-elimination reaction with time resulted from an irreversible inactivation of the enzyme rather than from accumulation of an inhibitor in the reaction mixture. BCA is capable of permanently inactivating KATII through a mechanism that, likely, involves formation of a covalent adduct between the active site lysine residue and the α–aminoacrylate intermediate, as already reported for AlaAT (42) and AspAT (44) (Scheme 4). Apparently, the covalently modified form of the enzyme is quite unstable, as it could not be

recovered neither after ultrafiltration nor after gel filtration on micro spin columns. This hampered the determination of the type of modification by mass spectrometry. The pseudo-first order rate constant, k_{obs}, for the inactivation process was obtained fitting to a single exponential decay the dependence of the percent of initial activity of KATII on time of incubation in the presence of 5 mM BCA (Figure 5C). The calculated value is k_{obs} = 0.7 min^{-1}. The time required for inactivating one-half the enzyme initially present ($t_{1/2}$) was obtained from the pseudo-first order rate constant k_{obs} using the equation $t_{1/2}$ = 0,693/ k_{obs} (69). The value calculated ($t_{1/2}$ ≈ 1') is comparable to those measured for other aminotransferase. Indeed, in the case of AlaAT the pseudo-first order rate constant for inactivation was 0.36 min^{-1}, with a $t_{1/2}$ ≈ 2' in the presence of 5 mM BCA (42). The partition ratio (moles of product per mole of inactivated enzyme) is about 500, a value comparable with those found for AlaAT, 1050 (42), and for kynureninase, 530 (71).

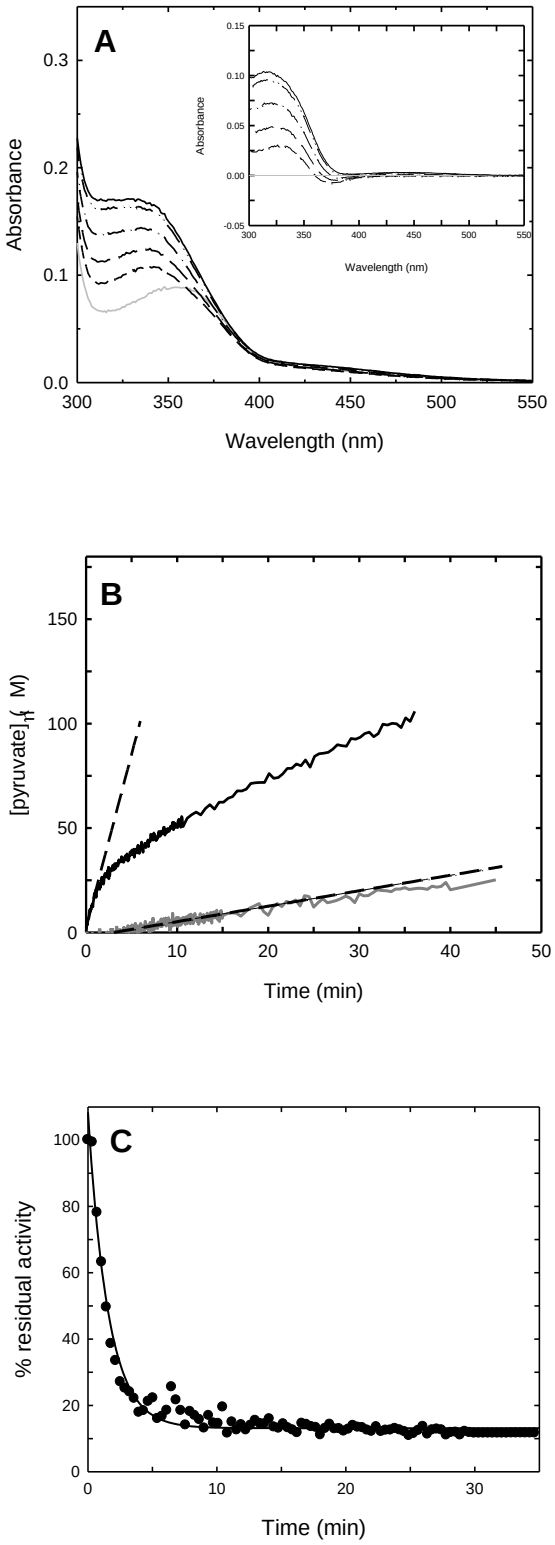

Figure 5. β-lyase activity of KATII on BCA.

A *Reaction of KATII with BCA.* The reaction mixture contained 15 μM KATII, 50 mM Hepes, pH 7.5, at 25°C, in the absence (solid gray line) and presence of 5 mM BCA, after 1, 5, 10, and 28 min after mixing (dashed lines). **Inset:** difference spectra obtained from raw spectra by subtracting the spectrum of the unreacted KATII.

B *Time courses of pyruvate formation by KATII and Y142F KATII.* The reaction mixture contained either 64 nM KATII or 64 nM Tyr142phe KATII (solid black line and solid gray line, respectively) and 5 mM BCA, 100 mM K_2PO_4, pH 7.5, at 25 °C. The black dashed lines represent the fitting to linear equations with slopes 17 μM/min and 0.74 μM/min for KATII and Tyr142phe KATII, respectively.

C *Monophasic progress curve for the inactivation process of hKAT II by BCA*. The plot of percent of initial activity versus time for hKAT II in the presence of 5 mM BCA (calculated from data in figure 5B) was best fit to a single exponential decay. The solid line represents the fitting to an exponential decay equation with k_{obs} = 0.7 min^{-1} and $t_{1/2}$ ≈ 1'.

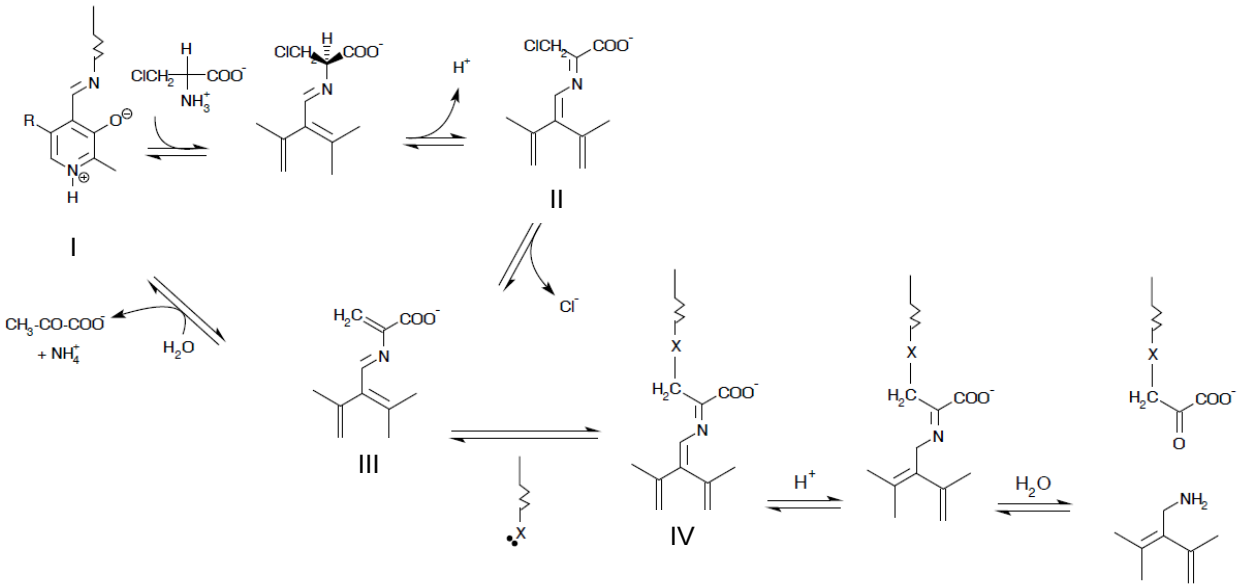

Scheme 4. Proposed mechanism for the reaction of KAT II with BCA and the syncatalytic inactivation proceeding from the α-aminoacrylate intermediate. Adapted from (42). Pirydoxal-5'-phosphate is bound to the active site via an aldimmine linkage with the ε-amino group of Lys263 (species I). Removal of the β-substituent from the deprotonated complex (species II) can lead to two different reaction pathways: the formation of an α-aminoacrylate-enzyme complex (species III), which then decomposes to pyruvate and ammonia regenerating the internal aldimine, that can catalyze another catalytic cycle. Otherwise, the three-carbon moiety derived from BCA covalently binds to a nucleophilic amino acid residue (X) within the active site resulting in the formation of the complex IV in which the enzyme is irreversibly inactivated. With aspartate aminotransferase, this X was demonstrated to be the ε-amino group of the lysine residue involved in the formation of an aldimine bond with the coenzyme (70,72). The fraction of enzyme that is covalently modified and

therefore irreversibly inactivated depends on the rates of the two different reaction of quinonoide intermediate decay.

BCA is considered the best substrate to test for β-elimination reaction, as chloride is a good β-leaving group. KAT II β-lyase activity was further tested on a different substrate, S-phenyl-cysteine (SPC). SPC was chosen as a substrate for β-elimination because cysteine S-conjugates are good substrates for the β-lytic activity of the related enzyme KAT I (43,46) and this activity could have important physiological consequences in the bioactivation of both potentially toxic cysteine S-conjugates or anti-cancer prodrugs. (43,53). As SPC strongly absorbs at 220 nm, the rate of pyruvate formation could not be measured by monitoring the absorbance increase at 220 nm. Therefore, the β-lytic activity of KAT II in the presence of SPC was evaluated by measuring the amount of ammonia produced by the Nessler's method. Moreover, SPC solubility limit did not allow for assay concentrations higher than 3 mM. Unlike BCA, SPC is transaminated by hKAT II, as measured by the GOX coupled assay that monitors the formation of glutamate. Therefore, in the case of SPC, the aminotransferase reaction competes with the β-elimination reaction. β-elimination results in generation of the PLP form of the enzyme, which is free to catalyze another round of β-elimination. A half-transamination reaction converts the PLP coenzyme into its pyridoxamine 5'-phosphate (PMP) form, which cannot catalyze a β-lyase reaction. When transamination competes with the β-elimination reaction, as in the case of SPC, maximal β-lyase activity requires the presence of an α-keto acid substrate in the reaction mixture. The α-keto acid forms a Schiff's base with PMP that is then converted to the corresponding amino acid and PLP. The PLP form of the enzyme can then support another round of β-lyase catalysis (53). Therefore, in the case of SPC, inclusion of KG in the reaction mixture was necessary to ensure maximal β-lyases activity. For a reaction of KAT II in the presence of 3 mM SPC and 10 mM KG, the specific activity was 42 pmol/μg·min. This value is comparable to that measured for rat KAT I/GTK on the same substrate (53 pmol/μg·min) (54). The β-lytic activity of Tyr142Phe KAT II was instead undetectable. We tested whether also SPC can inactivate hKAT II, as it was observed with BCA. A solution containing KAT II (129 μM) was incubated with 3 mM SPC for 60 minutes, at 25 °C. The reaction was diluted 200 fold in an assay solution containing 10 mM KYN and 10 mM KG. The activity of the enzyme reacted with SPC was found to be about 65% compared to the activity of the unreacted enzyme, suggesting that β-lytic activity of SPC may lead to syncatalytic inactivation of the enzyme. Furthermore, the β-lyase catalysis on the natural substrate KYN by KAT II was also evaluated. The specific activity measured using 20 mM KYN was $9 \cdot 10^{-6}$ μmol/min·μg, four orders of magnitude lower than that measured on BCA. The activity of the enzyme reacted with KYN was found to be identical to that of the unreacted enzyme, indicating that in this case the enzyme was not covalently inactivated as a consequence of the occurrence of the β-elimination reaction.

Discussion

PLP-dependent enzymes are reported to be quite promiscuous, with reference to both substrate and the type of catalyzed reaction. In particular, some ATs are known to be relatively efficient in catalyzing β-elimination as side reaction on substrates with good leaving groups, such as BCA and, more interestingly, on S-substituted cysteine derivatives (42-44,53,62,69,73). Cysteine S-conjugates β-lyase side reactions can have both negative and positive physiological consequences. Adverse effects may occur as a result of cysteine S-conjugates β-lyases catalysing reactions that generate toxic sulphur-containing fragments, whereas possible beneficial consequences of cysteine S-conjugates β-lyases activity include pharmacological applications in cancer therapy *via* the bioactivation of pro-drugs into anti-proliferative and pro-apoptotic agents (43,53-56). In the case of KAT II, the exploration of β-lyase activity was particularly intriguing in that structural comparisons suggested the presence of features normally observed in β-lyases, such as the conformation of the N-terminal region and a tyrosine residue in position 142 which is normally occupied by a tryptophan or a phenylalanine in most AT (65). We thus investigated the β-lytic activity of KAT II and Tyr142Phe KAT II with BCA and SPC. Whereas the Tyr142Phe mutation does not change the reactivity of KAT II towards AAD and KYN in the presence of KG, it heavily influences the β-lytic activity of the enzyme. In fact, both the wild type and the mutant are able to eliminate chloride from BCA, with production of equivalent amounts of ammonia and pyruvate, but Tyr142Phe mutant is twenty times less efficient. One possible explanation is that the tyrosine residue in position 142 plays a role in the balance between β-elimination and transamination. In the conditions tested here we could not reach saturation in a plot of initial velocity against BCA concentration. This is consistent with the observation that K_M values of transaminases for BCA are usually very high, preventing the determination of kinetic parameters. This also hampers the calculation of catalytic efficiency for chloride elimination by KAT II and Tyr142Phe KAT II. For this reason, we cannot rule out the possibility that the lower rate of β-elimination observed for Tyr142Phe KAT II is partly due to a higher K_M value. The K_M values exhibited toward BCA by various aminotransferases vary markedly. The values reported for mitAspAT (69), cytAsAT (69), AlaAT (42), BCATm (61), AGAT (62,66) are 50, 200, 0.1, 0.6, 0.07-0.1 mM, respectively. Evidently BCA binds favorably at the active site of some aminotransferases, but not others.

Although a detailed characterization of the β-lytic activity of this mutant is behind the aim of this work, we checked the β-lytic activity of wild type KAT II and the mutant enzyme in the presence of SPC. Also in this case we observed β-elimination with production of ammonia by the wild type enzyme but no activity by the Tyr142Phe mutant, a further indication of a reduction of β-lytic activity brought about by the mutation. Interestingly, the β-elimination, although quite inefficiently, takes also place on the natural substrate KYN. This unusual β-elimination reaction should produce *ortho*-amino benzaldehyde, as already reported in a controversial paper on the activity of

kynureninase (74). At present, it is not known whether this reaction has any physiological significance or is regulated by any effector, as in the case, for example of the mammalian serine racemase (40,41). However, it should be bear in mind that the β-elimination reaction requires the formation of an α-aminoacrylate intermediate that, in the case of KAT II, as demonstrated by experiments with BCA, leads to a concomitant syncatalytic inactivation of the enzyme. Furthermore, it is unlikely that a very inefficient reaction, when compared to the main one, would have any physiological significance, unless it is tuned by effectors and ligands. The understanding of this aspect of KAT II mechanism of action is beyond the aim of this work but should deserve further attention.

To date, β-lyase activity of hKAT II has not yet been investigated. Our preliminary evaluation demonstrates for the first time that hKAT II catalyzes β-elimination reactions on BCA and SPC, with efficiency comparable to that reported for other aminotransferases. These findings suggest further investigations (i.e. the reaction with TFEC, DVCD and other cysteine S-derivatives) to extend the specificity of hKAT II as a cysteine S-conjugates β-lyase, and, more importantly, to assess whether hKAT II might contribute in human brain to bioactivation of potentially toxic cysteine S-conjugates and act as a possible target for cysteine S-conjugate prodrugs in cancer therapy. It is worth noting that the mercapturate pathway, by which cysteine S-conjugates are produced, is most prominent in liver and kidney, but all the constituent enzymes are present in most other organs. Thus, many tissues have the capacity to generate cysteine S-conjugates (63). Moreover, cysteine S-derivatives that are formed in the liver can be released into the circulation and distributed to other organs, including the brain (63). DCVC, for example, is readily transported across the blood-brain barrier (75). Human KAT I, like its rat counterpart, has the potential to bioactivate DCVC and other halogenated cysteine S-conjugates (43). Better understanding of the catalytic properties of hKAT II is crucial not only for expanding the knowledge of its biological functions in human brain, but also for improved inhibitor design.

REFERENCES

1. Amori, L., Guidetti, P., Pellicciari, R., Kajii, Y., and Schwarcz, R. (2009) *J Neurochem* **109**(2), 316-325
2. Amori, L., Wu, H. Q., Marinozzi, M., Pellicciari, R., Guidetti, P., and Schwarcz, R. (2009) *Neuroscience* **159**(1), 196-203
3. Han, Q., Cai, T., Tagle, D. A., Robinson, H., and Li, J. (2008) *Bioscience reports* **28**(4), 205-215
4. Han, Q., Robinson, H., and Li, J. (2008) *The Journal of biological chemistry* **283**(6), 3567-3573
5. Pellicciari, R., Venturoni, F., Bellocchi, D., Carotti, A., Marinozzi, M., Macchiarulo, A., Amori, L., and Schwarcz, R. (2008) *ChemMedChem* **3**(8), 1199-1202
6. Swartz, K. J., Matson, W. R., MacGarvey, U., Ryan, E. A., and Beal, M. F. (1990) *Analytical biochemistry* **185**(2), 363-376
7. Shibata, K. (1988) *J Chromatogr* **430**(2), 376-380
8. Dalgliesh, C. E. (1952) *The Biochemical journal* **52**(1), 3-14
9. Wogulis, M., Chew, E. R., Donohoue, P. D., and Wilson, D. K. (2008) *Biochemistry* **47**(6), 1608-1621
10. Sowerby, J. M., and Ottaway, J. H. (1966) *The Biochemical journal* **99**(1), 246-252
11. Ling, D., Wu, G., Wang, C., Wang, F., and Song, G. (2000) *Enzyme and microbial technology* **27**(7), 516-521
12. Arima, J., Tamura, T., Kusakabe, H., Ashiuchi, M., Yagi, T., Tanaka, H., and Inagaki, K. (2003) *Journal of biochemistry* **134**(6), 805-812
13. Washko, M. E., and Rice, E. W. (1961) *Clinical chemistry* **7**, 542-545
14. Hirano, A., Moridera, N., Akashi, M., Saito, M., and Sugawara, M. (2003) *Analytical chemistry* **75**(15), 3775-3783
15. Marangoni, A. G. (2003) *Enzymes Kinetics - A Modern Approach*, John Wiley & Sons, Inc., Hoboken, New Jersey
16. Amori, L., Guidetti, P., Pellicciari, R., Kajii, Y., and Schwarcz, R. (2009) *J Neurochem*
17. Han, Q., Fang, J., and Li, J. (2002) *J Biol Chem* **277**(18), 15781-15787
18. Donini, S., Ferrari, M., Fedeli, C., Faini, M., Lamberto, I., Marletta, A. S., Mellini, L., Panini, M., Percudani, R., Pollegioni, L., Caldinelli, L., Petrucco, S., and Peracchi, A. (2009) *The Biochemical journal* **422**(2), 265-272
19. Kuramitsu, S., Hiromi, K., Hayashi, H., Morino, Y., and Kagamiyama, H. (1990) *Biochemistry* **29**(23), 5469-5476
20. Katsos, N. E., Labrou, N. E., and Clonis, Y. D. (2004) *Journal of chromatography* **807**(2), 277-285

21. Wilkinson, J. H., Baron, D. N., Moss, D. W., and Walker, P. G. (1972) *Journal of clinical pathology* **25**(11), 940-944
22. Karmen, A. (1955) *The Journal of clinical investigation* **34**(1), 131-133
23. Henry, R. J., Chiamori, N., Golub, O. J., and Berkman, S. (1960) *American journal of clinical pathology* **34**, 381-398
24. Fisher, H. F. (1985) *Methods in enzymology* **113**, 16-27
25. Peterson, P. E., and Smith, T. J. (1999) *Structure* **7**(7), 769-782
26. Eisenkraft, B., and Veeger, C. (1968) *Biochimica et biophysica acta* **167**(2), 227-238
27. LeJohn, H. B., and Stevenson, R. M. (1970) *The Journal of biological chemistry* **245**(15), 3890-3900
28. Caughey, W. S., Hellerman, L., and Smiley, J. D. (1957) *The Journal of biological chemistry* **224**(1), 591-607
29. Colen, A. H. (1978) *Biochemistry* **17**(3), 528-533
30. Cross, D. G., McGregor, L. L., and Fisher, H. F. (1972) *Biochimica et biophysica acta* **289**(1), 28-36
31. Eliot, A. C., and Kirsch, J. F. (2004) *Annual review of biochemistry* **73**, 383-415
32. John, R. A. (1995) *Biochimica et biophysica acta* **1248**(2), 81-96
33. Schneider, G., Kack, H., and Lindqvist, Y. (2000) *Structure* **8**(1), R1-6
34. O'Brien, P. J., and Herschlag, D. (1999) *Chemistry & biology* **6**(4), R91-R105
35. Jeffery, C. J. (1999) *Trends in biochemical sciences* **24**(1), 8-11
36. Han, Q., Fang, J., and Li, J. (2001) *The Biochemical journal* **360**(Pt 3), 617-623
37. Miles, E. W. (1987) *Biochemistry* **26**(2), 597-603
38. Bertoldi, M., and Borri Voltattorni, C. (2003) *Biochim Biophys Acta* **1647**(1-2), 42-47
39. Kochhar, S., and Christen, P. (1988) *Eur J Biochem* **175**(2), 433-438
40. Foltyn, V. N., Bendikov, I., De Miranda, J., Panizzutti, R., Dumin, E., Shleper, M., Li, P., Toney, M. D., Kartvelishvily, E., and Wolosker, H. (2005) *J Biol Chem* **280**(3), 1754-1763
41. Strisovsky, K., Jiraskova, J., Mikulova, A., Rulisek, L., and Konvalinka, J. (2005) *Biochemistry* **44**(39), 13091-13100
42. Morino, Y., Kojima, H., and Tanase, S. (1979) *J Biol Chem* **254**(2), 279-285
43. Cooper, A. J., Pinto, J. T., Krasnikov, B. F., Niatsetskaya, Z. V., Han, Q., Li, J., Vauzour, D., and Spencer, J. P. (2008) *Archives of biochemistry and biophysics* **474**(1), 72-81
44. Cooper, A. J., Bruschi, S. A., Iriarte, A., and Martinez-Carrion, M. (2002) *The Biochemical journal* **368**(Pt 1), 253-261
45. Graber, R., Kasper, P., Malashkevich, V. N., Strop, P., Gehring, H., Jansonius, J. N., and Christen, P. (1999) *J Biol Chem* **274**(44), 31203-31208
46. Cooper, A. J. (2004) *Neurochemistry international* **44**(8), 557-577

47. Commandeur, J. N., Stijntjes, G. J., and Vermeulen, N. P. (1995) *Pharmacological reviews* **47**(2), 271-330
48. Hayden, P. J., and Stevens, J. L. (1990) *Molecular pharmacology* **37**(3), 468-476
49. Dekant, W., Vamvakas, S., and Anders, M. W. (1994) *Advances in pharmacology (San Diego, Calif* **27**, 115-162
50. Volkel, W., and Dekant, W. (1998) *Chemical research in toxicology* **11**(9), 1082-1088
51. Dekant, W., Vamvakas, S., Koob, M., Kochling, A., Kanhai, W., Muller, D., and Henschler, D. (1990) *Environmental health perspectives* **88**, 107-110
52. Chen, Q., Jones, T. W., Brown, P. C., and Stevens, J. L. (1990) *The Journal of biological chemistry* **265**(35), 21603-21611
53. Cooper, A. J., and Pinto, J. T. (2006) *Amino acids* **30**(1), 1-15
54. Commandeur, J. N., Andreadou, I., Rooseboom, M., Out, M., de Leur, L. J., Groot, E., and Vermeulen, N. P. (2000) *The Journal of pharmacology and experimental therapeutics* **294**(2), 753-761
55. Rooseboom, M., Commandeur, J. N., and Vermeulen, N. P. (2004) *Pharmacological reviews* **56**(1), 53-102
56. Rooseboom, M., Vermeulen, N. P., Durgut, F., and Commandeur, J. N. (2002) *Chemical research in toxicology* **15**(12), 1610-1618
57. Stevens, J. L. (1985) *The Journal of biological chemistry* **260**(13), 7945-7950
58. Kato, Y., Asano, Y., and Cooper, A. J. (1996) *Developmental neuroscience* **18**(5-6), 505-514
59. Gaskin, P. J., Adcock, H. J., Buckberry, L. D., Teesdale-Spittle, P. H., and Shaw, P. N. (1995) *Human & experimental toxicology* **14**(5), 422-427
60. Adcock, H. J., Gaskin, P. J., Shaw, P. N., Teesdale-Spittle, P. H., and Buckberry, L. D. (1996) *The Journal of pharmacy and pharmacology* **48**(2), 150-153
61. Cooper, A. J., Bruschi, S. A., Conway, M., and Hutson, S. M. (2003) *Biochemical pharmacology* **65**(2), 181-192
62. Cooper, A. J., Krasnikov, B. F., Okuno, E., and Jeitner, T. M. (2003) *The Biochemical journal* **376**(Pt 1), 169-178
63. Cooper, A. J., Bruschi, S. A., and Anders, M. W. (2002) *Biochemical pharmacology* **64**(4), 553-564
64. Ueno, H., Likos, J. J., and Metzler, D. E. (1982) *Biochemistry* **21**(18), 4387-4393
65. Rossi, F., Garavaglia, S., Montalbano, V., Walsh, M. A., and Rizzi, M. (2008) *J Biol Chem* **283**(6), 3559-3566
66. Porter, D. J., Harrington, J. A., Almond, M. R., Chestnut, W. G., Tanoury, G., and Spector, T. (1995) *Biochemical pharmacology* **50**(9), 1475-1484
67. Barnes, A. R., and Sugden, J. K. (1990) *Pharm Acta Helv* **65**(9-10), 258-261

68. Gregerman, R. I., and Christensen, H. N. (1956) *J Biol Chem* **220**(2), 765-774
69. Morino, Y., Osman, A. M., and Okamoto, M. (1974) *The Journal of biological chemistry* **249**(20), 6684-6692
70. Morino, Y., and Okamoto, M. (1973) *Biochem Biophys Res Commun* **50**(4), 1061-1067
71. Kishore, G. M. (1984) *J Biol Chem* **259**(17), 10669-10674
72. Morino, Y., Okamoto, M., and Tanase, S. (1978) *The Journal of biological chemistry* **253**(17), 6026-6030
73. Bertoldi, M., Cellini, B., Paiardini, A., Montioli, R., and Borri Voltattorni, C. (2008) *Biochim Biophys Acta* **1784**(9), 1356-1362
74. Longenecker, J. B., and Snell, E. E. (1955) *J Biol Chem* **213**(1), 229-235
75. Patel, N. J., Fullone, J. S., and Anders, M. W. (1993) *Brain research* **17**(1-2), 53-58

CHAPTER 4

MECHANISMS OF INTERACTION WITH INHIBITORS

Introduction and aim of the work

Fluctuations in the brain levels of the neuromodulator KYNA may control cognitive process and play a role in several neurological brain diseases (1). Since KAT II accounts for the majority of KYNA formation in the human brain, a KAT II selective inhibitor is an important pharmacological tool to control KYNA levels favouring precognitive effects. The potential harmful complete depletion of this neuroprotective molecule would be prevented by the action of other KAT isoenzymes (2). Development of isozyme-specific inhibitors is notoriously difficult, especially in the case of PLP-dependent aminotransferases, since the members of this family share significant conservation of the active site (3). To this end, the different geometry of the ligand-binding pocket in KAT I and II isozymes was exploited for the synthesis of the first potent and selective rat KAT II inhibitor, (S)-4-ethylsulfonylbenzoylalanine (S-ESBA), a close structural analogue of KYN that bears a bulky substituent on the anthranilic ring (4). ESBA was found to be pharmacologically active on rats KAT II but poorly active towards the human ortholog, as signaled by a 20-fold higher IC_{50} value (*4, 5*). On the basis of the results of a molecular docking approach, it was proposed that this different inhibitory activity might arise from the presence in the catalytic site of human KAT II of two hydrophobic residues, Leu40 and Pro76, which are substituted by polar serine residues in the rat enzyme (5). Recently, a human KAT II double-mutant harboring the serine residues characterizing the rat ortholog active site was generated, in order to investigate the molecular basis for ESBA species-specificity (2). Unexpectedly, the site-directed mutagenesis approach did not provide further experimental support to explain the striking difference in ESBA inhibitory efficiencies toward rat and human KAT II, and underlined the need for more in depth biochemical investigation aimed at deciphering the mechanism of ESBA inhibition. It is also worth noticing that rat KAT II displays a K_M for KYN of 0.66 mM (*6*), a value about ten-fold lower than the value determined for hKAT II (*7*). This observation indicates that the rat enzyme has evolved to recognize the physiological substrate KYN with a higher affinity compared with the human KAT II. Interestingly, both KYN and ESBA bind more tightly to the active site of the rat KAT II, suggesting that their binding is controlled by a similar mechanism. In this respect, it can be noted that S-ESBA retains the general amino acid chemical structure, opening the question whether this molecule is actually more a substrate than an inhibitor in the case of the human enzyme (*2*). This hypothesis can be investigated by determining the mechanism of S-ESBA action on hKAT II.

The isotype-specificity of a rat KAT II inhibitor, cysteine sulphinate (CSA), has been demonstrated for brain slices (*8*) and might be the starting point for the development of potent and specific inhibitors of the synthesis of KYNA in the brain. In mammals, endogenous sulphur-containing

amino acids, such as homocysteine, cysteine sulphinate, homocysteine sulphinate and cysteate, display neuroexcitatory actions similar to those of glutamate. These cysteine derivatives were able to reduce the production of KYNA in cortical slices in rats, due to their interaction with KATs. Thus, they were considered endogenous modulator of KYNA synthesis in the CNS (*9, 10*). In particular, CSA displayed unique specificity, inhibiting only the action of rat KAT II and showing an IC_{50} of approximately 2 μM (*8*), relatively close to the physiological brain level of CSA (*11, 12*). The potency of CSA as an inhibitor of human KAT II has never been evaluated so far. Moreover, the mechanisms of both CSA and ESBA inhibition on human KAT II have not yet been studied in depth. Therefore, a detailed analysis of the mechanisms of action of these two inhibitors was carried out.

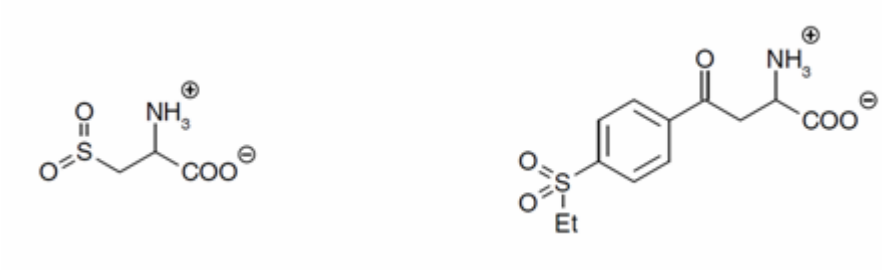

CSA **ESBA**

Materials and Methods

Materials. L-Kynurenine (K8625), CSA (C4418), glutamate oxidase from Streptomyces sp. (G5921), peroxidase from horseradish (P8375), o-dianisidine (D9143) were purchased from Sigma-Aldrich (St.Louis, MO). ESBA was synthesized as previously described (4, 5) and kindly provided by Prof. Roberto Pellicciari.

KAT transamination activity measured by a coupled glutamate oxidase-peroxidase assay. The amount of glutamate produced by transamination activity in the presence of KG was determined by an end-point assay based on the use of GOX and peroxidase. A reaction mixture containing 10 mM KG, 40 μM PLP and the potential aminogroup donor (CSA or ESBA), was equilibrated at the desired reaction temperature (25°C) in 50 mM Hepes, pH 7.5, before starting the reaction with addition of 2 μM KAT II. Aliquots (20 μL each) were removed after an appropriate incubation time, and stopped by mixing with 2 μL of 1.14 M phosphoric acid (final concentration 14 mM). Each aliquot was subsequently mixed with a detection solution containing 0.02 units of glutamate oxidase (GOX-Sigma G5921), 3 units of peroxidase (perox-Sigma P8375), 1 mM *O*-dianisidine (Sigma D9143) and 50 mM Hepes pH 7.5, in a final volume of 200 μL. The detection mixture was incubated at 37 °C for 30 minutes. Finally, the mixture was supplemented with 50 μL sulphuric acid

(final concentration 3.36 mM) to dissolve the occasional precipitates of oxidized *O*-dianisidine and to increase the sensitivity of the assay (*13*), before measuring the absorbance at 530 nm to quantify the extent of *O*-dianisidine oxidation. A calibration curve was prepared, using known concentrations of glutamate, ranging from 10 to 800 μM in the presence of 10 mM KG, 40 μM PLP, 14 mM phosphoric acid, 1 mM *O*-dianisidine (Sigma D9143), 0.02 units of glutamate oxidase (GOX-Sigma G5921), 3 units of peroxidase (Perox-Sigma P8375) and 50 mM Hepes pH 7.5, in a final volume of 200 μL. The reaction mixture was incubated and treated as above, and the absorbance at 530 nm was plotted against the initial amount of glutamate to generate a calibration curve. Blanks (control reactions) were set up using the same reagents as for the assay except for hKAT II that was replaced by the same volume of buffer.

KAT β-elimination activity measured by Nessler's assay. Reaction mixtures containing ammonia produced by β-elimination were tested with the Nessler's assay (*14*) using a ready-to-use solution (Fluka, code 72190). At pH 7.5 98% of ammonia is in the NH_4^+ form and the solubility of NH_3 in water at 25 °C is about 50 % (w/w), thus no significant loss of ammonia by evaporation is expected under these experimental conditions. A standard curve was built using ammonium sulfate solutions at concentrations in the range 1-20 mM. 40 μl of a solution containing ammonia were diluted with 860 μl of water. 100 μl of Nessler's reagent were added to the mixture and the absorbance of the solution immediately recorded at 436 nm.

Determination of CSA inhibition mechanism and dissociation constants. The mechanism of inhibition of CSA and its dissociation constants were determined by measuring the initial rate of reactions containing 870 nM hKAT II in 50 Mm Hepes pH 7.5 in the presence of 10 mM KG, 40 μM PLP and concentrations of KYN from 2.5 to 10 mM. The reactions were carried out at 25 °C in 0.1 cm optical path cuvettes either in the absence or presence of 4 mM and 20 mM CSA. Initial rates were measured from kinetic traces collected at 310 nm using the calculated $\Delta\varepsilon_{310\ nm}$ = 3625 M^{-1} cm^{-1} for KYNA.

Double reciprocal plots for uncompetitive inhibition of KAT II by CSA were globally fitted to linear equations of the type (*15*):

$$\frac{1}{V_0} = \left(\frac{appK}{appV}\right) \cdot \frac{1}{[KYN]} + \left(\frac{1}{appV}\right) \cdot \left(1 + \frac{[CSA]}{K_{ii}}\right) \qquad [1]$$

where appK and appV are apparent K_M and apparent V_{max}. The slope is the linking parameter, whereas the intercept is allowed to vary. A secondary plot of intercepts of the primary plots versus [CSA] gives an estimated K_{ii} as the abscissa intercept. Because the KYN concentration used in the assay is close to K_M, an approximated value of K_i can be obtained by the following:

$$K_i = \frac{K_{ii}}{2 \cdot \left(1 + \frac{[KG]}{K_M^{KG}}\right)} \qquad [2]$$

Determination of kinetics parameters for transamination reaction with ESBA. A continuous assay for the determination of kinetic parameters for the transamination reaction of ESBA with hKAT II was developed (see Results). Reactions (200 μL final volume) containing 50 mM Hepes pH 7.5, 10 mM KG, 40 μM PLP, and variable concentrations of ESBA (50 μM-15 mM) were incubated at 25°C. The reaction was started by the addition of 870 nM hKAT II and carried out at 25 °C in a 0.1 cm optical path cuvette. Initial rates were estimated exploiting the absorbance increase at 338 nm due to the accumulation of the ketoacid ESdiOBA (ε = 15,400 $M^{-1} \cdot cm^{-1}$).

Results

Reactivity with CSA.

CSA is a physiological substrate of AspAT (*16, 17*) due to its structural similarity with Asp. On the basis of structural considerations, CSA can, in principle, be a substrate for either transamination and β-elimination reaction catalyzed by KAT II, being sulfite a good leaving group. The reaction of hKAT II with CSA was first analyzed spectroscopically (Figure 1A). hKAT II reacts with 1.8 mM CSA showing a slow decrease of the intensity of the internal aldimine band at 360 nm and the accumulation of a species, likely PMP, absorbing at 330 nm. The reaction is completed in about 60 minutes. In the presence of the same enzyme concentration and 10 mM α-aminoadipate the reaction reaches equilibrium within 8 minutes (see Figure 1C in chapter 2). The occurrence of transamination activity on CSA in the presence of KG was demonstrated by a GOX-peroxidase coupled assay measuring the formation of glutamate. For the same reaction, the accumulation of ammonia was detected by a Nessler's assay, indicating that also a β-lytic side reaction takes place. Cysteine sulfinate is thus a poor substrate of KAT II rather than a pure, competitive inhibitor. To further investigate CSA mechanism of action, we exploited the new developed continuous spectrophometric assay for KYN aminotransferase activity monitoring the absorbance increase at 310 nm. hKAT II activity assays were carried out at two concentrations of cysteine sulfinate, namely 4 and 20 mM. A double reciprocal plot of the initial velocity against KYN concentration gave a series of parallel lines, indicative of an uncompetitive inhibition (Figure 1B). Double reciprocal plots for uncompetitive inhibition of hKAT II by CSA were globally fitted to equation 1 with a slope of 392±22 min and intercepts of 47±4, 68±6 and 94±6 mM^{-1} in the presence of 0, 4 and 20 mM CSA, respectively. A secondary plot of the intercepts of the first plot versus inhibitor concentration gave a straight line, allowing to estimate a K_{ii} for CSA of about 25 mM (Figure 1B,

inset) (*15*). The approximated value of K_i, calculated from equation 2, is 20 μM, in good agreement with the IC_{50} value from *in vivo* experiments on rats (*8*), which is about 2 μM. These experiments provide the first information on the mechanism of inhibition of hKAT II by CSA.

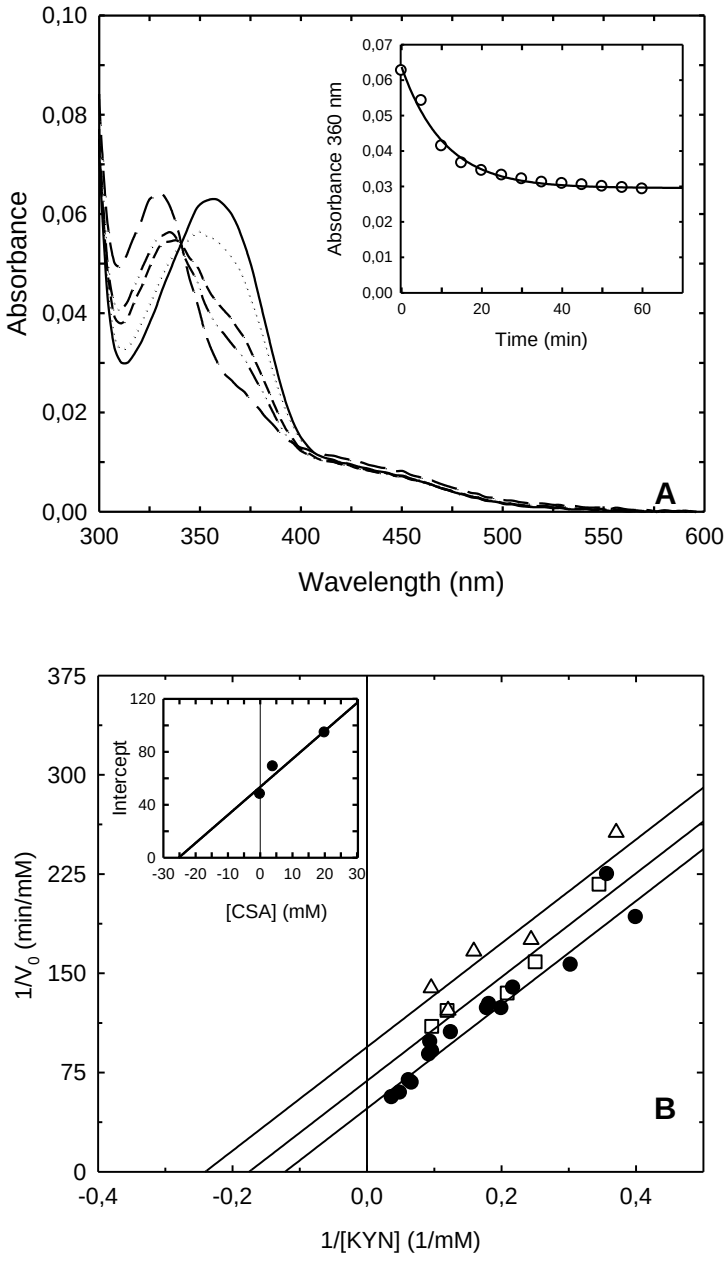

Figure 1. Reaction of hKAT II with CSA

A *Reaction of KATIIwith CSA monitored by absorption spectroscopy.*

Spectra of the reaction mixture containing 7 μM hKAT II in 50 mM Hepes, pH 7.5 at 25°C, were recorded in the absence (solid line) and presence of 1.8 mM CSA upon 5 (dotted line), 10 (short dashed line), 15 (dash dotted line) and 60 (long dashed line) minutes from the addition. **Inset**: time course of internal aldimine disappearance at 360 nm. The solid line represents the fitting to a monoexponential equation with k = 0.09 min^{-1}.

***B** Determination of the mechanism of inhibition and inhibition constants.*

The primary double reciprocal plot for KAT II inhibition by CSA was obtained by determining the rate of reaction in a mixture containing 870 nM hKAT II in 50 Mm Hepes pH 7.5 in the presence of 10 mM KG, 40 μM PLP and concentrations of KYN from 2.5 to 10 mM. The reaction was carried out at 25 °C in 0.1 cm optical path cuvettes either in the absence (closed circles) or presence of 4 mM (open squares) and 20 mM CSA (open triangles). The solid lines through data points represent a global fitting to equation 1 with a slope of 392±22 min and intercepts of 47±4, 68±6 and 94±6 mM^{-1} in the presence of 0, 4 and 20 mM CSA, respectively. **Inset:** secondary plot of the intercepts of the primary plot versus CSA concentration. The abscissa intercept, 25 mM, gives an estimate of the inhibition constant K_{ii}.

Reactivity with S-ESBA

ESBA is an aromatic compound analogous to the natural substrate KYN, that absorbs maximally at 287 nm, with an approximate extinction coefficient of 2050 M^{-1} cm^{-1} (Figure 2A, short dashed line). ESBA might be either a pure inhibitor, as previously proposed (4), or, more likely, a substrate analog. Indeed, the structure of ESBA bearing an amino acid moiety suggests that this molecule might be processed by the enzyme.

The interaction between ESBA and hKAT II was first investigated by analyzing the spectroscopic behaviour of the enzyme in its presence. Binding of ESBA to hKAT II, in the absence of 2-oxoacids, led to marked changes in the absorption spectrum, with intensity increase at 283 nm and at around 330 nm. (Figure 2A). The absorption spectrum of the reaction mixture changes with time up to 11' (dashed dotted line), indicating that ESBA is processed by the enzyme. Moreover, the final spectrum is similar but not coincident with the spectrum of PMP-KAT II, as collected in the presence of AAD (grey solid line). In particular, considering that in the absence of keto acids only one transamination cycle can take place, with consumption of an amount of ESBA equal to the amount of active sites, the product of the reaction show higher absorbance intensities at around 300 and 355 nm. The addition to the reaction mixture of 10 mM KG led to the accumulation of a species absorbing maximally at 338 nm (Figure 2B), likely the product of ESBA transamination, 4-(4-(ethylsulfonyl)phenyl)-2,4-dioxobutanoic acid (ESdiOBA) (Scheme 1). Spectral analysis of the product, after separation by ultrafiltration from the enzyme, showed a species with a single absorption peak centered at 338 nm (data not shown). As most αketo acids significantly absorb in the 320-340 nm region (*18*), it seems likely, from its spectroscopic properties, that this product represents the αketo acid generated by ESBA transamination. As a check, the occurance of transamination activity on ESBA was assessed by a GOX-peroxidase coupled assay for the same reaction mixture described in figure 2. The amount of ESBA transaminated by hKAT II at equilibrium (about 3 hours after the addition of KG) was found to be about the 90 % of the initial

ESBA concentration. Thus, the main product of the reaction is ESdiOBA, that is characterized by an extinction coefficient at 338 nm of 15,400 $M^{-1} \cdot cm^{-1}$.

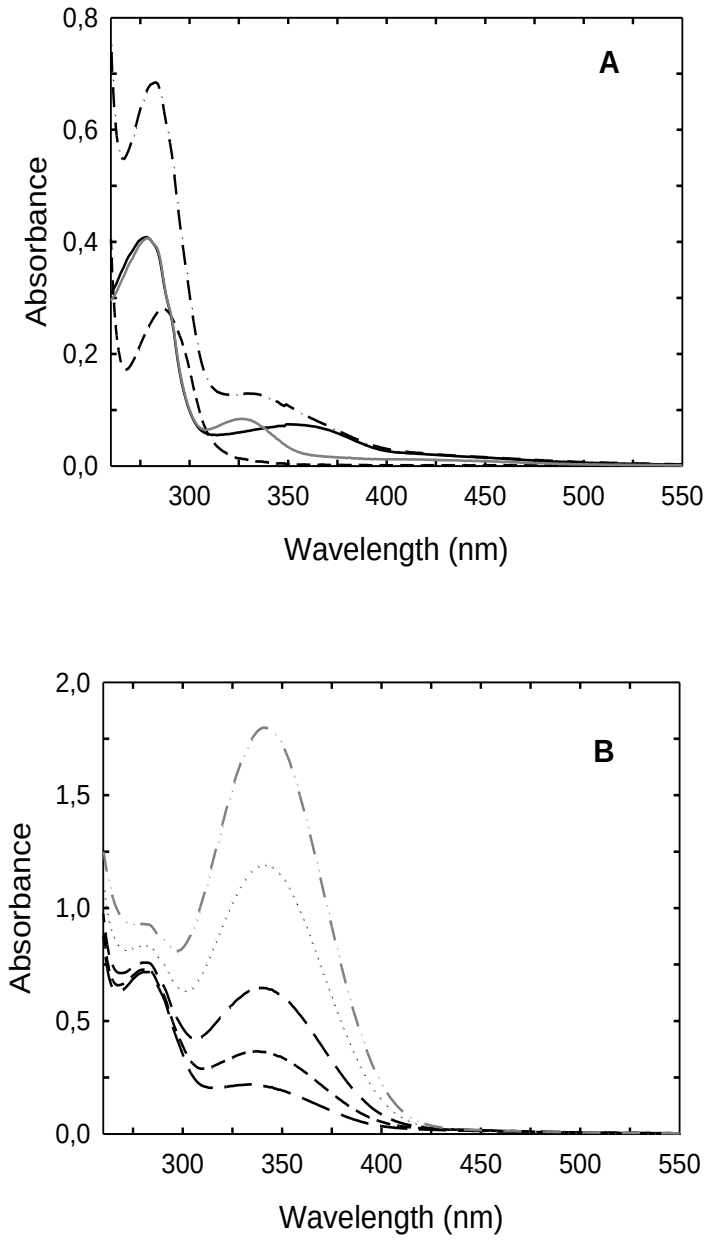

Figure 2. Reactivity of KATII towards ESBA

A Absorption spectra recorded for a solution containing 8 μM hKAT II in 50 mM Hepes, pH 7.5, 25 °C (black solid line), and in the presence of 100 μM ESBA at the equilibrium (dashed dotted line). For comparison, a spectrum of a solution containing 100 μM ESBA in 50 mM Hepes, pH 7.5 (short dashed line), and the spectrum of PMP-KAT II collected in the presence of AAD (grey solid line) are reported.

B Upon addition of 10 mM KG a series of spectra was collected after 1' (long dashed line) , 5' (short dashed line), 15' (medium dashed), 45' (dotted line) and 185' (grey dashed dot-dot line). Spectra were corrected for KG contribution.

Based on previous experiments carried out in the presence of compounds undergoing β-elimination, it was verify whether a β-lytic reaction takes place on ESBA. In fact, it is reported in the literature that p-substituted benzaldehyde is produced by the αβ elimination activity of kynureninase on kynurenine (*19*). If a β-elimination reaction on ESBA is taking place, accumulation of ammonia is expected and can be compared to the amount of ammonia produced in the reaction with the good β-elimination substrate BCA. The rate of β-elimination was determined by monitoring the formation of ammonia as a function of time for a solution containing 2 μM KAT II, 8 mM ESBA and 10 mM KG (Figure 3). The reaction is linear within 180', with a slope of 2.5 μM/min ammonia (e.g. the specific activity is 25 pmol/μg·min). This rate is expected to be a lower limit, since, for substrates with poor leaving groups, transamination reaction, in the presence of 2-oxo acids, is favoured with respect to the β-elimination reaction. As a comparison, the reaction of KAT II with 5 mM BCA gave a specific activity of 5 nmol/μg·min, thus indicating that ESBA is a poor substrate for β-elimination.

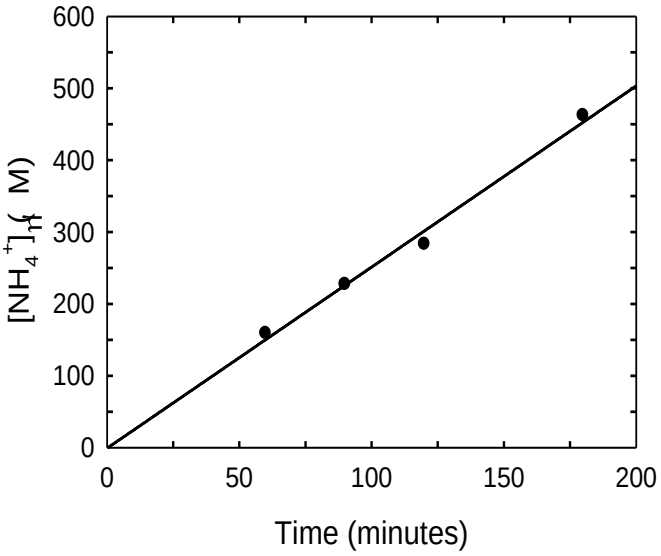

Figure 3. β-elimination kinetics of ESBA by hKAT II

The amount of ammonia formed in a reaction mixture containing 2 μM hKAT II, 8 mM ESBA and 10 mM KG was determined as a function of time with the Nessler's assay. The solid line through data points represents the fitting to a linear equation with slope 2.5 ± 0.18 μM/min.

Taken together these findings confirm that, as previously supposed, ESBA is a good substrate for hKAT II rather than a pure competitive inhibitor, and indicate two possible pathways for ESBA processing by hKAT II, as shown in Scheme 1. The reaction of hKAT II with ESBA proceeds mainly *via* a transamination reaction, producing 4-(4-(ethylsulfonyl)phenyl)-2,4-dioxobutanoic acid (ESdiOBA). This reaction is accompanied by a β-elimination side-reaction that likely gives a p-substituted benzaldehyde. Both products are expected to absorb at wavelengths lower than 350 nm (*18, 20*) and are merely hypothesized, as any attemps to identify them by mass spectrometry failed.

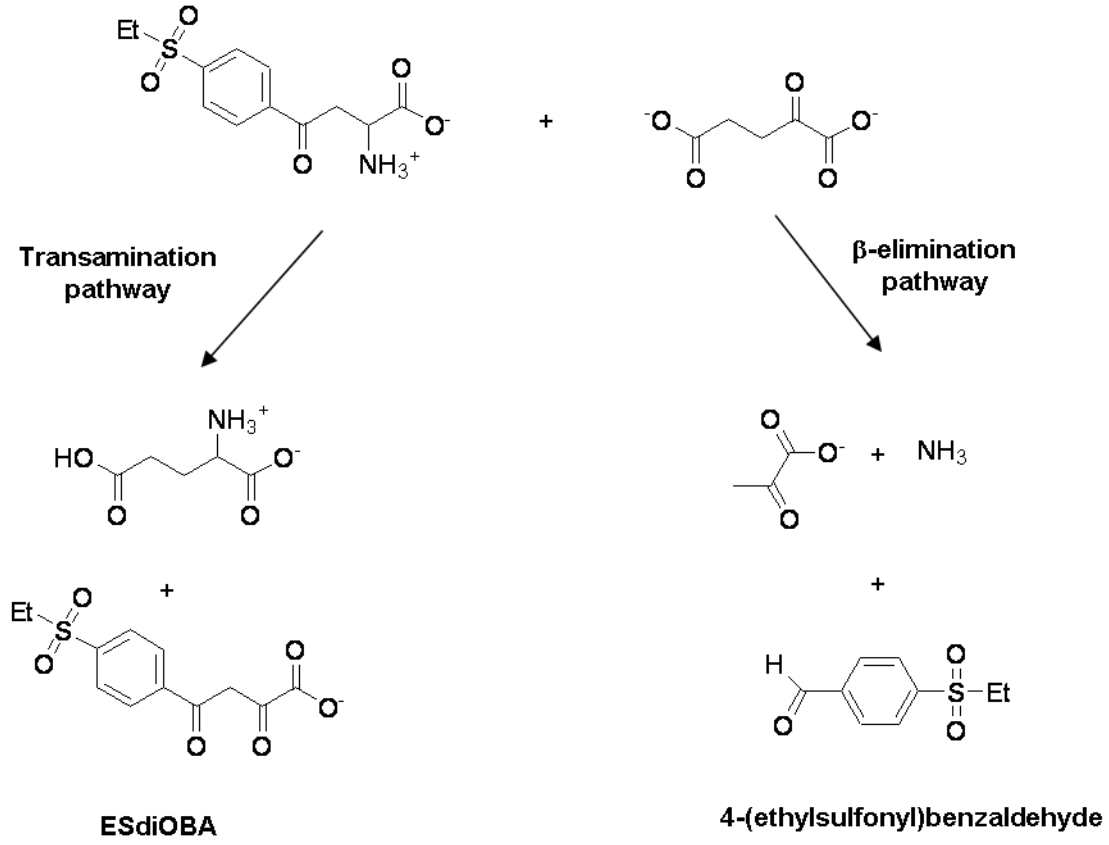

Scheme 1. Reaction pathways for ESBA (in the presence of KG as amino group acceptor) to give either 4-(4-(ethylsulfonyl)phenyl)-2,4-dioxobutanoic acid (ESdiOBA) or 4-(ethylsulfonyl)benzaldehyde.

We have also assessed whether ESBA or its reaction products inactivate hKAT II, as it was observed with BCA. A solution of KAT II (174 μM) was incubated with 8 mM ESBA for 60 minutes, at 25 °C. The reaction was diluted 200 fold in an assay solution containing 10 mM KYN and 10 mM KG. hKAT II reacted with ESBA was found to be two fold less active than the unreacted enzyme, suggesting that β-lytic activity of ESBA might lead to syncatalytic inactivation of the enzyme. The enzyme that reacted with ESBA was unstable, as a PLP-ESBA derivative could not be recovered

neither after ultrafiltration nor gel filtration on micro spin columns. This hampered the determination of the type of modification by mass spectrometry.

Unlike in the case of CSA, the mechanism of inhibition of ESBA on hKAT II could not be determined, due to the heavy interference of ESBA spectrum with spectroscopic signals used to monitor hKAT II activity. However, the affinity of ESBA for hKAT II could be estimated exploiting the absorbance increase at 338 nm due to the accumulation of the ketoacid ESdiOBA. Kinetic parameters for the transamination reaction of ESBA with hKAT II were determined by collecting kinetic traces at 338 nm at different ESBA concentrations. Data were fitted to the Michaelis Menten equation with K_M = 4.5 ± 0.9 mM and V_{max} = 7.8 ± 0.6 μM/min (Figure 4). k_{cat} for the reaction of hKAT II with ESBA is 9 min^{-1}, only about 2.5 fold less than the value of 25 min^{-1} for the reaction with KYN. Moreover, the inhibition of hKAT II by ESBA was further assessed by a colorimetric hightroughput screening assay, as illustrated in the following chapter.

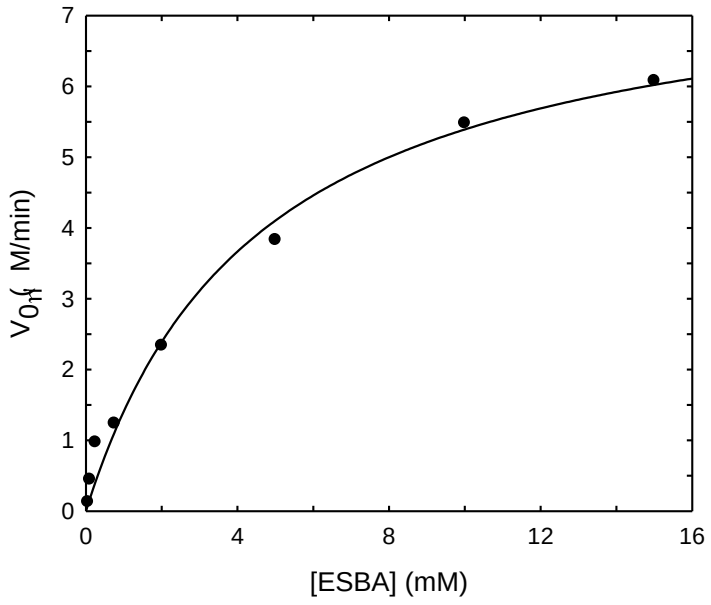

Figure 4. Dependence of the rate of reaction of hKATnII on ESBA concentration in the presence of KG. The reaction mixture contained 870 nM hKAT II in 50 mM Hepes pH 7.5 in the presence of 10 mM KG and variable concentrations of ESBA (50 μM-15 mM). The reaction was carried out at 25 °C in 0.1 cm optical path cuvettes. The solid line through data points represents the fitting to the Michaelis Menten equation with V_{max} = 7.8 ± 0.6 μM/min and K_M = 4.5 ± 0.9 mM.

Discussion

In vivo experiments have indicated that both CSA and ESBA are inhibitors of KAT II (*4, 5, 8*), but their mechanisms of action were never studied in depth. On the basis of structure-reactivity considerations, they might be substrates for either transamination and β-elimination reactions.

Their interactions with hKAT II were evaluated by both spectroscopic analysis and monitoring the accumulation of reaction products. Our findings demonstrate that both CSA and ESBA are substrate analogs and not purely competitive inhibitors.

CSA is a physiological substrate of AspAT that is able to catalyze both the transamination (*21, 22*) of CSA and its β-elimination as a side reaction (*23*). CSA is an effective amino donor substrate for AspAT, probably because a product of the aminotransferase reaction, β-sulfinylpyruvate, decomposes non enzymatically to SO_3^{2-} and pyruvate, and hence the aminotransferase reaction is irreversible (*21*). In the case of hKAT II, cysteine sulfinate is a very slow transamination substrate when compared to the natural substrate AAD. Inhibition of hKAT II by CSA was determined to be uncompetitive, a quite unexpected finding, considering that CSA is also a substrate of hKAT II, converting the PLP form of the enzyme to the PMP form. Uncompetitive inhibition involves the exclusive (or predominant) binding of the inhibitor to the enzyme-substrate complex or to any intermediate downstream of it (*15*). This mode of inhibition is quite rare in nature and is particularly encountered in multi-substrate reactions (*24-29*), where the inhibitor is competitive with respect to one substrate (S_2) but not with respect to another (S_1). The reaction scheme is represented by

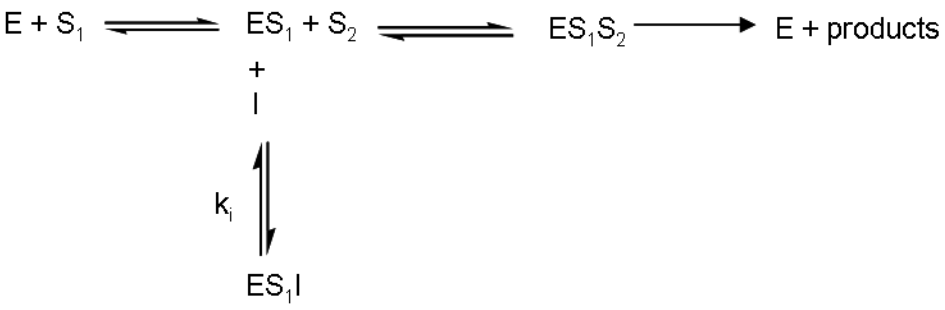

Inhibition occurs since ES_1I is catalytically inactive. As it can not form product, it is a dead end complex which has only one fate, to returns ES_1. The uncompetitive inhibition is most noticeable at high substrate concentrations (i.e. S_1 in the scheme above) and cannot be overcome as both the V_{max} and K_M are equally reduced. Normally, the uncompetitive inhibitor also bears some structural similarity to one of the substrates. In the case of CSA, uncompetitive inhibition could come from preferential binding of CSA to the PMP form of hKAT II, suggesting that CSA might better mimic KG than KYN or AAD.

In the case of ESBA, the mechanism of inhibition could not be determined due to its strong interference with the continuous spectrophotometric assay for KYN aminotransferse activity. However, the spectroscopic signal generated by the accumulation of the product of the reaction of ESBA with hKAT II was exploited to calculate the kinetic parameters for the transamination of ESBA by hKAT II and, thus, an approximate affinity of the inhibitor for the enzyme. An apparent K_M of 4.5 mM is in good agreement with a 64 % inhibition exerted by 1 mM ESBA (5). Any attempt to

identify the reaction products by mass spectrometry was unsuccessful. Although the identity of the product could not be assessed, it seems likely, from its spectroscopic properties, that it represents the α-ketoacid generated by ESBA transamination. Occurrence of transamination activity on ESBA was confirmed by the detection of the other product of transamination activity, glutamate. As expected on the basis of ESBA structure, this substrate analogue is processed by hKAT II mainly *via* a transamination reaction, which is accompanied by a β-lyase side activity. A rough estimate of the catalytic efficiency for β-elimination reaction, based on specific activity at a fixed substrate concentration, indicate that ESBA, as KYN, is a poor substrate for β-elimination, when compared to BCA. However, ESBA, like BCA, is capable of permanently inactivating hKAT II through a mechanism that, likely, involves formation of a covalent adduct between the active site lysine residue and the α–aminoacrylate intermediate, as already reported for alanine aminotransferase (*30*) and AspAT (*31*) (see Scheme 4 in chapter 3).

In conclusion, although both CSA and ESBA show good inhibitory properties on hKAT II, with, at least for CSA, inhibition constants in the micromolar range, these molecules are actually substrates. In particular, the nature of the reaction of ESBA with hKAT II, possibly involving a syncatalytic inactivation and a β-elimination reaction with production of an aromatic aldehyde, suggest caution in the clinical application of this molecule or its structural analogues. Understanding the mechanisms of hKAT II inhibitors is important not only to enable the design of better hKAT II inhibitors, but also to understand the enzyme reaction mechanisms. Control of reaction mechanism is particularly important for PLP-dependent enzymes because it is known that they catalyze side reactions at significant rates with substrates analogues or even with their natural substrates (*3*).

REFERENCES

1. Rossi, F., Valentina, C., Garavaglia, S., Sathyasaikumar, K. V., Schwarcz, R., Kojima, S., Okuwaki, K., Ono, S., Kajii, Y., and Rizzi, M. Crystal structure-based selective targeting of the pyridoxal 5'-phosphate dependent enzyme kynurenine aminotransferase II for cognitive enhancement, *Journal of medicinal chemistry 53*, 5684-5689.
2. Casazza, V., Rossi, F., and Rizzi, M. Biochemical and Structural Investigations on Kynurenine Aminotransferase II: An Example of Conformation-Driven Species-Specific Inhibition?, *Current topics in medicinal chemistry*.
3. Amadasi, A., Bertoldi, M., Contestabile, R., Bettati, S., Cellini, B., di Salvo, M. L., Borri-Voltattorni, C., Bossa, F., and Mozzarelli, A. (2007) Pyridoxal 5'-phosphate enzymes as targets for therapeutic agents, *Current medicinal chemistry 14*, 1291-1324.
4. Pellicciari, R., Rizzo, R. C., Costantino, G., Marinozzi, M., Amori, L., Guidetti, P., Wu, H. Q., and Schwarcz, R. (2006) Modulators of the kynurenine pathway of tryptophan metabolism: synthesis and preliminary biological evaluation of (S)-4-(ethylsulfonyl)benzoylalanine, a potent and selective kynurenine aminotransferase II (KAT II) inhibitor, *ChemMedChem 1*, 528-531.
5. Pellicciari, R., Venturoni, F., Bellocchi, D., Carotti, A., Marinozzi, M., Macchiarulo, A., Amori, L., and Schwarcz, R. (2008) Sequence variants in kynurenine aminotransferase II (KAT II) orthologs determine different potencies of the inhibitor S-ESBA, *ChemMedChem 3*, 1199-1202.
6. Guidetti, P., Amori, L., Sapko, M. T., Okuno, E., and Schwarcz, R. (2007) Mitochondrial aspartate aminotransferase: a third kynurenate-producing enzyme in the mammalian brain, *Journal of neurochemistry 102*, 103-111.
7. Han, Q., Cai, T., Tagle, D. A., Robinson, H., and Li, J. (2008) Substrate specificity and structure of human aminoadipate aminotransferase/kynurenine aminotransferase II, *Bioscience reports 28*, 205-215.
8. Kocki, T., Luchowski, P., Luchowska, E., Wielosz, M., Turski, W. A., and Urbanska, E. M. (2003) L-cysteine sulphinate, endogenous sulphur-containing amino acid, inhibits rat brain kynurenic acid production via selective interference with kynurenine aminotransferase II, *Neurosci. Lett. 346*, 97-100.
9. Han, Q., and Li, J. (2004) Cysteine and keto acids modulate mosquito kynurenine aminotransferase catalyzed kynurenic acid production, *FEBS letters 577*, 381-385.
10. Han, Q., Li, J., and Li, J. (2004) pH dependence, substrate specificity and inhibition of human kynurenine aminotransferase I, *European journal of biochemistry / FEBS 271*, 4804-4814.

11. Cuenod, M., Grandes, P., Zangerle, L., Streit, P., and Do, K. Q. (1993) Sulphur-containing excitatory amino acids in intercellular communication, *Biochemical Society transactions 21*, 72-77.
12. Kilpatrick, I. C., and Mozley, L. S. (1986) An initial analysis of the regional distribution of excitatory sulphur-containing amino acids in the rat brain, *Neuroscience letters 72*, 189-193.
13. Washko, M. E., and Rice, E. W. (1961) Determination of glucose by an improved enzymatic procedure, *Clinical chemistry 7*, 542-545.
14. Barnes, A. R., and Sugden, J. K. (1990) Comparison of colourimetric methods for ammonia determination, *Pharm Acta Helv 65*, 258-261.
15. Cook, P. F., and Cleland, W. W. (2007) *Enzyme Kinetics and Mechanism*, Taylor and Francis Group, LLC, New York.
16. Parsons, B., and Rainbow, T. C. (1984) Localization of cysteine sulfinic acid uptake sites in rat brain by quantitative autoradiography, *Brain Res. 294*, 193-197.
17. Weinstein, C. L., Haschemeyer, R. H., and Griffith, O. W. (1988) In vivo studies of cysteine metabolism. Use of D-cysteinesulfinate, a novel cysteinesulfinate decarboxylase inhibitor, to probe taurine and pyruvate synthesis, *J. Biol. Chem. 263*, 16568-16579.
18. Donini, S., Ferrari, M., Fedeli, C., Faini, M., Lamberto, I., Marletta, A. S., Mellini, L., Panini, M., Percudani, R., Pollegioni, L., Caldinelli, L., Petrucco, S., and Peracchi, A. (2009) Recombinant production of eight human cytosolic aminotransferases and assessment of their potential involvement in glyoxylate metabolism, *Biochem. J. 422*, 265-272.
19. Longenecker, J. B., and Snell, E. E. (1955) A possible mechanism for kynureninase action, *J. Biol. Chem. 213*, 229-235.
20. Dearden, J. C., and Forbes, W. F. (1958) LIGHT ABSORPTION STUDIES. PART XII. ULTRAVIOLET ABSORPTION SPECTRA OF BENZALDEHYDES, *Canadian Journal of Chemistry 36*, 1362-1370.
21. Kim, H., Ikegami, K., Nakaoka, M., Yagi, M., Shibata, H., and Sawa, Y. (2003) Characterization of aspartate aminotransferase from the cyanobacterium Phormidium lapideum, *Biosci Biotechnol Biochem 67*, 490-498.
22. Yagi, T., Kagamiyama, H., and Nozaki, M. (1979) Cysteine sulfinate transamination activity of aspartate aminotransferases, *Biochem. Biophys. Res. Commun. 90*, 447-452.
23. Graber, R., Kasper, P., Malashkevich, V. N., Strop, P., Gehring, H., Jansonius, J. N., and Christen, P. (1999) Conversion of aspartate aminotransferase into an L-aspartate beta-decarboxylase by a triple active-site mutation, *J. Biol. Chem. 274*, 31203-31208.
24. Ghosh, N. K., and Fishman, W. H. (1966) On the mechanism of inhibition of intestinal alkaline phosphatase by L-phenylalanine. I. Kinetic studies, *The Journal of biological chemistry 241*, 2516-2522.

25. Nahorski, S. R., Ragan, C. I., and Challiss, R. A. (1991) Lithium and the phosphoinositide cycle: an example of uncompetitive inhibition and its pharmacological consequences, *Trends in pharmacological sciences 12*, 297-303.
26. Hoylaerts, M. F., Manes, T., and Millan, J. L. (1992) Molecular mechanism of uncompetitive inhibition of human placental and germ-cell alkaline phosphatase, *The Biochemical journal 286 (Pt 1)*, 23-30.
27. Boocock, M. R., and Coggins, J. R. (1983) Kinetics of 5-enolpyruvylshikimate-3-phosphate synthase inhibition by glyphosate, *FEBS letters 154*, 127-133.
28. Pollack, S. J., Atack, J. R., Knowles, M. R., McAllister, G., Ragan, C. I., Baker, R., Fletcher, S. R., Iversen, L. L., and Broughton, H. B. (1994) Mechanism of inositol monophosphatase, the putative target of lithium therapy, *Proceedings of the National Academy of Sciences of the United States of America 91*, 5766-5770.
29. Fell, D. A., and Snell, K. (1988) Control analysis of mammalian serine biosynthesis. Feedback inhibition on the final step, *The Biochemical journal 256*, 97-101.
30. Morino, Y., Kojima, H., and Tanase, S. (1979) Affinity labeling of alanine aminotransferase by 3-chloro-L-alanine, *J. Biol. Chem. 254*, 279-285.
31. Cooper, A. J., Bruschi, S. A., Iriarte, A., and Martinez-Carrion, M. (2002) Mitochondrial aspartate aminotransferase catalyses cysteine S-conjugate beta-lyase reactions, *Biochem. J. 368*, 253-261.

CHAPTER 5

DEVELOPMENT OF A HIGH-THROUGHPUT SCREENING ASSAY FOR hKAT II INHIBITORS

Introduction and aim of the work

KYNA is a neuroinhibitory metabolite of the kynurenine pathway acting as an antagonist of both the α7-nicotinic acetylcholine receptor and the NMDA glutamate receptor (1-3). Since these effects are detected at KYNA concentrations found in the mammalian brain, altered KYNA levels could signal malfunctioning of neuronal excitability and synaptic plasticity. In particular, chronically increased levels of KYNA can lead to hypofunction of glutamatergic and cholinergic neurotransmission, which has been proposed to play a causative role in cognitive impairments seen in Alzheimer's disease (4), schizophrenia (5,6) and Down syndrome (7). In the brain as elsewhere, KYNA is formed enzymatically by the irreversible transamination of the pivotal kynurenine pathway metabolite kynurenine (KYN). At least, four aminotransferases can utilize kynurenine as the amino donor of the transamination reaction in the mammalian brain (8). However, only one of them, KAT II, accounts for the majority of cerebral KYNA synthesis in rat and human brain tissue (9). Hence, selective inhibition of KAT II is an attractive strategy for therapeutically normalization of increased levels of KYNA in the diseased brain (10,11). The ability to pharmacologically modulate KAT II has been limited, and only a rat-specific KAT II inhibitor, ESBA, with poor potency toward the human ortholog, has been reported (12-15). A different rat KAT II inhibitor, BFF 122, has been discovered recently (16), exhibiting also activity against human KAT II (17). The mechanisms of action of these two inhibitors have been ascertained: BFF 122 forms a hydrazone adduct with PLP and is thus an irreversible inhibitor (17), whereas ESBA is actually a substrate undergoing a transamination reaction (see above). Thus, although to date available KAT II inhibitors are good *in vitro* and are valuable experimental tools for the elucidation of the role of the kynurenine pathway in brain function (12,16), they should be improved for possible future orally administered *in vivo* drugs. Therefore, there is a need for novel and optimized KAT II inhibition structures. To select structures leading to potent KAT II inhibitors, it is necessary to develop a simple and sensitive high-throughput-compatible enzymatic screening tool. In recent years, assaying enzyme-catalyzed transformations in high-throughput systems has become crucial to enzyme discovery, enzyme engineering and the drug discovery process (18). In most high-throughput enzyme assays, catalytic activity is detected using labelled substrates or indirect sensor systems that produce a detectable spectroscopic signal upon reaction (19-23). To date, the discovery of KAT II inhibitors has been hampered by the inability to use the existing HPLC-based KAT assay for high-throughput screening. A very recent study (10) reports a modification of the conventional HPLC fluorescence

method that enabled the development of a 96-well microplate fluorescence assay for analysis of *in vitro* human KAT I activity. KYNA enzymatically produced from KYN is measured directly in the reaction mixture fluorimetrically (λ_{exc} = 344 nm, λ_{em} = 398 nm). The major advantages of this new assay is that it is amenable for high-throughput screening due to its simplicity and low cost compared to exiting HPLC method. However, a significant drawback of this assay is that compounds that fluoresce at similar wavelengths can be lost. Moreover, another important shortcoming of this method is the long incubation time (4 hours at 37°C), which harbours significant risks in compounds screening, such as formation of active breakdown products or compounds instability. This fluorescence-based method, which was reported for KAT I using KYN as substrate, could also detect activity of other KAT isoforms, as they all use KYN as amino group donor and have activity at the applied pH range (8,24-26). Therefore, this method is not a KAT II-specific assay. The lack of a specific assay for each individual KAT represents a significant drawback in clinic and pharmacological studies, as it is impossible to ascertain which isoenzyme being affected by the action of tested inhibitors. Among KATs isoforms, KAT II is unique in having aminoadipate (AAD) aminotransferase activity. We exploited this substrate specificity to develop a specific and sensitive method to assay KAT II activity, based on the coupling of KAT II activity to two reporter reactions catalyzed by glutamate oxidase and peroxidase. This end-point assay was efficiently implemented on a 96-well plate format for rapid high-throughput screening of hKAT II inhibitors. To validated the assay, we investigated its ability to differentiate between known KAT II inhibitors of various potencies. Although KAT II is considered an interesting drug target in the treatment of schizophrenia and other neurological disorders (11,13), only a few compounds have been so far described as potent KAT II inhibitors (12-14,16,27-29) (Scheme 1): cysteine sulfinate (CSA) on brain slices of rats (27), ESBA in dialysis experiments on rat hippocampus (13), 1-Methyl-4-phenylpyridinium (MPP^+) and 3-nitropropionic acid (3-NPA) on both cortical brain slices and partially purified KATs (29), *O*-phosphoserine (OPS) on rat brain tissue homogenates (28) and BFF122 on both rat brain tissue homogenates (16) and recombinant human KAT II (17). MPP^+ is the metabolite of 1-Methyl-4-phenyl-1,2,3,6-tetrahydropyridine (MPTP), a contaminant of “street drugs”, whereas 3-NPA is a toxin produced by fungi and plants. Both MPP^+ and 3-NPA are mitochondrial toxins that inhibit the mitochondrial respiratory complex I and II, respectively (29-33). Compromised energy metabolism associated with these two mitochondrial toxins has been supposed to increase the vulnerability of neurons to the endogenous glutamate and thus initiate changes leading to neurodegeneration (34). Enzymatic studies revealed that MPP^+ inhibits the activity of rat KAT II, but not the activity of rat KAT I, whereas 3-NPA affects the activity of both enzymes (29). Thus, the neurotoxic consequences evoked by MPP^+ and 3-NPA may be at least partially associated with the decrease of KYNA production. Although MPP^+ was proved to be able to discriminate between KAT I and KAT II, stimulating the design of isoform-specific inhibitors, the use of this compound triggers Parkinsonian symptoms (35). Therefore, we tested only the inhibition

activity of 3-NPA. We tested also the inhibition brought about OPS as in rat brain tissue homogenates, some metabotropic glutamate receptor (mGluR) ligands, such as quisqualate and OPS, inhibited KAT II activity, but not KAT I, therefore reducing KYNA formation (28). This effect should be taken into consideration when novel mGluR ligands are developed for the treatment of neurological and psychiatric diseases.

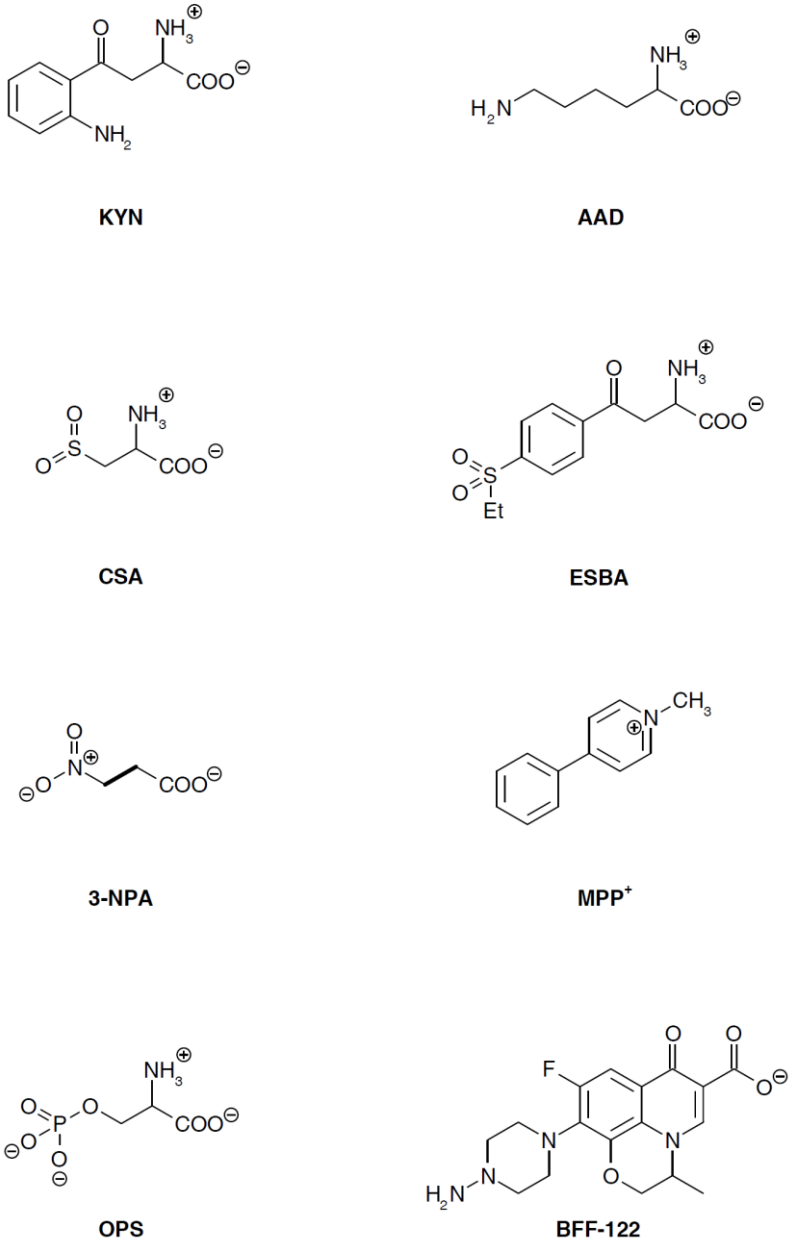

Scheme 1. Natural substrates (KYN and AAD) and inhibitors [ESBA (13,14), CSA (27), MPP^+, 3-NPA (29), OPS (28), BFF-122 (16,36)] of KATII.

Materials and methods

Materials. KYN (K8625), AAD (A0637), CSA (C4418), 3-NPA (N5636), OPS (P0878), glutamate oxidase from Streptomyces sp. (G5921), peroxidase from horseradish (P8375) and *O*-dianisidine (D9143) were purchased from Sigma-Aldrich (St.Louis, MO). ESBA was synthesized as previously described (13,14) and kindly provided by Prof. Roberto Pellicciari.

KAT transamination activity measured in a 96-well microplate by a coupled glutamate oxidase-peroxidase assay (GOX-peroxidase coupled assay). Reactions were performed in 96-well tissue culture plate (Sarstedt). According to final optimized conditions, reaction mixtures containing 10 mM AAD, 10 mM KG, 40 μM PLP, 2.2 μM hKAT II, 50 mM Hepes, pH 7.5, were incubated at 25 °C for 30 minutes. The reactions were stopped with 14 mM phosphoric acid. 0.015 units of glutamate oxidase (GOX-Sigma G5921), 2.25 units of peroxidase (perox-Sigma P8375) and 0.75 mM *O*-dianisidine were added to the solution. The mixture was incubated at 37 °C for 90 minutes. 3.36 mM sulphuric acid was added and the absorbance was measured at either 500 or 550 nm using a home-developed plate reader. Blanks were set up using the same reagents as for the assay except hKAT II was replaced by the same volume of buffer. A calibration curve using known concentrations of glutamate, ranging from 10 to 800 μM in the presence of 10 mM KG, 40 μM PLP and 14 mM phosphoric acid, was build to measure the amount of glutamate produced in the enzymatic reactions. Inhibition assays were set up by adding in the reaction mixture either cysteine sulfinate (CSA), β-chloroalanine (BCA), (R)-2-amino-4-(4-(ethylsulfonyl)-4-oxobutanoic acid (ESBA), 3-nitropropionic acid (3-NPA) or *O*-phosphoserine (OPS). CSA, CSA, 3-NPA, OPS and ESBA at the same concentrations used for the inhibition assays were also tested for transamination activity in the presence of 10 mM KG. All measurements were performed in duplicate.

Results

Because hKAT II is a potential target for pro-cognitive interventions in schizophrenia and other neurological disorders, a high-throughput screening assay to identify hKAT II inhibitors was developed. The assay implemented on a 96-well microplate format is based on the end-point associated with the consumption by glutamate oxidase of glutamate produced during the transamination of AAD, or other substrates, in the presence of KG. GOX specifically catalyzes the oxidative deamination of L-glutamate with the formation of α-ketoglutarate, ammonia and hydrogen peroxide (37). The latter reacts with *O*-dianisidine in the presence of peroxidase to form a stable coloured product, absorbing at 530 nm that is proportional to the glutamate concentration. When measured in microplate, the oxidized *O*-dianisidine spectrophotometric signal was linearly proportional for a wide range of glutamate concentration (10 μM to 800 μM), hence fulfilling the

requirement for detection system linearity. The conditions of the GOX-peroxidase end-point system were optimized to ensure assay sensitivity, reliability and reproducibility, as already described in chapter 3. Incubation time and reagents concentrations allow for product to accumulate to readily detectable levels in the presence of relatively low substrate concentrations, which in turns helps avoid saturation of the reaction. This assay is well suited to monitor both the transamination of potential substrates and the inhibition brought about by molecules rationally designed or, more importantly, by libraries of compounds to be screened. Using the optimized GOX-peroxidase endpoint assay we performed a 96-well microplate assay in order to assess at the same time the transamination activity with potential amino donor substrates and the inhibition of AAD transamination activity in the presence of compounds which have been described as KAT II inhibitors. Results of 96-well plate assay are shown in Figure 1. A mixture containing 2.2 μM hKAT II and 10 mM KYN, incubated for 30 min, led to the formation of 810 ± 91.9 μM glutamate, i.e. 8.1 ± 0.9 % of KYN was transaminated within the incubation time. When the reaction was carried out in solution and the transamination determined directly by the absorption intensity of KYNA ($\varepsilon_{310\ nm}$ = 3625 $M^{-1}cm^{-1}$), the same degree of KYN transamination was measured. The transamination reaction in the presence of 10 mM AAD generated a higher amount of glutamate (1.1 ± 0.0997 mM) due to the higher catalytic efficiency of KAT II towards AAD with respect to KYN (26). 1 mM ESBA, 200 μM CSA and 2 mM OPS gave a measurable transamination, which was about 8 ± 0.78, 1.4 ± 0.07 and 41 ± 4.2 % of the transamination with AAD, respectively (Figure 1B). Transamination in the presence of either 5 mM BCA or 50 mM 3-NPA was found to be negligible (Figure 1B). Furthermore, the assay allows to identify compounds that specifically inhibit KAT II activity. It was found that the presence of either 1 mM or 100 μM ESBA leads to 71 ± 4.9 % and 63 ± 1.4 % hKAT II activity inhibition, respectively (Figure 1B), in good agreement with data previously obtained (64 % inhibition exerted at 1 mM ESBA) (14). CSA, BCA, 3-NPA and OPS inhibition of hKAT II was also measured (Figure 1B) and found to be in good agreement with data reported in the literature, showing an IC_{50} value of approximately 2 μM for CSA (27), and inhibition of 24% and 38% exerted at 5 mM NPA (29) and 1 mM OPS (28), respectively.

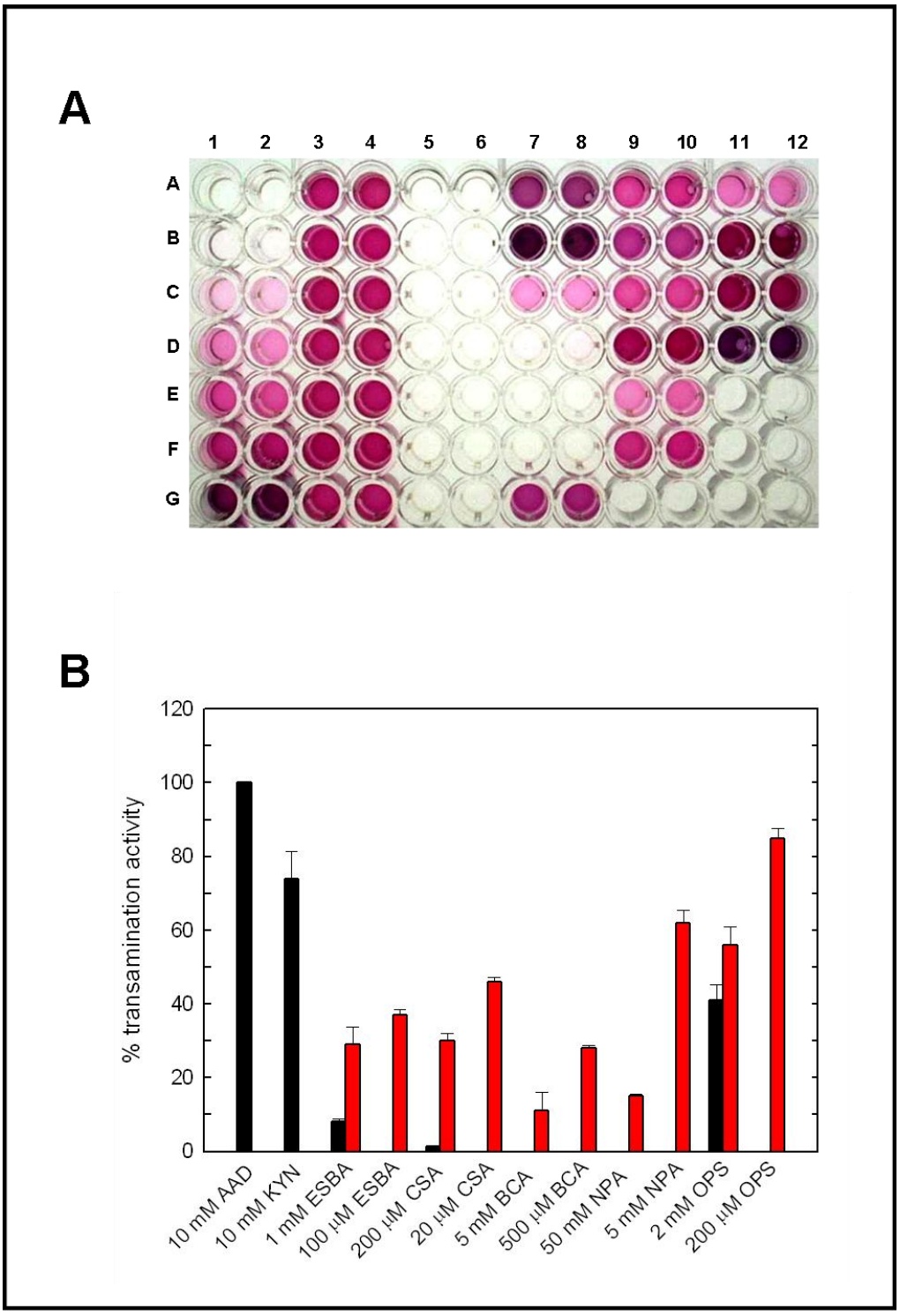

Figure 1. Representative 96-well microplate assay for substrates and inhibitors of hKAT II.

A Each reaction well contained 10 mM KG and 40 µM PLP in 50 mM Hepes, pH 7.5. Reactions were allowed to proceed for 30 minutes at 25 °C and stopped with phosphoric acid to a final concentration of 14 mM. To the reaction mixture, a solution containing 0.75 mM *O*-dianisidine, 0.015 U GOX and 2.25 U peroxidase was added. The reaction was allowed to develop for 90 minutes at 37 °C, and stopped with 3.66 M sulfuric acid. Each reaction well was duplicated (odd

and even lines). Wells in lines **1** and **2** were used to build a calibration curve using the following glutamate concentrations: 0 (A), 10 μM (B), 50 μM (C), 100 μM (D), 200 μM (E), 400 μM (F), 800 μM (G). The effect of tested molecules on the reporter GOX-peroxidase reaction is shown in line **3** and **4**. Each well contains 400 μM GLU and 10 mM KYN (A), 10 mM AAD (B), 1 mM ESBA (C), 200 μM CSA (D), 5 mM BCA (E), 50 mM NPA (F), 2 mM OPS (G). Wells in lines **5** and **6** are blanks containing only tested molecules at the higher concentration. The transamination activity of 10 mM KYN (A), 10 mM AAD (B), 1 mM ESBA (C), 200 μM CSA (D), 5 mM BCA (E), 50 mM 3-NPA (F) and 2 mM OPS (G) in the presence of 2.2 μM hKAT II is shown in lines **7** and **8**. In lines **9-12** each molecule is tested for inhibition of the transamination reaction in the presence of 10 mM AAD and 2.2 μM hKAT II using the following concentrations of inhibitors: 1 mM ESBA (A9-10), 100 μM ESBA (B9-10), 200 μM CSA (C9-10), 20 μM CSA (D9-10), 5 mM BCA (E9-10), 500 μM BCA (F9-10), 50 mM NPA (A11-12), 5 mM NPA (B11-12), 2 mM OPS (C11-12) and 200 μM OPS (D11-12).

B. Percentage of transamination activity of hKAT II in the presence of either AAD, KYN, ESBA, CSA, BCA, NPA, and OPS (black bars) or AAD and ESBA, CSA, BCA, NPA, and OPS (red bars), at concentrations shown in the figure. The activities are expressed as a percentage of the degree of transamination measured in the presence of 10 mM AAD.

Discussion

The high-throughput search for specific and potent enzyme inhibitors strongly takes advantage of fast, simple, cheap and reliable activity assays. High-throughput enzyme assays for screening large compound libraries are generally set up as endpoints tests with comparatively long reaction times (19,38-40), in contrast to rapid kinetic assay systems for IC_{50} determinations (41-43). Most high-throughput assays are based on chromogenic and fluorogenic substrates or sensors. Recent advances in the development of high-throughput enzyme assays have identified new labels and chromophores to detect a wide range of enzymes activities (18). These conditions allow multiple 96-well, 384-well, or higher density well plates to be set up in parallel by hand or simple robotics (19). Due to the lack of such a method for hKAT II, we developed and validated a simple and sensitive enzymatically coupled absorbance assay to enable routine high-throughput screening for hKAT II inhibitors. The GOX-peroxidase coupled assay was efficiently adapted to a 96-well microplate format and allowed to assess quickly and sensitively both the transamination activity on potential substrates and the inhibition potency of selected compounds. The assay is very sensitive and is linear in an 80-fold concentration range of glutamate (between 10 and 800 μM). Furthermore, very low amounts of enzyme are used for the assay. The assay was optimized for about 20 μg of hKAT II/assay and an incubation of 30 minutes. By increasing the incubation time, the amount of enzyme can be proportionally decreased. One of the criteria for high-throughput

screening assay is to provide the best sensitivity while using the minimal amount of reagents for which supply may be limited, such as enzymes. This assay is therefore compatible with the low yields of hKAT II expression. The development of new hKAT II inhibitors can take advantages of this high-throughput screening compatible activity assay. Indeed, it is the first KAT II assay amenable for high-throughput screening due to its simplicity, quick readout and low cost compared to existing HPLC methods. Moreover, it was intended for use in conjunction with the continuous spectrophotometric assay monitoring KYNA accumulation at 310 nm. The GOX-peroxidase coupled assay implemented on a 96-well microplate allows the fast evaluation of libraries of compounds as potential hKAT II inhibitors *via* an initial visual inspection. Subsequently, for compounds showing good inhibitory properties, the mechanisms of inhibition and dissociation constants can be estimated with the continuous spectrophotometric assay. Notably, as the GOX-peroxidase end-point assay works with both AAD and KYN, two different applications are possible. First, using AAD as aminogroup donor, only KAT II activity can be specifically assayed. One of the main drawbacks of the discontinuous HPLC-based KAT II assay is lack of isoform-specificity (44), as under the same assay conditions, also KAT I, III and IV have detectable activity (8,24,25). Differently from KYN, that can be used as the amino group donor by all four known KAT isoezymes, AAD is efficiently used only by KAT II (26,44). A KAT II-specific activity assay has never been reported so far. On the other hand, if KYN is used as amino group donor, the end-point assay can also be adapted for use with different members of the KAT superfamily, thus allowing the quantitative comparison of substrate preferences among the different isoforms and the selectivity of potential inhibitors.

In conclusion, the assay system we have developed will be a valuable tool to the high-throughput screening of large compounds libraries, with the objective to discover currently unknown potent hKAT II inhibitors leading to novel drugs for cognitive dysfunction. New hints toward the development of a KAT II-specific inhibitor come from the recent observation that large molecules with bulky substituents specifically bind to the II-isoform of the enzyme (29,36), probably as a consequence of the higher mobility of the N-terminal domain of KAT II with respect to that of other aminotransferases (36). These observations together with the tools developed here for the high-throughput screening of KAT II specific inhibitors will aid in the development of anti-schizophrenic and precognitive drugs.

REFERENCES

1. Hilmas, C., Pereira, E. F., Alkondon, M., Rassoulpour, A., Schwarcz, R., and Albuquerque, E. X. (2001) *J Neurosci* **21**(19), 7463-7473
2. Kessler, M., Terramani, T., Lynch, G., and Baudry, M. (1989) *Journal of neurochemistry* **52**(4), 1319-1328
3. Pereira, E. F., Hilmas, C., Santos, M. D., Alkondon, M., Maelicke, A., and Albuquerque, E. X. (2002) *Journal of neurobiology* **53**(4), 479-500
4. Baran, H., Jellinger, K., and Deecke, L. (1999) *J Neural Transm* **106**(2), 165-181
5. Erhardt, S., Blennow, K., Nordin, C., Skogh, E., Lindstrom, L. H., and Engberg, G. (2001) *Neuroscience letters* **313**(1-2), 96-98
6. Erhardt, S., Olsson, S. K., and Engberg, G. (2009) *CNS drugs* **23**(2), 91-101
7. Baran, H., Cairns, N., Lubec, B., and Lubec, G. (1996) *Life sciences* **58**(21), 1891-1899
8. Han, Q., Cai, T., Tagle, D. A., and Li, J. *Cell Mol Life Sci* **67**(3), 353-368
9. Guidetti, P., Amori, L., Sapko, M. T., Okuno, E., and Schwarcz, R. (2007) *Journal of neurochemistry* **102**(1), 103-111
10. Wong, J., Ray, W. J., and Kornilova, A. Y. *Analytical biochemistry*
11. Rossi, F., Schwarcz, R., and Rizzi, M. (2008) *Curr Opin Struct Biol* **18**(6), 748-755
12. Amori, L., Wu, H. Q., Marinozzi, M., Pellicciari, R., Guidetti, P., and Schwarcz, R. (2009) *Neuroscience* **159**(1), 196-203
13. Pellicciari, R., Rizzo, R. C., Costantino, G., Marinozzi, M., Amori, L., Guidetti, P., Wu, H. Q., and Schwarcz, R. (2006) *ChemMedChem* **1**(5), 528-531
14. Pellicciari, R., Venturoni, F., Bellocchi, D., Carotti, A., Marinozzi, M., Macchiarulo, A., Amori, L., and Schwarcz, R. (2008) *ChemMedChem* **3**(8), 1199-1202
15. Casazza, V., Rossi, F., and Rizzi, M. *Current topics in medicinal chemistry*
16. Amori, L., Guidetti, P., Pellicciari, R., Kajii, Y., and Schwarcz, R. (2009) *Journal of neurochemistry*
17. Rossi, F., Valentina, C., Garavaglia, S., Sathyasaikumar, K. V., Schwarcz, R., Kojima, S., Okuwaki, K., Ono, S., Kajii, Y., and Rizzi, M. *Journal of medicinal chemistry* **53**(15), 5684-5689
18. Goddard, J. P., and Reymond, J. L. (2004) *Current opinion in biotechnology* **15**(4), 314-322
19. Wolf, N. M., Morisseau, C., Jones, P. D., Hock, B., and Hammock, B. D. (2006) *Analytical biochemistry* **355**(1), 71-80
20. Sawai, T., Koma, D., Hara, R., Kino, K., and Harayama, S. (2007) *Journal of microbiological methods* **71**(1), 32-38
21. Dixon, S. M., Li, P., Liu, R., Wolosker, H., Lam, K. S., Kurth, M. J., and Toney, M. D. (2006) *Journal of medicinal chemistry* **49**(8), 2388-2397

22. Shanks, E. J., Ong, H. B., Robinson, D. A., Thompson, S., Sienkiewicz, N., Fairlamb, A. H., and Frearson, J. A. *Analytical biochemistry* **396**(2), 194-203
23. Zhang, B., Senator, D., Wilson, C. J., and Ng, S. C. (2005) *Analytical biochemistry* **345**(2), 326-335
24. Han, Q., Li, J., and Li, J. (2004) *European journal of biochemistry / FEBS* **271**(23-24), 4804-4814
25. Han, Q., Robinson, H., Cai, T., Tagle, D. A., and Li, J. (2009) *Molecular and cellular biology* **29**(3), 784-793
26. Han, Q., Cai, T., Tagle, D. A., Robinson, H., and Li, J. (2008) *Bioscience reports* **28**(4), 205-215
27. Kocki, T., Luchowski, P., Luchowska, E., Wielosz, M., Turski, W. A., and Urbanska, E. M. (2003) *Neuroscience letters* **346**(1-2), 97-100
28. Battaglia, G., Rassoulpour, A., Wu, H. Q., Hodgkins, P. S., Kiss, C., Nicoletti, F., and Schwarcz, R. (2000) *Journal of neurochemistry* **75**(5), 2051-2060
29. Luchowski, P., Luchowska, E., Turski, W. A., and Urbanska, E. M. (2002) *Neuroscience letters* **330**(1), 49-52
30. Burns, R. S., Chiueh, C. C., Markey, S. P., Ebert, M. H., Jacobowitz, D. M., and Kopin, I. J. (1983) *Proceedings of the National Academy of Sciences of the United States of America* **80**(14), 4546-4550
31. Langston, J. W., Ballard, P., Tetrud, J. W., and Irwin, I. (1983) *Science (New York, N.Y* **219**(4587), 979-980
32. Huang, L. S., Sun, G., Cobessi, D., Wang, A. C., Shen, J. T., Tung, E. Y., Anderson, V. E., and Berry, E. A. (2006) *The Journal of biological chemistry* **281**(9), 5965-5972
33. Urbanska, E. M. (2000) *Polish journal of pharmacology* **52**(1), 55-57
34. Beal, M. F. (1992) *Annals of neurology* **31**(2), 119-130
35. Dauer, W., and Przedborski, S. (2003) *Neuron* **39**(6), 889-909
36. Rossi, F., Valentina, C., Garavaglia, S., Sathyasaikumar, K. V., Schwarcz, R., Kojima, S.-i., Okuwaki, K., Ono, S.-i., Kajii, Y., and Rizzi, M. (2010) *Journal of Medicinal Chemistry*, In press
37. Arima, J., Tamura, T., Kusakabe, H., Ashiuchi, M., Yagi, T., Tanaka, H., and Inagaki, K. (2003) *Journal of biochemistry* **134**(6), 805-812
38. Venhorst, J., Onderwater, R. C., Meerman, J. H., Vermeulen, N. P., and Commandeur, J. N. (2000) *Eur J Pharm Sci* **12**(2), 151-158
39. Marks, B. D., Goossens, T. A., Braun, H. A., Ozers, M. S., Smith, R. W., Lebakken, C., and Trubetskoy, O. V. (2003) *AAPS pharmSci* **5**(2), E18
40. Soriano, A., Radice, A. D., Herbitter, A. H., Langsdorf, E. F., Stafford, J. M., Chan, S., Wang, S., Liu, Y. H., and Black, T. A. (2006) *Analytical biochemistry* **349**(2), 268-276

41. Dietze, E. C., Kuwano, E., and Hammock, B. D. (1994) *Analytical biochemistry* **216**(1), 176-187
42. Jones, P. D., Wolf, N. M., Morisseau, C., Whetstone, P., Hock, B., and Hammock, B. D. (2005) *Analytical biochemistry* **343**(1), 66-75
43. Morisseau, C., Du, G., Newman, J. W., and Hammock, B. D. (1998) *Archives of biochemistry and biophysics* **356**(2), 214-228
44. Han, Q., Cai, T., Tagle, D. A., and Li, J. (2010) *Cell Mol Life Sci* **67**(3), 353-368

CHAPTER 6

OPTIMIZATION OF hKAT II HETEROLOGOUS EXPRESSION

Introduction and aim of the work

As a part of the activities carried out during the thesis, we report here the attemps to increase the expression yield of soluble hKAT II. Recombinant expression of hKAT II was investigated by a novel culture method, called EnBase™ (BioSilta - enzyme-based-substrate-delivery), which exploits the principle of fed-batch culture, traditionally used within bioreactors, to provide controlled growth at micro-scale by enzymatic substrate release. EnBase™ (BioSilta) is an enhanced novel microbial culture system in which enzyme-based supply of glucose allows a glucose-limited growth, providing high cell densities and high recombinant protein yields.

Culture for recombinant protein production today in laboratory scale is mainly based on shaken media which are generally performed in batch (i.e. all nutrients are added at the beginning of the process). Shake flask cultures are known to be easy and low cost, but generally their reliability and final product yield is poor. Compared to industrial fed-batch processes, shaken cultures are characterised by low volumetric cells and product yields (*1*). Cell cultures in shake flasks often fail to reach high cell densities and high protein productivity per cell due to oxygen depletion, lack of pH control and the necessity to use low induction cell densities. Shake flask cultures are normally run without monitoring and control of any parameters such as pH and the level of dissolved oxygen (*2*). Under such circumstances, high cell densities cannot be reached since the high respiratory rate of fast growing bacteria exceeds the oxygen transfer capacity of the medium, and the culture is relatively soon depleted of oxygen (*3*). Under oxygen limitation growth is slow and recombinant protein production is poor. Moreover, oxygen limitation leads to anaerobic responses (*4, 5*), which multiply the stress caused by the recombinant protein synthesis. In addition to oxygen limitation, uncontrolled batch cultures may suffer from acetate accumulation by overflow metabolism. The drop of pH due to accumulation of overflow acetate and anaerobic metabolites impairs cell growth and leads to poor recombinant protein formation (*2*). Uncontrolled cell growth is often associated with uncontrolled protein synthesis rate and incorrect protein folding. High local concentration of recombinant protein together with insufficient amount of folding-promoting proteins may lead to formation of insoluble protein aggregates (inclusion bodies).

In contrast to variable shaking cultures, in well controlled bioreactor scale cultures, high cell densities can be successfully achieved by applying the fed-batch principle, which has been widely utilized since late 1980's (*6-8*). In most fed-batch processes, a continuous supply of a growth limiting substrate (generally glucose) by an external pump provides a metabolic control. In this way, the growth rate can be controlled to match the oxygen transfer rate, allowing for the growth to

be run in aerobic mode. Higher cell densities (up to 50-200 OD_{600}) are therefore reached compared to shake flask cultures. In shaken cultures substrate-limited growth is not commonly applied as it is not trivial to implement a continuos well-controlled feed flow in a shaking enviroment. However, recently a novel technology to provide feeding without external devices have been developed (*1*). The novel techology, called EnBase™ (BioSilta), or enzyme-based-substrate-delivery, combines a continuos diffusion of a metabolic inactive polymer, starch, from a gel phase into the culture medium and the enzymatic conversion by glucoamylase of the starch to glucose substrate. In this system, the glucose release rate and the growth rate of the culture can be simply controlled by the amount (and principally by the activity) of the enzyme glucoamylase, in a similar way as the pump speed of the feed solution is changed to control the growth of cells in a biorector. This solves the problems of uncontrolled growth, oxygen limitation and severe pH drop in shaken cultures. The enzymatic glucose release principle has recently been developed into a fully liquid phase cultivation system, EnBase™ Flo (BioSilta), where the glucose-releasing polymer is fully soluble and no gel phase is necessary (*2*). This novel method was directly applied in microwell plates and shake flasks without any requirements for additional sensors or liquid supply systems. The feasibilility of this method was demonstrated by overproduction in *Escherichia coli* of three different recombinant proteins, the A-domain of human protein disulphide isomerase (PDI), alcohol dehydrogenase (ADH) from *Lactobacillus* and a multifunctional enzyme from *Drosophila melanogaster* (2). In this study, these three proteins were expressed in EnBase™ Flo (BioSilta), conventional Luria-Bertani (LB), Terrific Broth (TB) and mineral salt medium. By examination of cell growth, medium pH development and protein yields, results demonstrated that sigificant improvements in protein yield can be achived by this new cultivation method. With EnBase™ Flo (BioSilta), the final cell densities were typically 10 times higher compared to the standard cultures in LB, TB and mineral salt medium. The enzymatic glucose release system together with a well-balanced combination of mineral salts and complex medium additives provided high cell densities, high protein yields and a considerably improved proportion of soluble proteins in harvested cells. This increase was coupled with equal or improved yields of soluble recombinant proteins. This improvement is thought to result from a well controlled physiological state during the whole process. Indeed, this novel culture method consist of two phases (figure 1): in the first step cells grow in fed-batch like mode controlled by the activity of amylase, and, in the second phase, addition of medium boosters together with an inducer guaranties stable pH conditions and balanced supply of extra energy source for optimal protein expression. The boosting step is followed by a slow growth period during which the recombinant protein is slowly synthesized and folded.

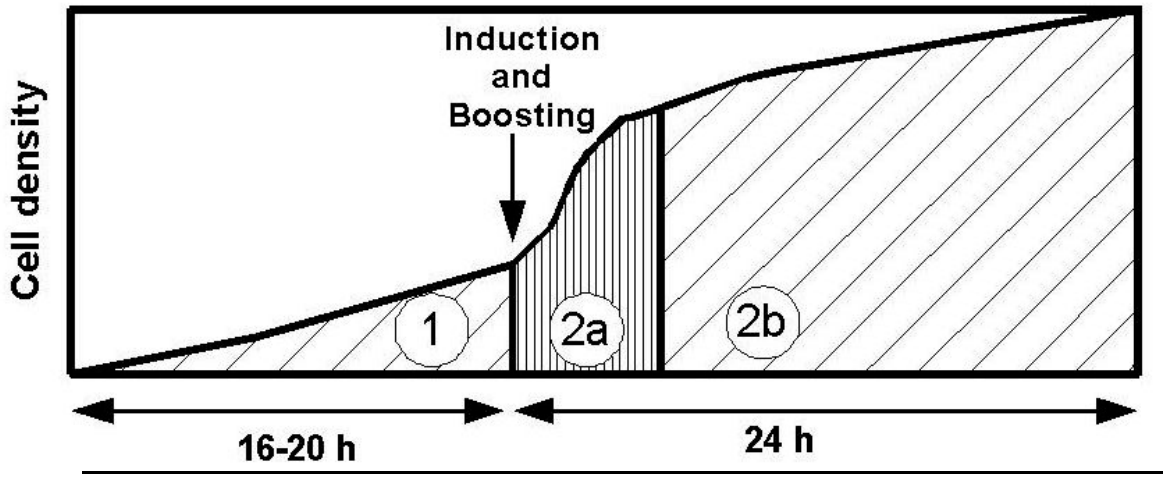

Figure 1. Schematic picture of the EnBase™ (BioSilta) culture principle (*1*).
Phase 1 = controlled culture in optimized mineral salt medium with a low concentration of complex additives (peptones, yeast extract). Phase 2 = induction with IPTG and addition of complex nutrients (booster mixture). Phase 2a of increased growth rate is followed by phase 2b of low growth rate and slow production of soluble protein.

EnBase™ Optiset (BioSilta) is a handy tool to select an optimal culture medium for the production of the target recombinant protein. It includes a total of 4 different culture media. For each medium variant, the conditions for testing can be differentiated by the presence of absence of inducer and medium boosters. One of the test media is the medium routinely used for recombinant protein production. The other culture options utilize the patented EnBase™ media of Biosilta. EnBase™ media are based on an optimised mineral salt medium (MSM) composition, where small amounts of complex medium additives (yeast extract and peptones) have been added to ensure a fast adaptation of cells to the medium.

The expression system for recombinant human KAT II production has been developed and optimized by Proff. Franca Rossi and Menico Rizzi (University of Piemonte Orientale), but is still poor, yielding about 1.5 mg of soluble protein from 2 litre culture broth, as most of the enzyme is inside inclusion bodies. The search for specific and potent hKAT II inhibitors will strongly take advantages of an optimized recombinant expression process enabling to obtain higher volumetric protein yields (i.e. soluble or active protein per culture volume) compared to the standard shake flask protocol. Therefore, we tested hKAT II heterologous expression in a 24-wells plate culture format using two versions of EnBase™ Optiset (BioSilta). The first version of EnBase™ Optiset included two gel-based Enbase media (MSM2 and MSM10) and a liquid EnBase™ Flo medium. Recently, the EnBase™ Optiset was updated by BioSilta so that the gel-based media were excluded. The most recent EnBase™ Flo Optiset contains three different variants of the liquid

EnBase™ Flo medium (Flo-02, Flo-10 and Flo-20). These three culture media differ from each other only in the amount of complex nutrients.

Materials and methods

Standard protocol for hKAT II expression and purification. The *E.coli* strain BL21(DE3) expressing human KAT II was constructed by Prof. Franca Rossi, Università Piemonte Orientale. The DNA fragment coding for the His-tagged hKAT II sequence was ligated into the pET16b expression vector (Novagen). The resulting pET16b-hKAT II construct was transformed in BL21(DE3) competent bacteria for the expression of native enzyme. pET16b-hKAT II transformed BL21(DE3) bacteria were inoculated in 1 liter of LB medium (50 μg/mL ampicillin); bacterial culture was grown at 22°C under vigorous shaking, omitting the addition of IPTG. 18-20 post-inoculation, bacteria were collected by centrifugation (11,000 x *g* for 15 min. at 4°C), washed once in PBS and flash frozen in liquid nitrogen for storage at –80°C until subsequent use. Bacterial pellet from 1 liter of native hKAT II expressing culture was dissolved in 40 mL of buffer A (20 mM Tris-HCl, pH 8.0, 50 mM NaCl, 40 μM PLP and a commercial proteases inhibitors cocktail from Sigma) and disrupted by sonication. The clarified bacterial lysate was added with 50 mM imidazole and incubated with 5 mL of drained Ni-NTA Agarose resin (Quiagen) for 1 hr at 20° C, under gentle agitation. After extensive washes in buffer A containing 75 mM imidazole, the elution of the absorbed protein was obtained at 200 mM imidazole in buffer A. Pure hKAT II containing fractions, as determined by standard SDS-PAGE analysis, were pooled, dialyzed against buffer A and concentred using a 30,000 MWCO disposable device (Vivascience) to a final protein concentration ≥ 10 mg/mL, as determined by Bradford assay (Sigma), using bovine serum albumin as standard. Aliquots of hKAT II were frozen at -80 °C for long term storage.

Expression of hKAT II with EnBase™ Optiset (BioSilta). The pET16b-hKAT II construct, provided to us by Proff. Franca Rossi and Menico Rizzi, Università Piemonte Orientale, was transformed in *E.coli* Tuner (DE3) (Novagen) competent bacteria. Tuner (DE3) bacteria encoding pET16b-hKAT II were inoculated in four different culture media: 1) Luria-Bertani (LB) medium, which is the standard medium for hKAT II heterologous expression; 2) EnBase gel with mineral salt medium (MSM2), 3) EnBase gel with balanced medium (MSM10) and 4) EnBase Flo medium. The media composition is reported in (*2*). Culture procedures were carried out as indicated in the user manual included in Biosilta™ Optiset kit. *E.coli* cells expressing hKAT II from premade glycerol stocks were streaked on a LB-agar plate (50 μg/ml Amp) and incubated overnight at 37°C. All the cells from the LB-agar plate cultured overnight at 37°C were collect by rinsing with 3-4 mL of EnBase medium for dilution. The optical density of cell suspension was measured at 600 nm with a Cary 400 Scan spectrophotometer (Varian Inc.). To each bottle of culture medium a volume of inoculum was added in order to obtain an initial OD_{600} of 0.15. Supplements including ampicilline

(50 μg/ml final concentration), thiamine, magnesium, inoculum and the enzyme glucoamylase, were aseptically added to the medium bottles according to the user manual. Bottles were carefully mixed after supplements addition. The plastic storage seal was removed from the 24-wells plate and 3 mL of each medium-cell mixture was dispensed per well as indicated with colours in the plate layout 1:

	1	2	3	4	5	6
A	**EnBase MSM2**	**EnBase MSM2 + IPTG**	**EnBase MSM2 + IPTG**	**EnBase Flo**	**EnBase Flo + IPTG**	**EnBase Flo + IPTG**
B	**EnBase MSM2 + medium boosters**	**EnBase MSM2 + medium boosters + IPTG**	**EnBase MSM2 + medium boosters + IPTG**	**EnBase Flo + medium boosters**	**EnBase Flo + medium boosters + IPTG**	**EnBase Flo + medium boosters + IPTG**
C	EnBase MSM10	**EnBase MSM10 + IPTG**	**EnBase MSM10 + IPTG**	**LB medium**	**LB medium + IPTG**	**LB medium + IPTG**
D	**EnBase MSM10 + medium boosters**	**EnBase MSM10 + medium boosters + IPTG**	**EnBase MSM10 + medium boosters + IPTG**	**LB medium + medium boosters**	**LB medium + medium boosters + IPTG**	**LB medium + medium boosters + IPTG**

Enbase gel with MSM2 medium: wells A1, A2, A3, B1, B2, B3, green.
EnBase gel with MSM10 medium: wells C1, C2, C3, D1, D2, D3, red.
EnBase Flo medium: wells A4, A5, A6, B4, B5, B6, yellow.
Standard medium (LB): wells C4, C5, C6, D4, D5, D6, white.

The plate was sealed with an oxygen permeable membrane and the culture was immediately started at 30°C, 200 rpm on a shaker with amplitude of 30 mm.
After 2 hours, IPTG (15 μM final concentration) and a mixture of medium booster were added to the wells containing the LB standard medium, as marked on the plate layout 1. Growth was continued at 30°C. Samples of LB cultures for protein analysis were harvested at 3-4 hours after IPTG addition. For total protein analysis, aliquots corresponding to a 500 μL culture with OD_{600} of 0.7 were pelleted by centrifugation (13 000 rpm for 10 min. at 4°C), supernatants were discarted, the pellets were resuspended in 40 μL of sample buffer and further analyzed by SDS-PAGE. For the analysis of the soluble and insoluble fractions after cellular lysis, aliquots of 500 μL were collected from each well. The samples were pelletted by centrifugation (13 000 rpm for 10 min. at 4°C), supernatants were discarted and the pellets were frozen at –20°C.

After overnight growth (16-20 hours), the EnBase™ cultures were supplemented with a "booster solution", providing additional complex medium additives and glucoamylase; product synthesis was simultaneously induced by addition of IPTG (15 μM final concentration). 24 hours after induction, aliquots of the EnBase™ cultures were withdrawn for OD_{600} measurement. For total protein analysis, aliquots corresponding to a 500 μL culture with OD_{600} of 0.7 were harvested and treated as descibed for LB samples. For the soluble and insoluble fractions analysis, the volume of each EnBase™ sample was calculated so that the resulting cell density was the same in all LB and EnBase™ samples. The samples were pelletted by centrifugation (13 000 rpm for 10 min. at 4°C), supernatants were discarted and the pellets were frozen at –20°C.

Expression of hKAT II with EnBase™ Flo Optiset (Biosilta). Four different media were used for bacteria growth: 1) Luria-Bertani (LB) medium; 2) EnBase Flo-02 medium, 3) EnBase Flo-10 medium and 4) EnBase Flo-20 medium. For each medium variant, the conditions for testing were differentiated by the presence or absence of inducers (IPTG or lactose) and medium boosters. Therefore, 24 different growth conditions were tested, as indicated with colours in the plate layout 2:

	1	2	3	4	5	6
A	**EnBase Flo-02 + medium boosters**	**EnBase Flo-02 + medium boosters + lactose**	**EnBase Flo-02 + medium bosters + IPTG**	**EnBase Flo-02**	**EnBase Flo-02 + lactose**	**EnBase Flo-02 + IPTG**
B	**EnBase Flo-10 + medium boosters**	**EnBase Flo-10 + medium boosters + lactose**	**EnBase Flo-10 + medium boosters + IPTG**	**EnBase Flo-10**	**EnBase Flo-10 + lactose**	**EnBase Flo + IPTG**
C	**EnBase Flo-20 + medium boosters**	**EnBase Flo-20 + medium boosters + lactose**	**EnBase MSM10 + medium boosters + IPTG**	**EnBase Flo-20**	**EnBase Flo-20 + lactose**	**EnBase Flo-20 + IPTG**
D	**LB medium + medium boosters**	**LB medium + medium boosters + lactose**	**LB medium + medium boosters + IPTG**	**LB medium**	**LB medium + lactose**	**LB medium + IPTG**

Enbase Flo-02 medium: wells A1-A6, green.

EnBase Flo-10 medium: wells B1-B6, yellow.

EnBase Flo-20 medium: wells C1-C6, red.

Standard medium (LB): wells D1-D6, white.

The growth process was the same as that described above, except for the incubation temperature and time. Growth was carried out at 15°C and induction with IPTG or lactose was at 2 hours and about 18 hours for the control (LB medium) and the optimized EnBase™ Flo media, respectively. Cell samples were harvested at 4 hours and about 48 hours after induction for the control and the optimized EnBase™ Flo media, respectively. For each growth conditions, samples for total and soluble protein analysis were collected as previuosly described.

Analysis of the soluble fraction after cellular lysis. Cell pellets were suspended in 500 μL of 20 mM Tris-HCl, pH 8.0, 50 mM NaCl, 40 μM PLP and then disrupted by three freezing (-20°C) and thawing (42°C) cycles. Cellular lysis was then carried out by adding to each sample 50 μL of a fresh made 10 mg/mL lisozyme solution, samples were incubated at 37°C for 20 minutes. Complete cells disruption was ensured by one minute of sonication on ice. To obtain the soluble protein fraction, the disrupted cell solution was centrifuged at 13,000 rpm for 10 min. at 4°C. Pellets were resuspended in 50 μL of sample buffer, whereas supernatants were concentrated using Vivaspin 10,000 (Sartorius) up to 30 μL final volume; then 20 μL of sample buffer were added to the concentrated supernatants and soluble protein fractions were analysed by SDS-PAGE and Western Blotting.

Western Blotting procedure. Sample proteins were first separated by SDS-PAGE, then blotted using Chemichrome Western Control (Sigma C4236) or ProSieve Color Protein Markers (Lonza 50550) as control. A sheet of nitrocellulose membrane and four pieces of filter paper were soaked in transfer buffer (48 mM Tris, 39 mM glycine, 1.3 mM SDS, 20 % methanol, pH 9.0-9.4). The gel and membrane were gently pressed together by using a Pasteur pipette as a rolling pin to avoid the occurence of air pockets between the “sandwich” layers. By applying electric current (30 minutes at 10 Volt), proteins were trasferred from the gel to the nitrocellulose membrane, retaining the same separation pattern they had on the gel. The blotted membrane was washed with TBST solution (Sigma T94447) and then incubated overnight at room temperature with a commercial solution containing milk proteins (TBS with 3% fat milk, Sigma T8793). TBS solution was then discarted and the membrane washed with TBST solution. The colorimetric detection of the target recombinant protein was carried out using monoclonal anti-polyHistidine antibodies conjugated with peroxidase (dilution 1:20 000) and TMB as substrate (Sigma PQ0101).

Results

Expression of hKAT II with EnBase Optiset (BioSilta).

The growth process was performed as indicated in the protocol included in the kit, inoculating the 24-wells plate with cells obtained from a fresh-made LB-agar plate. LB broth was used as standard medium. For each medium variant, protein expression was tested either in the absence and presence of medium boosters and IPTG. Therefore, 16 different growth conditions were tested, as marked in plate layout 1. Growth was carried out at 30°C and induction with IPTG (15 μM final concentration) was at 2 hours and about 18 hours for the control and the optimized EnBase™ media, respectively. Cell samples were collected after 4 hours and about 18 hours induction for the control and the optimized EnBase™ media, respectively. The presence of the target protein was assayed by SDS-PAGE and Western Blotting on the total amount of cellular proteins and on the soluble and insoluble fractions. The volume of each sample was calculated so that the resulting cell density was the same in all samples. Therefore, protein productivity per cell in different samples can be directly compared on the basis of the protein band thickness. EnBase™ Optiset allowed a 5-fold increase in the amount of cells present at the end of the induction. Normalized results show a further 2-3 fold increase in the amount of total protein. Taken together these data indicate a 10-15 fold increase in protein yield. Results demonstrated that sigificant improvements in protein yield can be achieved by this new culture method, but unfortunately, the analysis of the soluble fractions (figure 2) showed that almost all the target protein was in the pellet. As also the standard medium LB did not show any protein in the soluble fraction, the growth temperature (30°C) was likely too high with respect to that normally used, 22°C. Therefore, we repeated the expression tests at a lower temperature (15°C), using an updated version of Opiset BioSilta, which contains no more gel-based media, but three different variants of the liquid EnBase Flo medium. Low temperature may trigger the production of intracellular chaperone type proteins, which may further improve protein folding during synthesis or refolding after synthesis.

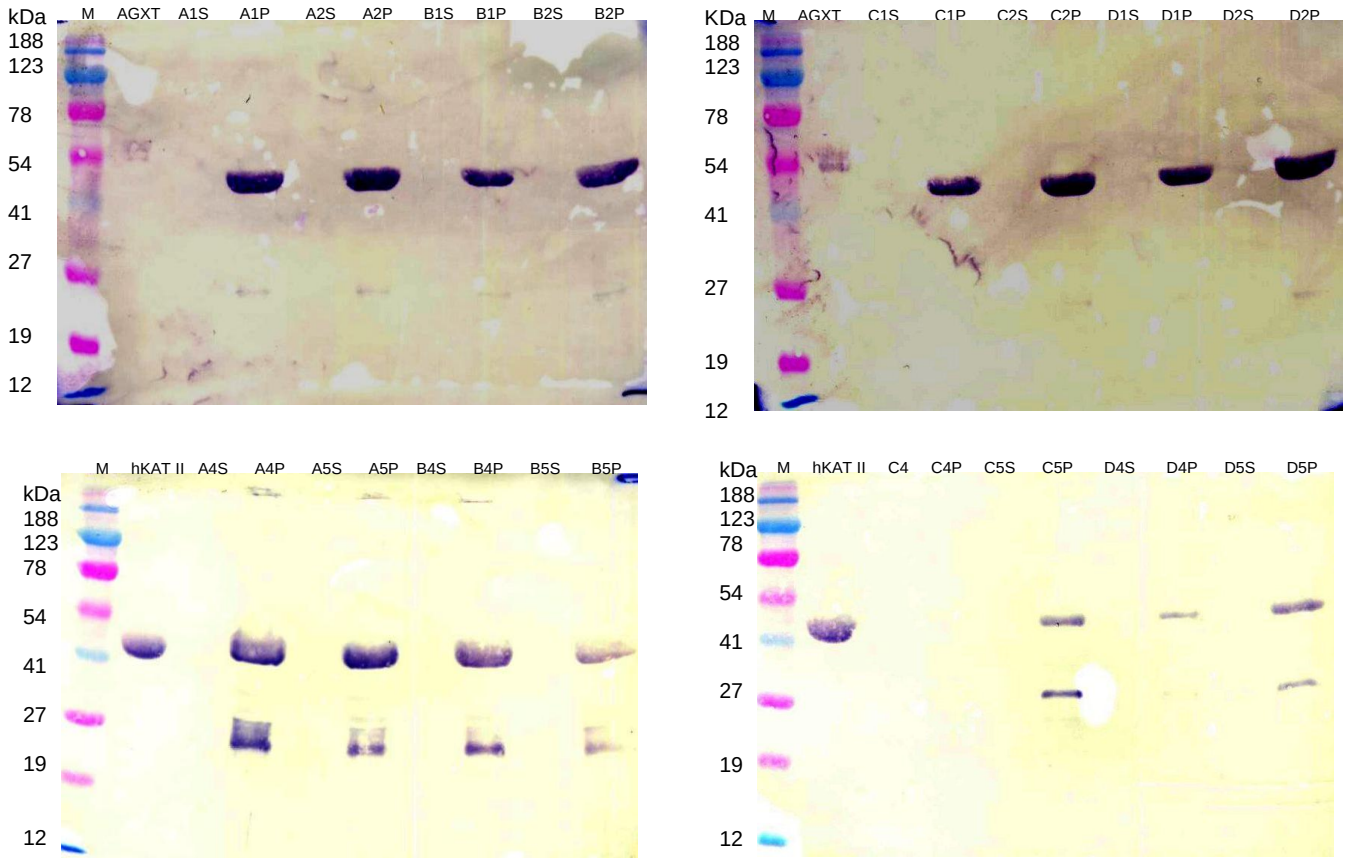

Figure 2. Analysis of the soluble and insoluble fractions after cellular lysis.

Recombinant hKAT II was produced in EnBase™ Optiset (Biosilta) 24-well plate format using 4 different culture media. To facilitate direct comparison between different culture media, all samples were diluited to equal cell concentration before cell lysis and loading on a gel. M = ProSieve Color Protein Markers (Lonza 50550). His-tagged recombinant proteins were used as control: AGXT = 3 μg of alanine-glyoxilate aminotransferase, hKAT II = 7 μg of recombinant hKAT II. The different growth conditions are indicated in plate layout 1 (A1=MSM2, A2=MSM2 + IPTG, B1= MSM2 + booster mixture, B2=MSM2 + booster mixture + IPTG. C1=MSM10, C2=MSM10 + IPTG, D1=MSM10 + booster mixture, D2=MSM10 + booster mixture + IPTG. A4=Flo, A5=Flo + IPTG, B4=Flo + booster mixture, B5=Flo + booster mixture + IPTG. C4=LB, C5=LB + IPTG, D4=LB + booster mixture, D5=LB + booster mixture + IPTG). For each growth condition, soluble and insoluble fraction are indicated as “S” and “P”, respectively.

Expression of hKAT II with EnBase™ Flo Optiset (Biosilta).

Expression procedures were carried out following the usual protocol, inoculating the 24-wells plate with cells coming from a fresh-made LB-agar plate. Growth was carried out at 15°C and induction with IPTG or lactose was at 2 hours and about 18 hours for the control (LB medium) and the optimized EnBase™ Flo media, respectively. Cell samples were harvested at 4 hours and about 48 hours after induction for the control and the optimized EnBase ™ Flo media, respectively. In addition to decreasing the culture temperature, we tried induction with lactose (0.5 mg/mL final concentration), instead of IPTG. Some limited data (private comunications from BioSilta company) indicate that lactose might be a slower inducer than IPTG, and this could be beneficial for soluble expression of the target protein. As in the Optiset 24-wells plate there are three parallel wells for each medium variant, we omitted the addition of inducer in one well, induced with lactose in one of them and with IPTG (15 μM final concentration) in the last one. Therefore 24 different growth conditions were tested, as shown in plate layout 2. For each growth condition, total and soluble protein samples were analyzed by SDS-PAGE and Western Blotting. Enbase™ Flo Optiset allowed a 3-fold increase in the amount of cells present at the end of induction. Normalized results show a further 2-3 fold increase in the amount of total protein. Taken together data indicate a 6-9 fold increase in protein yield. Unfortunately, the analysis of the soluble fraction after cellular lysis (figure 3), showed that even at decreased temperature almost all the target protein aggregated in inclusion bodies. Thus, reducing the growth temperature is not an adequate strategy to improve the expression of our target protein in a soluble form. Different strategies aimed at optimizing the heterolous expression of recombinant hKAT II in a soluble form should be taken into account.

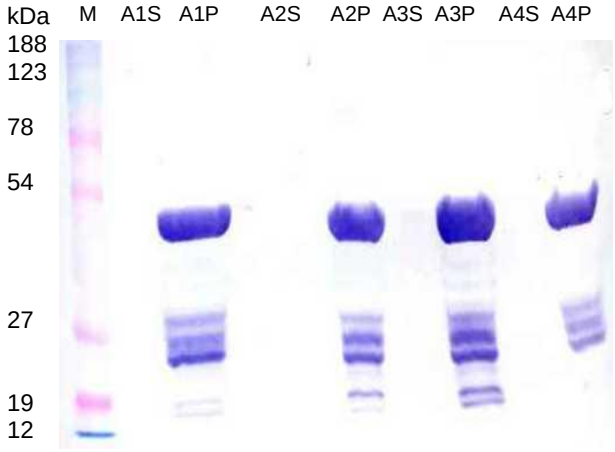
kDa
M
A1S
A1P
A2S
A2P
A3S
A3P
A4S
A4P
188
123
78
54
27
19
12

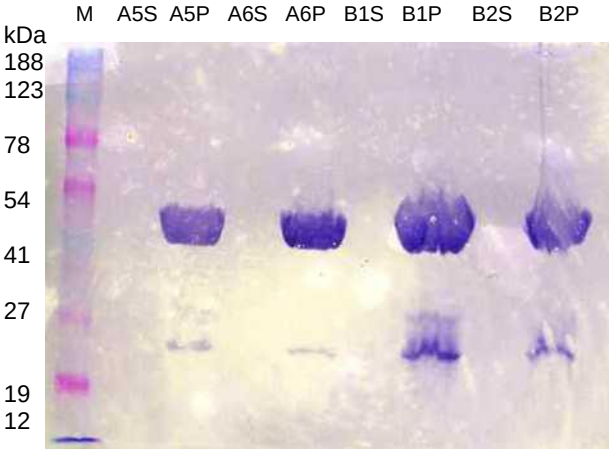
kDa
M
A5S
A5P
A6S
A6P
B1S
B1P
B2S
B2P
188
123
78
54
41
27
19
12

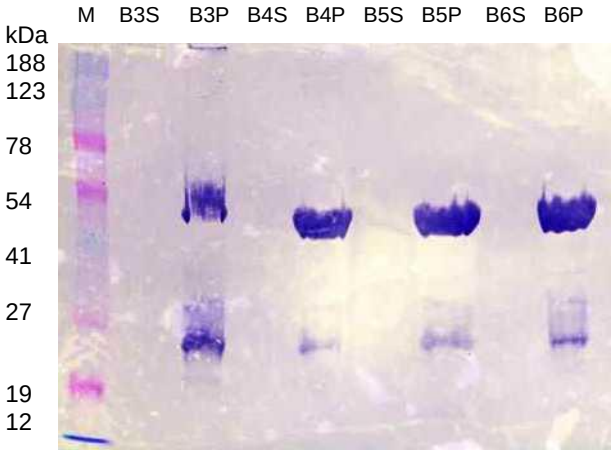
kDa
M
B3S
B3P
B4S
B4P
B5S
B5P
B6S
B6P
188
123
78
54
41
27
19
12

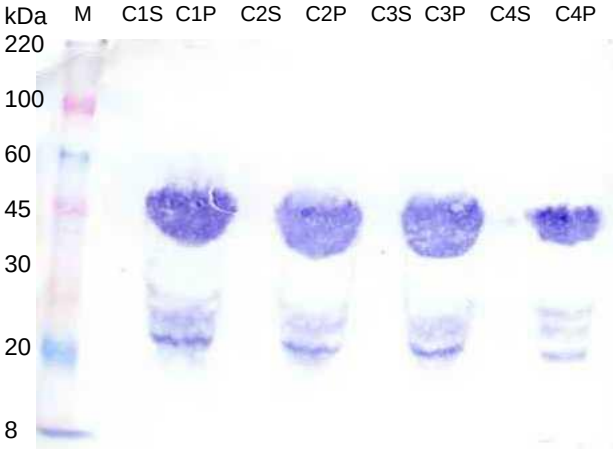
kDa
M
C1S
C1P
C2S
C2P
C3S
C3P
C4S
C4P
220
100
60
45
30
20
8

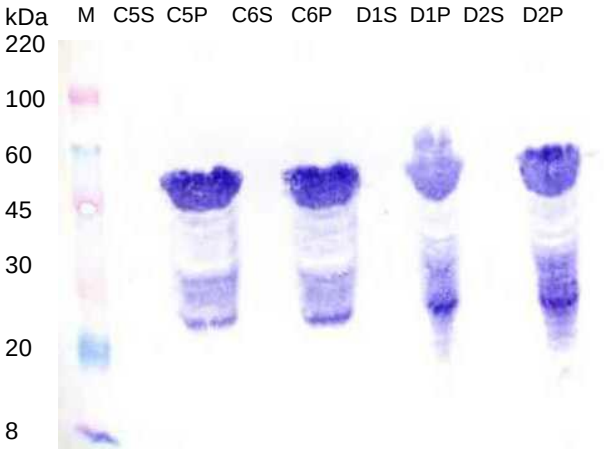
kDa
M
C5S
C5P
C6S
C6P
D1S
D1P
D2S
D2P
220
100
60
45
30
20
8

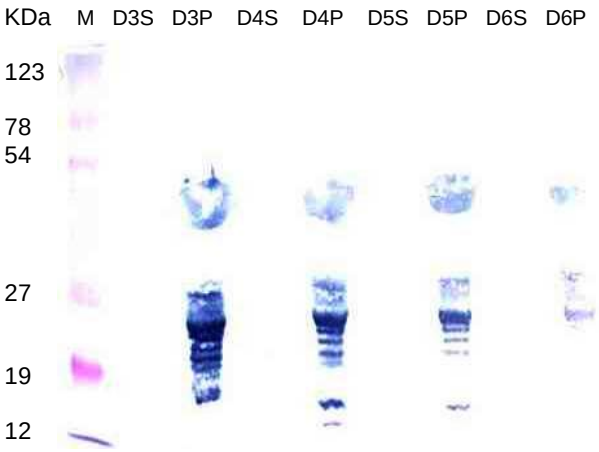
KDa
M
D3S
D3P
D4S
D4P
D5S
D5P
D6S
D6P
123
78
54
27
19
12

Figure 3. Analysis of the soluble and insoluble fractions after cellular lysis.
Recombinant hKAT II was produced in EnBase™ Flo Optiset (Biosilta) 24-well plate format using 4 different cultivation media. To facilitate direct comparison between different cultivation media, all samples were diluited to equal cell concentration before cell lysis and loading on a gel. M = Chemichrome Western Control (Sigma C4236) or ProSieve Color Protein Markers (Lonza 50550). The different cultivation conditions are indicated in plate layout 2 (A1=Flo-02 + booster mixture, A2=Flo-02 + booster mixture + lactose, A3= Flo-02 + booster mixture + IPTG, A4=Flo-02, A5=Flo-02 + lactose, A6=Flo-02 + IPTG. B1=Flo-10 + booster mixture, B2=Flo-10 + booster mixture + lactose, B3=Flo-10 + booster mixture + IPTG, B4=Flo-10, B5=Flo-10 + lactose, B6=flo-10 + IPTG. C1=Flo-20 + booster mixture, C2=Flo-20 + booster mixture + lactose, C3=Flo-20 + booster mixture + IPTG, C4=Flo-20, C5=Flo-20 + lactose, C6=Flo-20 + IPTG. D1=LB + booster mixture, D2=LB + booster mixture + lactose, D3=LB + booster mixture + IPTG, D4=LB, D5=LB + lactose, D6=LB + IPTG. For each cultivation condition, soluble and insoluble fraction are indicated as “S” and “P”, respectively.

Discussion
The expression system for hKAT II synthesis in bacterial host has been developed and optimized by our collaborators Proff. Franca Rossi and Menico Rizzi, Università Piemonte Orientale. However, the protein yield (about 1.5 mg from 2 litre culture broth) is still too low and most of the protein is inside inclusion bodies. As a part of the activities carried out during the thesis, we have carried out several unsuccesful attemps to increase the expression yield of hKAT II in a soluble form. The avaibility of higher amounts of hKAT II, together with the activity assays previously described, are useful in the development of anti-schizophrenic and pro-cognitive drugs.
Cultures for recombinant protein production in shake flasks as a batch process often lead to oxygen limitation, medium acidification, and overflow metabolism. High cell densities are not routinely reached in this batch process and consequently low product yield rates occurs. By contrast, in the feed-batch process used in industrial bioreactors, the microbial growth is controlled by substrate limitation to avoid inhibitory effects and provide high cell densities and high product yields. In typical bioreactor process the main substrate feed, mostly glucose, is added by a pump. In EnBase™ no external glucose feed is required, but glucose is released in into the growth medium by enzymatic degradation of starch. Starch is supplied directly dissolved in the medium or embedded in a gel from which it slowly diffuses into the growing culture suspension. The potential of the system is that the microbial growth rate and oxygen consumption can be simply controlled by the amount, and principally by the activity, of the starch degrading enzyme glucoamylase. By utilising controlled growth within EnBase™, accumulation of growth limiting compounds from overflow metabolism, and oxygen starvation can be significantly reduced or eliminated. The EnBase™ technology based on catalytically controlled glucose delivery results in controlled growth

of *E.coli* to high cell densities and enhanced protein production. The 24-deep well plate of the Optiset enables a direct comparison between the traditional expression method and three different EnBase™ media and also includes growths with an additional boosting step. We tried the first version of BioSilta™ Optiset for the expression of hKAT II. Results indicated a 10-15 fold increase in protein yield, therefore sigificant improvements in protein yield can be achieved by this new culture method. Unfortunately, we did not succeed in the expression of the target soluble protein as all the proteins accumulated in inclusion bodies. One possible reason for this was the induction temperature: the standard protocol is optimized at 22 °C for 48 h, while we have tried Optiset at 30 °C, following exactly the protocol of the kit. Inclusion bodies are insoluble aggregates of misfolded protein lacking biological activity. Although the reasons for inclusion bodies formation are not well understood, two factors that might contribute are the rate of translation and the rate of protein folding, which are almost an order of magnitude faster in *E.coli* as compared with eukaryotic systems (*9*). It is well known that a reduced growth rate usually leads to more soluble expression and hence reduces the tendency to form inclusion bodies. A well known technique to limit the *in vivo* aggregation of recombinant proteins consist of growth at low temperature (*10*). Moreover, aggregation reactions are in general favoured at higher temperatures due to the strong temperature dependence of hydrophobic interactions that determine the aggregation reactions (*11*). In order to improve the fraction of soluble protein, we tried the recent version EnBase™ Flo Optiset, using a lower temperature, 15 °C and collecting samples after 48 hours of induction. Final protein yield with EnBase Flo media was about 6-9 fold higher than that obtained with the standard medium LB, but, even with growth at reduced temperature, the formation of inclusion bodies occured. EnBase™ guarantees more cells, due to the enzymatic glucose release and a well-balanced combination of mineral salts and complex medium additives, which provide high cell densities. The increased specific protein yield, measured as soluble or active protein per cell and better solubility, is depending on the expression system. If the reason for inclusion bodies formation is the stress due to oxygen limitation or too fast growing cells, then EnBase™ might be the solution for improvement of solubility. With EnBase™ the following parameters can be optimised to increase the solubility: inducer concentration, temperature (EnBase™ is working up to 10°C), medium composition (percentage of complex additives) and growth rate (controlled in a fed-batch manner by glucoamylase concentration). Should these modifications prove insufficient to increase soluble expression, more comprehensive strategies can be considered. These include the use of fusion tags, co-expression with chaperones or other folding-machinery components, and the use of an alternative host organism. Another possible strategy is refolding from inclusion bodies, but this procedure is in many cases considered undesiderable. The major obstacles are the poor recovery yields, the requirements for optimization of refolding conditions for each target protein and the possibilty that the resolubilization procedures could affect the integrity of the refolded proteins. In addition, the purification of highly expressed soluble protein is less expensive and time

consuming than refolding and purification from inclusion bodies (*10*). One of the most successfull methods used to improve soluble expression of aggregation prone proteins consist in engineering the target protein with solubility fusion tags (*12*). These tags are protein or peptides that are fused to the protein of interest and, in the best case, help to properly fold their partners leading to enhanced solubility of the target protein (*13, 14*). Among the most potent solubility enhancing proteins characterized to date are the *E.coli* maltose binding protein (MBP), N-utilizing substance A (NusA), thioredoxin (Trx) and glutathione-*S*-trasferase (GST). Both MBP and GST have an additional benefit in that they can function as affinity tags to facilitate the purification process. However, E.*coli* MBP proved to be a much more effective solubility partner than the highly soluble GST and thioredoxin proteins (*15*). A precise mechanism for the solubility enhancement of MBP has not been found. However, MBP might act as a chaperone by interactions through a solvent exposed "hot spot" on its surface which stabilizes the otherwise insoluble target protein (*16, 17*). Numerous examples of MBP and NusA as functional solubility enhancers are found in the literature (*10, 18, 19*). Aggregation of recombinant proteins overexpressed in bacterial cells could results either from accumulation of high concentration of folding intermediates or from inefficent processing by molecular chaperones. Another possible strategy for the prevention of inclusion body formation is the co-overexpression of chaperone encoding genes and the recombinant target protein. Some chaperones drive folding attemps, whereas others prevents protein aggregation (*20-22*). Numerous *E.coli* specialized host strains have been developed to improve soluble expression of aggregation prone proteins. Recently, a novel improved BL21(DE3) host strain, called SoluBL21, has been developed and it's now commercially available by amsbio (AMS Biotechnology). The SoluBL21 strain contains mutations that make this strain able to express insoluble proteins in a soluble form, fully or partially, in most tests conducted.

In conclusion, hKAT II recombinant expression with EnBase^{TMTM} Optiset demonstrated that sigificant improvements in protein yield can be achieved by this new culture method. Nevertheless, other steps are necessary in order to overcome the protein propensity for aggregation in inclusion bodies. One or more strategies listed above could be applied in the future to enhance protein solubility.

REFERENCES

1. Panula-Perala, J., Siurkus, J., Vasala, A., Wilmanowski, R., Casteleijn, M. G., and Neubauer, P. (2008) Enzyme controlled glucose auto-delivery for high cell density cultivations in microplates and shake flasks, *Microbial cell factories 7*, 31.
2. Krause, M., Ukkonen, K., Haataja, T., Ruottinen, M., Glumoff, T., Neubauer, A., Neubauer, P., and Vasala, A. A novel fed-batch based cultivation method provides high cell-density and improves yield of soluble recombinant proteins in shaken cultures, *Microbial cell factories 9*, 11.
3. Vasala, A., Panula, J., Bollok, M., Illmann, L., Halsig, C., and Neubauer, P. (2006) A new wireless system for decentralised measurement of physiological parameters from shake flasks, *Microbial cell factories 5*, 8.
4. Overton, T. W., Griffiths, L., Patel, M. D., Hobman, J. L., Penn, C. W., Cole, J. A., and Constantinidou, C. (2006) Microarray analysis of gene regulation by oxygen, nitrate, nitrite, FNR, NarL and NarP during anaerobic growth of Escherichia coli: new insights into microbial physiology, *Biochemical Society transactions 34*, 104-107.
5. Salmon, K. A., Hung, S. P., Steffen, N. R., Krupp, R., Baldi, P., Hatfield, G. W., and Gunsalus, R. P. (2005) Global gene expression profiling in Escherichia coli K12: effects of oxygen availability and ArcA, *The Journal of Biological Chemistry 280*, 15084-15096.
6. Jung, G., Denefle, P., Becquart, J., and Mayaux, J. F. (1988) High-cell density fermentation studies of recombinant Escherichia coli strains expressing human interleukin-1 beta, *Annales de l'Institut Pasteur 139*, 129-146.
7. Konstantinov, K., Kishimoto, M., Seki, T., and Yoshida, T. (1990) A balanced DO-stat and its application to the control of acetic acid excretion by recombinant Escherichia coli, *Biotechnology and bioengineering 36*, 750-758.
8. Shiloach, J., and Fass, R. (2005) Growing E. coli to high cell density--a historical perspective on method development, *Biotechnology advances 23*, 345-357.
9. Chatterjee, D. K., and Esposito, D. (2006) Enhanced soluble protein expression using two new fusion tags, *Protein expression and purification 46*, 122-129.
10. Sorensen, H. P., and Mortensen, K. K. (2005) Soluble expression of recombinant proteins in the cytoplasm of Escherichia coli, *Microbial cell factories 4*, 1.
11. Kiefhaber, T., Rudolph, R., Kohler, H. H., and Buchner, J. (1991) Protein aggregation in vitro and in vivo: a quantitative model of the kinetic competition between folding and aggregation, *Bio/technology (Nature Publishing Company) 9*, 825-829.
12. Esposito, F., Fogliano, V., Cardi, T., Carputo, D., and Filippone, E. (2002) Glycoalkaloid content and chemical composition of potatoes improved with nonconventional breeding approaches, *Journal of agricultural and food chemistry 50*, 1553-1561.

13. Makrides, S. C. (1996) Strategies for achieving high-level expression of genes in Escherichia coli, *Microbiological reviews 60*, 512-538.
14. Sorensen, H. P., and Mortensen, K. K. (2005) Advanced genetic strategies for recombinant protein expression in Escherichia coli, *Journal of Biotechnology 115*, 113-128.
15. Kapust, R. B., and Waugh, D. S. (1999) Escherichia coli maltose-binding protein is uncommonly effective at promoting the solubility of polypeptides to which it is fused, *Protein Sci 8*, 1668-1674.
16. Bach, H., Mazor, Y., Shaky, S., Shoham-Lev, A., Berdichevsky, Y., Gutnick, D. L., and Benhar, I. (2001) Escherichia coli maltose-binding protein as a molecular chaperone for recombinant intracellular cytoplasmic single-chain antibodies, *Journal of Molecular Biology 312*, 79-93.
17. Fox, J. D., Kapust, R. B., and Waugh, D. S. (2001) Single amino acid substitutions on the surface of Escherichia coli maltose-binding protein can have a profound impact on the solubility of fusion proteins, *Protein Sci 10*, 622-630.
18. Smyth, D. R., Mrozkiewicz, M. K., McGrath, W. J., Listwan, P., and Kobe, B. (2003) Crystal structures of fusion proteins with large-affinity tags, *Protein Sci 12*, 1313-1322.
19. Goh, L. L., Loke, P., Singh, M., and Sim, T. S. (2003) Soluble expression of a functionally active Plasmodium falciparum falcipain-2 fused to maltose-binding protein in Escherichia coli, *Protein expression and purification 32*, 194-201.
20. Hartl, F. U., and Hayer-Hartl, M. (2002) Molecular chaperones in the cytosol: from nascent chain to folded protein, *Science (New York, N.Y 295*, 1852-1858.
21. Mogk, A., Mayer, M. P., and Deuerling, E. (2002) Mechanisms of protein folding: molecular chaperones and their application in biotechnology, *Chembiochem 3*, 807-814.
22. Schwarz, E., Lilie, H., and Rudolph, R. (1996) The effect of molecular chaperones on in vivo and in vitro folding processes, *Biological Chemistry 377*, 411-416.

LIST OF PUBLICATIONS

Elisabetta Passera, Barbara Campanini, Franca Rossi, Valentina Casazza, Menico Rizzi, Roberto Pellicciari, and Andrea Mozzarelli. Human kynurenine aminotransferase II: reactivity with substrates and inhibitors. Manuscript submitted.

Ileana Ramazzina, Stefano Amato, Elisabetta Passera, Stefano Sforza, Gianni Mistrello, Rodolfo Berni and Claudia Folli. Recombinant production and characterization of the lipid transfer protein from pear (Pyr c 3), an allergen with an *in vivo* low allergenic potential. Manuscript submitted.